Study Project
Ice Forces against Offshore Structures
Phase 2 Report

Ice Force Studies in the Bothnian Bay

Phase 2 1989-94

VBB VIAK

Swedish National Maritime Administration

Hamburgische Schiffbau-Versuchsanstalt

R4816-000
ICE FORCE STUDIES
IN THE BOTHNIAN BAY
Phase 2 1989-94

CONTENTS:

FOREWORD

The second phase of the project ICE FORCES AGAINST OFF-SHORE STRUCTURES was initiated in 1989 as an extension of the first phase of the study, conducted between 1985 and -88. The 2nd phase has been sponsored by

* **MOBIL Research and Development Corporation, USA**
* **Canadian Marine Drilling Ltd. (CANMAR), Canada**
* **The Swedish National Maritime Administration (NMA)**

Experience from the 1st phase of the study has been summarized in a series of five reports and, as an introduction, in the present report in which the achievements during the 2nd phase are then accounted for.

VBB VIAK has been responsible for the management of project. The main part of the field work has been carried out by **NMA**. Hamburgische Schiffbau-Versuchsanstalt **HSVA** has been responsible for the testing and operation of the Ice Force Sensing Panel System with assistance of the NMA staff.

The essence of our findings during the two phases of the project is presented in Chapter 9 in the form of a generalized model for numerical characterization of ice force time-histories and observations concerning important physical features of the ice-structure interaction, whether periodical or of a more chaotic character.

Stockholm March 21, 1994
VBB VIAK

Alf Engelbrektson

LIST OF SYMBOLS ETC

Units

SI units are generally used in this study

Symbols

h: ice thickness
b: instantaneous width of ice-structure contact area
d: diameter of a cylindrical indentor

f_u: uniaxial strength of the ice (compressive if not otherwise stated)

f_{um}: "mean uniaxial strength", averaged over the contact area (compressive if not otherwise stated)

p: contact pressure between the ice and the structure

p_{eff}: "mean effective ice pressure", the unidirectional ice pressure averaged over a defined gross contact area, normally h x b, i.e.

$$p_{eff} = \frac{F}{h \times b}$$

F: "global ice force" i.e. the total unidirectional ice force on a structure, instantaneous or averaged over a certain period of time

F_{max}: the "peak global ice force" during a certain period of global ice force variations (in our studies the "peak force" is in fact also averaged, since it is related to the measured response of a structure, but it is normally averaged over a very small fraction of the period of the most significant mode of structural vibrations)

ΔF: amplitude of ice force fluctuation around the mean global ice force averaged during a certain period of time or determined as a low-frequency (filtered) load.

k_S: "shape factor", the ratio between global ice loads on e.g. cylindrical and plane indentors

k_I: "indentation factor", for factoring the ice load with respect to the aspect ration b/h

k_C: "contact factor", for factoring the ice load with respect to imperfect contact between the ice and the structure

$k = \frac{p_{eff}}{f_{um}}$ a common factor, accounting for all the abovementioned and other factors for transformation of the uniaxial ice strength to effective ice pressure on a structure

v: ice drift velocity

v_R: velocity of indentation or relative velocity between the moving ice and a vibrating or otherwise moving structure

v_S: velocity of the contact surface of the structure in the ice drift direction

$K_\phi = \frac{F\ Z_F}{\phi}$ rotational stiffness factor

ϕ: inclination of the lighthouse (above ice level and for static ice loads if not otherwise indicated)

Z_F: distance between the resultant ice force and the base of the structure

x_1, x_2, x_3, x_4 displacements corresponding to instruments Nos 1-4 (locations) and directions given in the text

$x(t), \dot{x}(t), \ddot{x}(t)$ time functions of the parameters of motion in horizontal direction

$\ddot{x}_R(t)$ time functions of the recorded acceleration

$\ddot{x}_\phi(t)$ time function of the fraction of gravity caused by the inclination of the structure

$\bar{x}, \bar{\dot{x}}, \bar{x}$ etc. dashed symbols indicate mean values or low-frequent components of motion

$F(f)$ Fourier wave amplitudes

$\Theta(f)$ phase angle of a component wave

$\alpha = \frac{\ddot{x}}{x}\phi$ ratio between "tilt acceleration" and displacement

Symbols used in the computer calculations and plotted diagrams

A1, A2	Structural acceleration and signal No. (Signals 1 and 2 are relating to the upper instrument level.)
V1, V2	Structural velocity and signal No.
D1, D2	Structural displacement and signal No.
I3, I4	Inclinometer signals.
T3, T4	Tilt angles corresponding to I3, I4.
F1, F2	Ice force components in directions Nos 1 and 2.
Fres	Resultant ice force.
Fdir	Direction of resultant ice force

KEY TO COORDINATE SYSTEMS, SCALES AND TRANSFORMATION OF UNITS

Norströmsgrund lighthouse

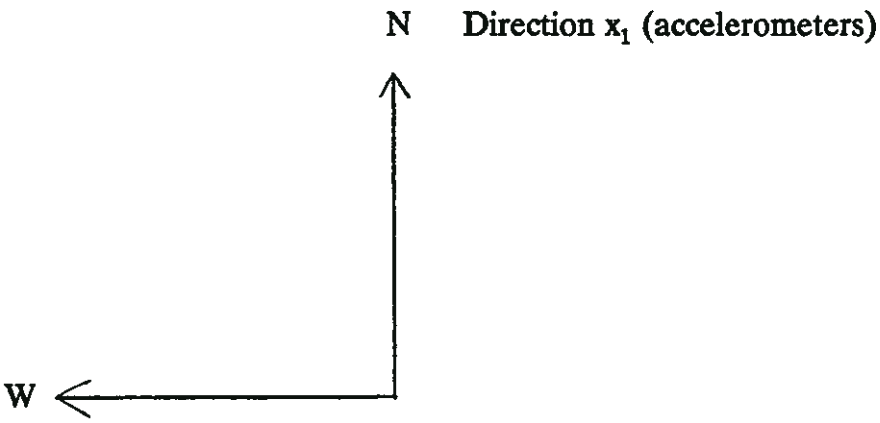

Direction x_2 (acc.)

ϕ_4 and x_4 (incl.)

Instrument reading units:

- Accelerometers u_1, u_2

- Inclinometers u_3, u_4

Transformation of instrument reading units to units used in calculations:

- Accelerometers $\tilde{x}_R1 = - u_1 \cdot 0.00191 \text{ m/s}^2$

$\tilde{x}_R2 = u_2 \cdot 0.00191 \text{ m/s}^2$

- Inclinometers $\phi_3 = u_3 \cdot 2.564 \cdot 10^{-7}$ radians *

$\phi_4 = u_4 \cdot 2.564 \cdot 10^{-7}$ radians *

$x_3 = \phi_3 \cdot g/\alpha_f$

$x_4 = \phi 4 \cdot g/\alpha_f$

$\alpha_f = 0.315$ **

$k = \frac{M}{\phi} = 7.378 \cdot 10^{11}$ Nm/radians

$F = M/z_F$

---

* u_3 and u_4 are filtered and calculated after the isolation of the horizontal acceleration component form the gravity component

** Determined by pull tests in July, 1988

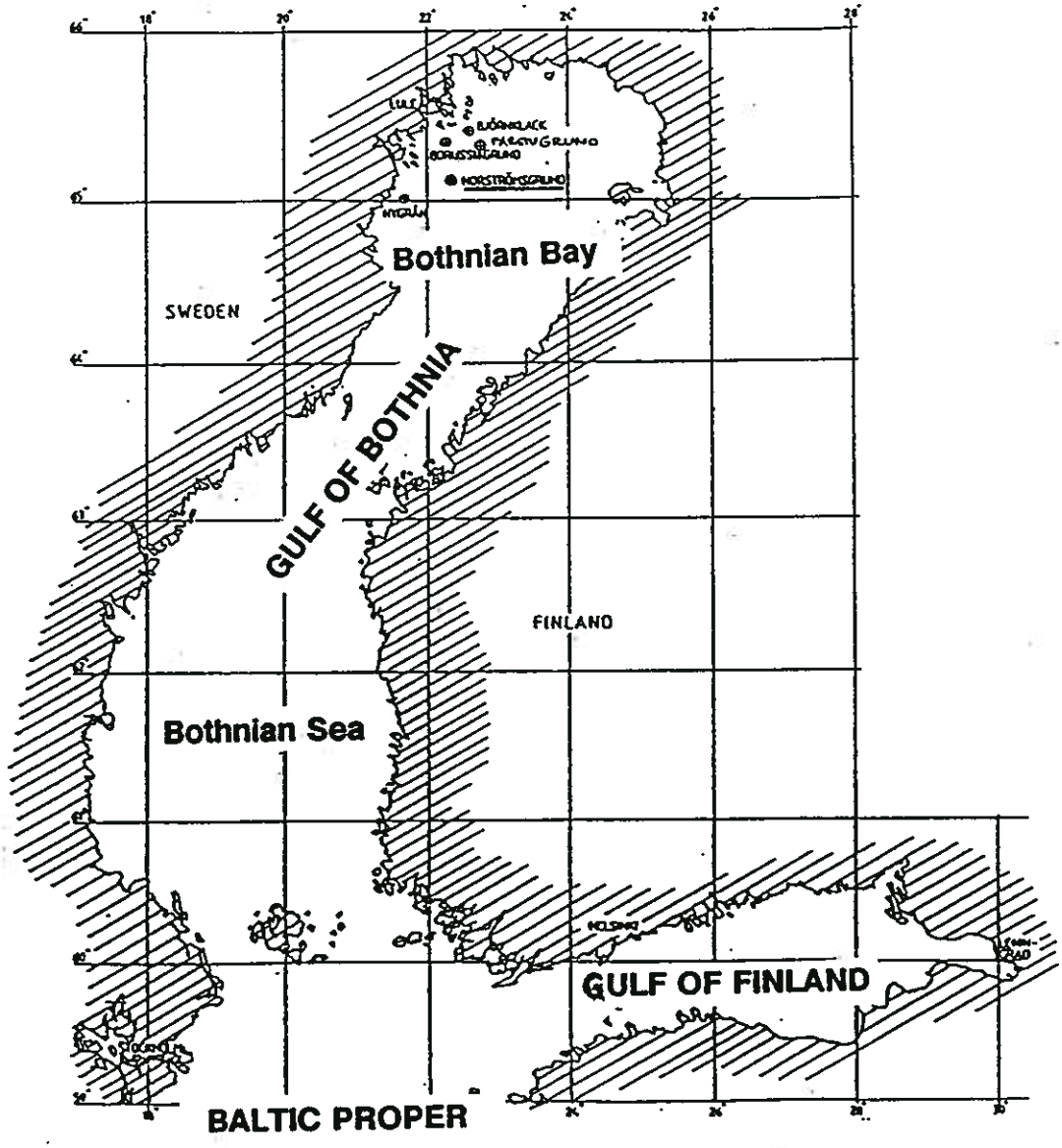
Bothnian Bay
SWEDEN
GULF OF BOTHNIA
FINLAND
Bothnian Sea
GULF OF FINLAND
BALTIC PROPER

1. INTRODUCTION

1.1 Background

For about 30 years ice action on offshore lighthouse structures in the Gulf of Bothnia has been increasingly studied. Largely, each decade represents a specific stage of development.

During the 1960's the studies were quite unsophisticated: simply a follow-up of the performance of the structures when affected by drifting ice, ice-piling, icing etc. On the basis of the rather poor knowledge of ice action at that stage and, apparently, a portion of good intuition, ice forces were predicted rather closely to the optimum risk level. A few cases of damage gave fairly clear indications as regards particular ice conditions, requiring adjustments of the design loads.

During the 70's the problem of ice-induced vibrations was realized and the most strongly affected structure was instrumented. Vibration records sampled during that decade, together with the continued follow-up and analysis of a few cases of static and dynamic overloading of Finnish and Swedish lighthouses, improved the understanding of ice-structure interaction considerably.

During the 80's the studies were expanded appreciably, quantitatively as well as qualitatively. Taking advantage of the Gulf of Bothnia as a convenient facility for Arctic research, several independent ice study projects with international participation have been conducted and some are still in progress. The product is a continuous inflow of parametrically well-defined data and subsequent improvements of the bases for ice-force predictions for Arctic areas, wherever the fundamental ice parameters can be quantified and where ice conditions are not essentially different from those prevailing in the Gulf of Bothnia.

1.2 The first phase of the Joint Industry Ice Force Study

In 1985 the studies of ice-structure interaction were intensified in that a joint study project was agreed between Arco, Exxon and Mobil (USA), Norwegian Contractors, Canadian Coast Guard, Mitsubishi, the Swedish National Industrial Board, Hamburgische Schiffbau-Versuchanstalt and VBB. The latter two companies, cooperating with the Swedish National Maritime Administration and with the University of Luleå obtained financial and advisory support for a comprehensively extended field study of ice-structure interaction, by employing two large lighthouses in the Bothnian Bay as objects for data sampling and other observations.

The lighthouses were provided with instrumentation for measuring and recording ice-induced structural responses and the character of ice

action. During a three years' period the database was greatly enlarged, and new analysis methods were developed for transformation of measured structural response to ice forces. Since the instrumented lighthouse structures serve, in principle, as full-scale elastic obstacles and measurement devices with calibrated constitutive properties, static as well as dynamic relations between the structural response and the ice forces were determined within uncertainty ranges that are judged to be quite acceptable for most engineering purposes.

A summary of the outcome of this first phase of the study as well as the applied methodology is presented in Chapter 3 of the present report. Very briefly the outcome may be characterized as model for prediction of ice-forces exerted by drifting ice on a vertical-sided (even slender and vibrating) offshore structure with ice strength and thickness as input parameters and with a particular attention paid to the time-history of the ice force in the case of resonance vibrations.

During the course of the first phase of the study, HSVA proposed an extension of the investigations, employing a set of ice force sensing panels mounted on the lighthouse. Costs beyond the project budget were covered by HSVA and the German government and to some extent by the Swedish Maritime Administration.

The Steering Group accepted the proposal and the panel system was fabricated, installed and tentatively operated in winter 1987/88. However, the sealing of the panels appeared not to be completely watertight and the panels had to be removed and the sealing improved.

1.3 Phase 2 activities

At the end of the first phase of the project, the Steering Group decided on a second phase, including reinstallation of the ice force sensing panels which was implemented before the winter 1988/89. The ice drift events causing strong vibrations were few during that winter, but a collection of more or less "dynamic" ice force records were still obtained, at least sufficiently for confirmation of the efficiency of the panel system. Since the formal start of the second project phase was delayed for several reasons, the costs had still to be covered mainly by the German sponsors and partly by the Swedish Maritime Administration. After the winter season the panels were removed for service and repair. An attempt to reinstall the panels in late 1989 was interrupted by rapidly increasing winds and waves, and for similar reasons several attempts during 1990 and 1991 were unsuccessful until July 15, 1991, when the reinstallation was successfully completed. Supplementary installation work and testing was carried out in the autumn 1991.

The instrumentation for structural response measurements and the video cameras were removed from the two lighthouses after the termi-

nation of the first phase. The reinstallation was conducted in early 1992. All the equipment and efforts were now concentrated to one lighthouse for reasons explained in Chapter 4.

Thus, after a long period of preparatory work (and expenses beyond the budget, carried mainly by the Maritime Administration, VBB and HSVA) the lighthouse Norströmsgrund was fully equipped with its test devices in early January, 1992. Until then, the winter had been extraordinarily warm (actually the 5th in a series of warm winters, see Appendix 6, page 45) and there was merely very thin ice in the Bothnian Bay.

However, no significant drifting ice appeared during the whole winter and, still worse, even the following winter was essentially free from drifting ice of such persistence that ice force measurements could be expected to be successful. Until mid 1993 the maintenance and repair work had proceeded in accordance with the work plans from -91 and -92 (Appendix 5). The cost of this work and the operation of the power system, etc. of the lighthouse consumed so much of the budget, that in mid 1993 it was clear, that the budget would not permit any more comprehensive repair of the panels. During the autumn personnel from HSVA and NMA made a number of expeditions to the lighthouse in order to examine the panels and necessary service systems as regards operability. It was reported that a large number of the sensors of the panels were out of operation so that one panel was definitely useless and it was questionable, whether any reliable data could be expected to be obtained from the others. The power system of the lighthouse was also out of operation due to leaks in the fuel system, etc. It was obvious that neither the budget nor the available time and resources would be sufficient for removal, repair and reinstallation of the panels before the winter.

These circumstances were explained in letters of January 11, 1994, to MOBIL and CANMAR, where it was recommended, among other things, that no more means be spent on trying to operate an incomplete measurement system but rather to postpone the activities until after the present winter or to break off the project, temporarily or definitely. At the present stage, final decisions have not been made as regards the future of the project, but, whatever happens in the future we have decided to finalize the previously drafted report covering the work which has been carried out until the present date and the outcome of that work. Thus, although it has not been possible to sample any ice force measurement data during Phase 2 of the project, it has been possible to improve the model outlined during Phase 1 for characterization of ice forces on offshore structures, as accounted for in Chapter 9.

2. STUDY OBJECTIVES

The following study objectives were formulated at the start of the second phase of the project. Although it has not been possible to sample data as intended, the initial outline of targets for the study follows here unchanged.

The basic objective of the second phase of the study is to improve the previously proposed model for characterization of ice forces acting on vertical-sided offshore structures, notably the model that was the outcome of the Phase 1 studies. The model has been described in the project reports of Phase 1 and, more briefly, in a report to the POAC 89 conference, [1]. For the sake of continuity and completeness the most important features of the model and its background are also described in Chapter 3 of the present report.

Also, as regards the objectives of the study, it is judged to be appropriate to start out from the basic objective outlined before the start of the first phase of the study. Subsequent to such a recapitulation of the "basic objective", the particular Phase 2 objectives will be addressed.

The basic incentive for the study project was, of course, the existence of a large number of offshore tower-shaped lighthouse structures in the Gulf of Bothnia, offering a unique opportunity to study ice-structure interaction in an Arctic field, comprehensively although without unreasonable efforts. Also, the outcome of simple ice-structure interaction studies that had already been in progress in the Gulf of Bothnia during almost two decades, indicated, that extended investigations would most likely provide data for considerable improvement of the understanding of ice-structure interaction phenomena and hopefully generate well-supported generally applicable models for derivation of ice forces for the design of offshore structures. Thus, the basic incentive was twofold, an obvious need for a better understanding of ice-structure interaction and the existence of an already established experimental field with properties, both as regards the structures and the ice conditions, representative for a relatively broad range of conditions expected to be met with in various Arctic waters.

Thus, basically, the goal for the study was a model with a broad applicability for prediction of ice forces on vertical-sided offshore structures, based on field data from the northernmost part of the Gulf of Bothnia (which part is called the Bothnian Bay). Obviously, such a model must include a parametric formulation of ice forces, taking into account the following conditions primarily:

- the ice effective strength or the effective contact pressure (p_{eff}) and its time-dependent variations, particularly when drifting ice is crushed against a vertical-sided indentor.

- the gross contact area (A) between the ice and the structure.

- the time-history of the global ice force, particularly in the case of resonance vibrations of the structure.

- the relationship between the effective ice pressure p_{eff} and measurable ice strength characteristics such as the average uniaxial compression strength of standard test cores (f_{um}).

In its most simple form the global ice force was therefore expressed by the following relationship

$$F(t) = p_{eff}(t) \cdot A = k(t) \cdot f_{um} \cdot A \qquad (2:1)$$

In this formula the coefficient k(t) must then represent not only the time dependence of the contact pressure but also its well-known dependence on the size of the gross contact area, the degree of contact, the aspect ratio (i.e. width/height of the gross contact area) and the shape of the indentor (flat, circular-cylindric, etc.).

Thus, in compliance with conventions generally applied when equating static ice forces and after introducing a separate time function to account for the dynamic effects, the general ice force formula may be written

$$F(t) = k_S \cdot k_I \cdot k_C \cdot f(t) \cdot f_{um} \cdot A \qquad (2:2)$$

where the coefficients k_S, k_I and k_C are intended to account for effects of structural shape, multiaxial ice stress conditions (depending on the aspect ratio among other things) and the degree of contact (which may also include size effects), respectively. Normally the relationship between the average ice pressure and the uniaxial ice strength f_{um} is also accounted for by k_C.

However, it must be realized, that, particularly when considering the time dependence, these effects are not easily separated. They are obviously more or less interrelated and depending on the variable ice stress conditions and failure modes. Even during one single cycle of a periodic ice force sequence, these conditions and thus the above coefficients must be expected to vary considerably, which the results of the Phase 1 study clearly demonstrate. In particular, the coefficient k_C, assumed to express the degree of contact, e.g. the ratio between the net and the gross contact area, is obviously also depending on the mode of ice failure etc. The very mechanism of a fluctuating local ice pressure could thus be reflected by expressing merely k_C as a time function $k_C(t)$ and by using values averaged in time for the other coefficients, when expressing the global ice force:

$$F(t) = k_{Sm} \cdot k_{Im} \cdot k_C(t) \cdot f_{um} \cdot A \qquad (2:3)$$

However, since it is not a primary purpose of the study to evaluate shape and aspect ratio influences, a common factor k has been used in the global ice force time function

$$F(t) = p_{eff}(t) \cdot h \cdot b = k(t) \cdot f_{um} \cdot h \cdot b \qquad (2:4)$$

as well as for peak values, e.g.

$$F_{max} = k_{max} \cdot f_{um} \cdot h \cdot b \qquad (2:5)$$

where the coefficient k is relating to the global ice force acting on a cylindrical, vertical-sided indentor and to aspect ratios for which k_I is generally assumed to be unity. Other shapes and aspect ratios may be accounted for with reasonable accuracy by using empirical factors averaged for stationary ice force conditions. The function k(t) may thus be adjusted, approximately by means of time-independent proportioning, to account for other shapes, aspect ratios etc than the above.

The primary goal for the first phase of the study was thus the establishment of generic time functions F(t) for the global ice force, based on measured responses of the affected lighthouse structure and, to the largest possible extent, to relate the ice force to the uniaxial ice strength, determined from sampled ice cores. In the next chapter of this report, where the achievements during Phase 1 are summarized, such time functions are presented.

The second phase of the ice force study has several purposes which can be summarized as follows:

(1) Sampling of more data, primarily in the form of structural response data (acceleration, inclination), to be transformed into global ice forces.

(2) Improvement of the procedure for transformation of the above response data, based on an increased number of instruments and measurement points and improvement of the calculation program, separating various modes of structural vibration and thus admitting a more accurate representation of higher-frequency components of the ice force time function.

(3) Sampling of local ice pressure data by means of the ice force sensing panel system in order to evaluate the distribution of the ice pressure in space and time and to correlate the time-histories of the local ice forces with those of the global force.

These evaluations are expected to provide a basis for a better understanding of the mechanism of ice-structure interaction, and may possibly support the more or less hypothetical explanations presented on the basis of the Phase 1 results.

In principle, the final goal is, of course, to establish ice force prediction formulae as indicated in Eq(2:4), however with improved accuracy in regard of the time-function k(t), with its "static" as well as its "dynamic" part.

In comparison with Items Nos 1 and 2 which may be regarded as direct extensions of the Phase 1 study, employing largely the same soft- and hardware facilities, Item No. 3 introduces a completely new feature into the project in the form of the ice force sensing panels and thus a novel device for ice force measurements. The panel system which was introduced and tested already during Phase 1 has been given a high priority both by the former and the present Steering Group, and even merely the testing of the performance of the system may be regarded as an important objective of the study. Consequently, a major part of the project budget has been allocated to the installation and operation of the panel system.

The introduction of the ice force sensing panel system and the limited financing means for the second phase of the ice force study, calls for a concentration of this phase on the dynamic character or the global and local ice forces. A low priority has to be given to the relationships with the laboratory-measured ice strength, as defined by standard tests.

The measured effective ice pressure functions $p_{eff}(t)$, averaged over the one, two or three panels or over the whole width of the structure, are primarily evaluated and compared. Secondly they are related or normalized to well-defined ice pressure characteristics which can in turn be related to a standard ice strength parameter. In the Phase 1 Summary Report an average of the peak global ice forces was suggested to constitute this field strength characteristic. The importance of a clear definition of the selected characteristic must be underlined, having in mind that the "effective strength" of ice when being crushed varies with time as well as the size of the gross contact area, not to speak of the net area.

3. PREVIOUS STUDIES

3.1 Objectives

As indicated in the introduction the objectives of the ice force studies, although basically the same, viz. to understand and quantify ice forces on offshore structures, were somewhat changed during the course of investigations. Before the 1970's the studies were mainly aiming at evaluation of "static" maximum ice force for various ice and structural conditions, based largely on experiences of cases of damages by ice "overloading" of lighthouse structures in the Gulf of Bothnia. At the start of the Phase 1 studies in 1985 the importance of dynamic ice action was focused at as well. In the initial declaration of the objectives, a static and a dynamic part of the ice load were defined, the latter with a "saw-tooth"-like time function, the amplitude of which was to be determined as well as the static ice load part. The intention was to study the "static" as well as the "dynamic" ice forces under a variety of structural and ice condition, since it was anticipated, that the ice-structure interaction would appear to be very sensitive to such variations.

Another important objective of Phase 1 one was the development and follow-up of various systems for data acquisition, such as instruments for measurement of structural "static" and "dynamic" responses with an extremely good resolution, video systems for automatic recording of ice drift situations and the ice force sensing panels.

Based on experience during the course of the investigations, the objectives were somewhat changed.

In particular, improved understanding of the mechanism of ice-induced vibrations (i.e. that the vibrations are "self-induced" as much as they are ice-induced and that the frequencies of the ice-load components are governed by the eigenfrequencies of the structures) made it clear, that it was better to concentrate on one single well-equipped structure located where ice drift is most frequent, than to spread out the resources. Data from FARSTUGRUND lighthouse was thus of the same character as data from NORSTRÖMSGRUND, but scarcer. Furthermore, the need of comparison between global and local ice forces as well as the need of a denser instrumentation for the refinement of the calculation model were good reasons for moving all he equipment to NORSTRÖMSGRUND, which was implemented before the observation period 1992.

It can be concluded, that the modifications of the initial objectives reflect a transition in the direction from a probabilistic to a more deterministic treatment of the ice-structure interaction problem. Initially, the phenomenon was assumed to be more complex and depending on "statistical" parameters to a greater extent than it now appears to be. At the present stage a deterministic formulation of ice-force expressions, such

as Eq(2:4), appears to be a good basis for further research and for design purposes also, with conservative safety factors applied, particularly to the ice parameters. These parameters (strength, thickness) are likely to be the predominant contributors to the uncertainty of ice force predictions.

3.2 Scope and methodology

Since the scope of the previous studies is rather similar to that of the extended investigations and since the methodology for data acquisition and analysis is the same to a large extent, the presentation of the present report starts out from a recapitulation of the scope and methodology of Phase 1. In this section only a brief summary is presented, but more comprehensive descriptions are included in **Appendices 1 and 2**, where procedures for data acquisition and analysis are described quite in detail. These appendices are referred to also in the descriptions of the Phase 2 studies in Chapter 3 and the following chapters, where mainly novel features and thus not the procedures established during previous studies are addressed.

The structural responses due to ice action were measured and recorded by means of a system of accelerometers and inclinometers, including computer and filter units as well as tape recorders.

By means of the accelerometer systems the horizontal acceleration of the structures when vibrating were measured and recorded with a very good accuracy ever since the instruments were installed. A few outages occurred, but they were of minor importance.

The low-frequency or "static" deflection of the ice-affected structures were measured by inclinometers.

The accelerometers, as well as the inclinometers, are inertia sensing instruments of, in principle, similar basic design. The latter are, however, designed for measurement of extremely small inertia forces, primarily due to gravity in case of small changes of the tilt angles.

Great efforts were devoted to the development of such a system for measurement of the low-frequency components of the structural responses that constitute the basis for assessing the corresponding low-frequency ice force components. Realizing that the very small structural deflections had to be related to gravity, a pendulum system was tested parallel to the installation of inclinometers. After some trial operations and laboratory testing the preference was given to the latter instruments. Methods had then been developed for Fourier-processing of the signals in order to separate low-frequency from higher-frequency wave components and to distinguish between horizontal (inertia) and vertical (gravity) components. After one winter season of tentative operation the

resolution of the inclinometer system was increased and during the winter season 1987-88 the performance of the inclinometers as well as other parts of the response measurement system was satisfactory.

Data regarding ice conditions have been acquired by means of video cameras, field sampling and study of reports regarding the large scale ice and weather conditions in the Bothnian Bay.

Video cameras mounted on the lighthouses were triggered automatically, when structural movements exceeded a certain acceleration limit. The ice drift velocity and the mode of ice failure could generally be determined by studying the video records and sometimes the thickness of broken ice could be estimated.

The field investigations were focused on measurement of ice thickness and ice temperature, and on sampling of cores for laboratory investigation of strength and other physical and mechanical properties.

A large collection of structural response data was acquired in the form of acceleration records, from accelerometers as well as from inclinometers. In order to avoid signal disturbances as much as possible, the signals were digitized before being recorded on magnetic tapes and, later, on diskettes. The data sequences were labelled so that they could be synchronized with the video records.

The most complete collection of response and video records was acquired during the winter season 1987-88. This collection contains a large number of records from ice drift events associated with more or less pulsating ice forces, many of which of pronounced resonance character. Some records from the 28th of March are particularly valuable, since resonance ice-structure interaction is represented as well as more "static" indentation and since field samples were taken shortly before the ice started to move.

The transformation of response data to ice force was performed by mathematical modelling of the structures and their constitutive properties etc. Finite element models were employed for determining the modes of deflection.

The dynamic ice-structure interaction was assessed by determining the dynamic equilibrium of simplified one-degree-of-freedom systems, the spring stiffness and internal damping of which could be determined within a narrow uncertainty range, since the fundamental structural frequency and the damping could be unambiguously identified in several records of free vibrations.

Whereas the transfer function, coupling the dynamic mode of deflection to the ice force, could thus be determined without further calibration measures, the corresponding static transfer function, i.e. the spring

stiffness coupling static load and deflection, could only be roughly estimated without calibration tests. Pull tests were therefore performed in 1987 by means of a large tugboat. The time-histories of the applied forces were measured by means of load cells and the corresponding deflection time-histories were registered by means of the inclinometer system.

Several procedures for transformation of the response signals to ice force functions were developed and tested. Problems that had to be solved were associated with, for instance, the identification of small-amplitude, low-frequency signals in the strongly pulsating inclinometer output and then to dissolve those signals into horizontal and vertical components. Other problems were associated with base-line errors and difficulties to identify the true zero base-line in the response signals. It appeared, that integration could not be carried out over any longer time intervals without causing problems such as amplification of small base-line errors.

However, the problems were essentially solved by introducing Fourier-processing of the signals. By dissolving them into sinusoidal components the various filtering processes and base-line corrections were greatly facilitated. Moreover, the spectral characterization of the signals appeared to be beneficial to the understanding of the interaction mechanism and the generalization of the ice force, as will be further demonstrated.

The analysis procedures are described step by step in **Appendix 2.**

3.3 Survey of sampled data

Data sampled during the period 1979-85 (before the start of Phase 1) was presented and analysed in Report No. 2 of Phase 1. Data sampled during the course of Phase 1 was dealt with in Report No. 5.

The quality of the data has been improved continuously. Therefore, although early data were very useful as a basis for improving the understanding of the ice-structure interaction phenomenon and for further development of data acquisition systems and analysis methods, data from the end of the second period is preferred for deterministic analysis, due to its completeness and comparatively high resolution. Actually, as pointed out in Report No. 5, there was good reasons for concentrating the analysis on selected data from the winter season 1987-88, which records are unique, since both low-frequency and high-frequency responses were recorded with a very good accuracy and since the ice parameters could be assessed reasonably well, particularly during some sequences of strong resonance vibrations.

Some data from this period has been selected for reexamination, employing the improved analysis methods developed during Phase 2.

An overview of data from the winter season 1987-88 was presented in Report No. 5. Table 3-1 is reproduced from that report.

3.4 Proposed model of ice-structure interaction

As a result of the Phase 1 studies a model for assessment of forces exerted by drifting ice on offshore structures was proposed. Basically, this model consisted of one quantitative and one qualitative part.

The quantification was expressed in the form of a generalized time-history of the global ice force or the effective ice pressure (to be multiplied by the gross contact area to obtain the global ice force).

$$p_{eff}(t) = p_0 + \Sigma p_n \cdot \sin(n\omega_1 + \Theta_n) \qquad (3:1)$$

Ice drift period	Max. acc.	Remarks
880113	0.35g	A few sequences of strong vibration
880117-20	0.40g	A few sequences of medium to strong vibrations
880205	0.10g	Field sampling 880210. 14 hours' intermittent vibration
(880110, 14)		Ice pressure (stationary)
880216	0.10g	Short vibration sequence
880211-26	0.25g	Many short and some long sequences
880301	0.20g	Several short and some long sequences
880303	0.25g	Several long and some short sequences
880307	0.20g	Many long and short sequences (mainly small amplitudes)
880310-11	0.20g	Many long and short sequences (mainly small amplitudes)
880320-26	0.10g	Many long and short sequences (mainly small amplitudes)
880328	0.35g	Field sampling 880328. Strong vibrations

Table 3-1: Observed ice drift periods in 1988 at Norströmsgrund

The loading function was thus represented by a constant p_0 and a series of sine waves with n = 1, 2, 3, 4 etc., the angular frequencies $n\omega_1$ of which are multiples of the fundamental structural frequency ω_1. The coefficients p_0, p_1 .. p_4 were tentatively quantified in relation to the peak pressure p_{max}. Typical relations between the effective pressure and the uniaxial ice strength were also indicated.

The qualitative part of the model was an attempt to explain the mechanism of ice-structure interaction, primarily the "dynamic" phenomena, although coupled to "static" indentation. Of course, these explanations were partly hypothetical, but were suggested as a basis for the planning of continued studies, particularly investigation of the distribution of the ice pressure not only in time but also in space.

The model thus proposed was described briefly in a report to the POAC 89 conference, which report is enclosed as **Appendix 3.**

4. METHODOLOGY

4.1 Evaluation of global ice forces

In principle, the evaluation of global and local ice forces utilizes similar mechanisms for acquisition of data and transformation of measured quantities to ice forces, viz. basically the spring mechanism. In the case of local ice forces, it is the elastic strain in the panel supports that is measured and transformed into reaction forces on the basis of calibrated constitutive relationships between the measured strain and the corresponding stresses. In the case of global ice force evaluation, the entire lighthouse structure serves as an elastic obstacle, the deflection of which is measured and transformed into global ice forces also on the basis of constitutive relationships and, in respect of dynamic response, also on the basis of relationships between measured response motion characteristics and the masses, eigenfrequencies and damping properties of the structure. All these relationships have been quantified on the basis of calibration tests and, in respect of eigenfrequencies and eigenmodes, observations of free vibrations initially generated by ice loads.

Thus, the evaluation of global ice forces comprises the following activities, basically:

* Measurement of the response of the lighthouse structure by means of accelerometers and inclinometers, placed at different levels.

* Mathematical processing of the obtained acceleration records in order to eliminate base line errors and to determine the low-frequency ("static") tilt angle of the structure.

* Transformation of acceleration and inclination response data to global ice forces on the basis of the above constitutive and dynamic transfer functions.

The instrumentation for response measurements is, in principle, the same as described in Chapter 3 for the Phase 1 measurements. More comprehensive descriptions are given in **Appendix 1**. However, since the measurements are now concentrated to Norströmsgrund lighthouse, the instrumentation of this structure has been doubled. The additional instruments are used for the purpose of redundancy in two respects. One is for malfunction of the instruments, the other is for checking of measured quantities by comparing acceleration records at different points. The latter also enables an improved accuracy in determining the modal shapes of the structure.

The locations of the instruments are shown in Figure 4:1.

Also, the procedures for processing the response data are to a large extent the same as those previously developed and applied during

Phase 1. Thus, the procedures briefly described in Chapter 3 and more comprehensively in **Appendix 2** have been applied with some exceptions to Phase 2 as well.

The exceptions are relating to an improved accuracy in the transformation of resonance vibrations to "dynamic" ice forces by accounting for secondary modes of vibration as well as the fundamental cantilever mode. The latter is doubtless of a predominant importance, since it governs the "self-induced" vibrations and thus the very mechanism of ice-structure interaction, but if the other modes are disregarded in the derivation of the ice force time-history (as in Phase 1), an unnecessary approximation is made.

The confirmation of the phenomenon of self-induced vibration and the fact that the ice force at resonance is composed of component sine loads with frequencies which are multiples of the fundamental frequency, facilities a more accurate derivation of the various sine components of the load and thus of a more accurate shape of the composed load time-history. Furthermore, a selective choice of measurement points makes it possible to improve the accuracy of the FE-model, in respect of the shapes of higher modes of vibration particularly.

For each sine component of the load the following procedure is applied:

* The load component is $F_n = F_{n\,max} \cdot \sin(\omega_n t + \Theta_n)$

* The response at the reference point of the lighthouse is $\vec{x}_n = \vec{x}_{n\,max} \cdot \sin(\omega_n t + \varphi_n)$

* $F_{n\,max}/\vec{x}_{n\,max}$ and $\Theta_n - \varphi_n$

  are determined by means of the FE-model

* The quantities $\vec{x}_{n\,max}$ and φ_n are determined from each particular sequence of recorded (stationary) accelerations that is to be analysed after disintegration and discretization into individual sine components, corresponding to the frequencies ω_n.

The procedure is demonstrated in **Appendix 4.**

Of course, when comparing this procedure with that of Phase 1, it must be kept in mind that the latter was developed and used not only for sequences of steady-state resonance vibrations but for general derivation of ice force time-histories based on various types of responses. However, one of the conclusions of the previous investigations was, that the stationary resonance conditions are likely to be predominantly decisive to the design of offshore structures susceptible to ice-induced vibrations. Therefore, for practical purposes and for the purpose of developing a generic model for "dynamic" ice load prediction, the present procedure

is judged to be preferable, and it is consequently generally adopted in the present phase of the study.

In the case that other than steady-state vibration sequences are considered, the method used in the previous studies may be applied. However, the accuracy would be improved if the response of the fundamental mode could be isolated. The quantities $\ddot{x}$,$\dot{x}$ and x of the isolated first mode should then be introduced into the general equation of motion, the solution of which yields the instantaneous values of the total ice force.

The isolation of individual modal responses from the acceleration records is, however, a complicated procedure, requiring a sharp identification of the various modal shapes, if a high precision called for. This in turn calls for a considerable number of instrument levels. For reasons given above such efforts are not within the frame of the present study. Since the steady-state vibrations are focused at, the more straightforward analysis method with a direct transformation of responses without modal separation is preferred. The particular advantage of this method is that the realism of the derived ice force function can be demonstrated simply by applying the derived ice force time-history as an input to the FE-model and comparing the computed output responses with the instrumental observations.

4.2 Evaluation of local ice forces

As declared in Chapter 2 an important objective of the present study is to sample local ice force data, enabling an evaluation of the ice force distribution not only in time but also in space. Such an evaluation was considered important already during Phase 1, when preparations for local measurements were made which were expected to provide additional bases for prediction of ice forces and for explanation of the mechanisms involved.

The lighthouse Norströmsgrund was provided with arrangements for being lined with ice force sensing panels around the entire circumference. However, due to the considerable costs for manufacturing and installations of the panels, their number had to be restricted at three panels, each with a width of 0,6 m. Thus a maximum of 16 per cent of an exposed half-circle can be expected to be covered by the panels, but the important thing is, that the panels are spaced so that the simultaneous ice force time-histories at the panels can be compared with each other and with the global ice force time-history.

The ice force sensing panel system is described in the next chapter and in **Appendix 5.**

4.3 Uncertainty assessments

The accuracy of the derived global ice load time functions depends, of course, on the accuracy of the simulation of various structural properties in the FE-model. A perfect result requires, that the model shapes and the model eigenfrequencies are perfectly simulated. Since perfection cannot be obtained with reasonable efforts (for example without a large number of measurement points and tests in order to map the exact model shapes) a certain degree of uncertainty must be tolerated. The uncertainty can, however, be limited to a level, where it is practically negligible. The following aspects are important in this respect:

* The model shall be applied merely to conditions of steady-state vibrations.

* Loads and responses shall be disintegrated into their sine components by Fourier processing.

* The eigenfrequencies of the first three modes of the model shall agree well with those of the lighthouse structure. (A frequency range up to about 20 Hz is then covered.)

* Since it is difficult to assess the modal shapes with a good precision based on a few measurement points, it is important to use response values, to which the second and third modes contribute as little as possible. In particular, the second mode should be avoided. Accelerometer are therefore placed closely to the zero deflection point of this mode. The reason for this is, that the frequency of the second mode is fairly close to the frequencies of the 2nd to 3rd sine components of the load. Closely to resonance the amplitudes and phase angles of the structural modes are very sensitive to these frequency relations, the evaluation of which may not be perfectly exact. The accuracy of the quantities used for transformation from response to load components is therefore improved, the more the influences of the 2nd and 3rd modes are avoided. The 3rd mode, however, has little influence even at resonance, since its zero point of deflection is located closely to the ice load.

* The structural damping is, of course, a potential uncertainty factor. Inaccurate modal damping ratios introduced in the model mainly affects load sine components close to resonance. Since resonance effects of the higher structural modes are minimized, as mentioned above, it is only the amplitude of the first mode that is significantly affected. Based on studies of sequences of free vibrations, the damping ratio of the first mode has been estimated at 0.040 ± 0.005. The corresponding uncertainty range of the fundamental ice force amplitude is of the order of 10 per cent. Damping effects due to friction between the vibrating structure

and fragmented ice is not likely to affect the above damping value very much. Consequently, such forces, if any, are included in the evaluated global ice force time-history.

* The uncertainties of the quantifications of more high-frequent load components are a little larger due to the abovementioned "disturbances" from the second and third modes of vibration. However, since the fundamental sine component of the load as well as of the response is of a predominant importance as a design prerequisite, the order of ± 10 per cent may be taken as a characterization of the general uncertainty of the dynamic load formulation. The uncertainty of the magnitudes of the "static" load components is somewhat larger.

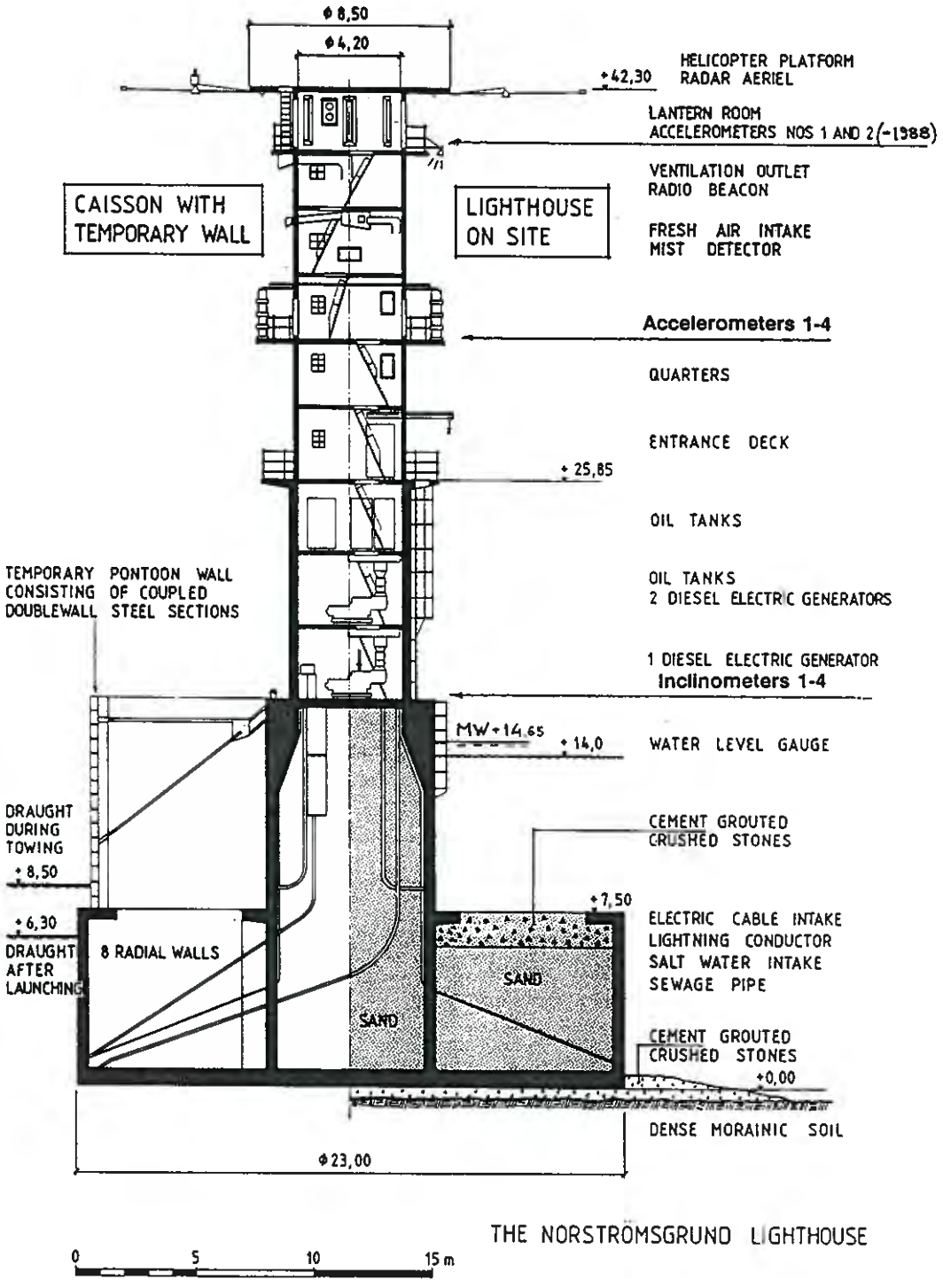

Figure 4:1

The NORSTRÖMSGRUND lighthouse

5. ICE FORCE SENSING PANELS

5.1 Principle design and function

For the purpose of measuring local ice forces on the lighthouse Norströmsgrund, HSVA has developed a twodimensional ice force panel (TIP) which measures the total load acting on the panel. The normal as well as the tangential (horizontal) component of the load is measured.

The principle design of the panel is shown in Figure 5:1.

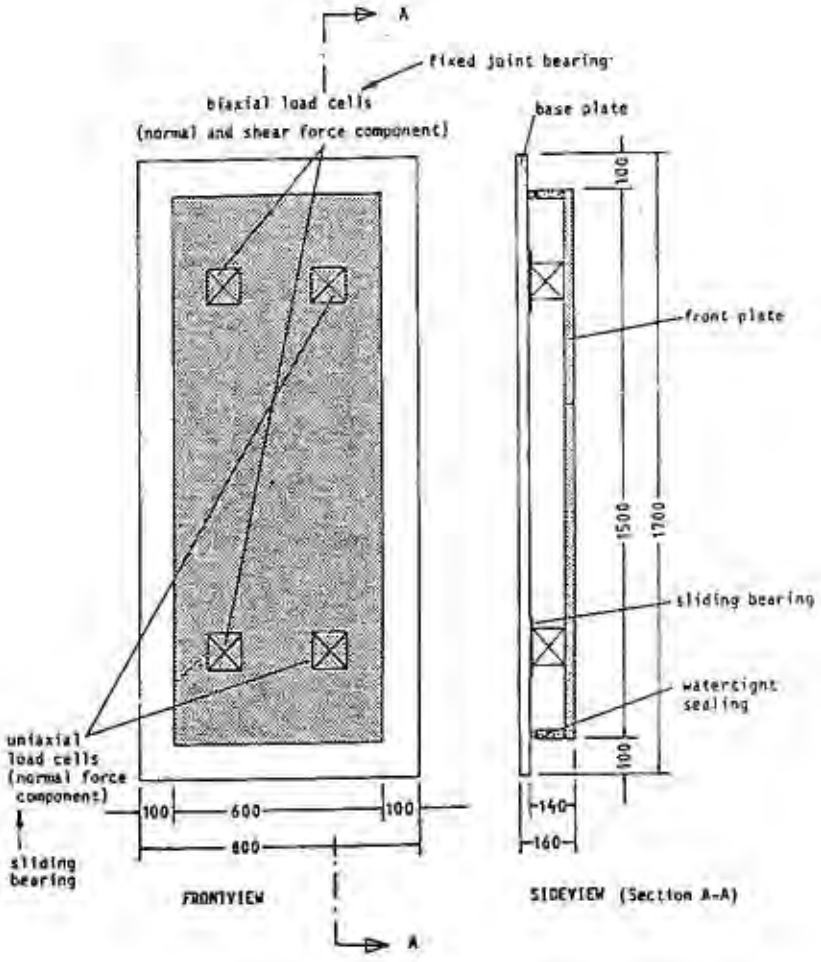

Figure 5:1
Principle design of an ice force sensing panel

The panel has a thick front plate exposed to the ice action and all the load paths towards the support base plate, i.e. the bearing points, are

instrumented with strain gauged load cells. The support reactions are superposed so that the total ice force on the panel will be measured. A unique feature of the TIP-panel is its capability of measuring two components of ice forces: the normal ice force component as well as the tangential component which acts horizontally (parallel to the waterline).

The base plate of the panel is mounted against a polygonal steel shield which is rigidly fixed to the lighthouse. The free space between the base plate and the front plate is entirely sealed, in order to avoid ice accretion and thus uncontrolled load paths. In order to upgrade the safety against water leakage and ice accretion, an internal heating system as well as passive protective means have been installed. All around the panel, the base plate extends over the dimensions of the front plate to provide the possibility of clamping the panel against the supporting steel shield.

The four load cells installed in each of the TIP ice force panels are strain gauged cylindrical load measuring bolts, supplied by Dr. Brandt GmbH, Bochum. The operational load of each load measuring bolt is 400 kN, thus providing a load capacity of 1 600 kN to the entire panel.

Two of the load cells are uniaxial to record normal load components, whereas the other two are biaxial for recording the normal as well as the tangential load components.

All functional elements of the panel have been designed to be fully operational down to a minimum temperature of -50°C.

Those structural components of the TIP-panel which are not made from stainless steel, are painted with an epoxy coating. The outer surface of the front plate is coated with a highly abrasion-resistant epoxy coating.

More details of the panel system are given in **Appendix 5.**

5.2 Static and dynamic calibration tests

Each single load measuring bolt as well as the complete TIP-ice force panels have been checked within the frame of a comprehensive testing program. Loads were applied in several steps up to the design load in normal as well as in tangential direction. The panel was loaded at various locations on the front plate, e.g. closely to the edges, in order to prove, that the response of the panel is independent of the point of load application. The test results show, that the linearity, i.e. the deviation from the straight line, is less than 5% of the design load, for normal as well as for tangential loading. The panel response on dynamic, saw-tooth like load time-histories was quite accurate.

5.3 Panel arrangement

Around the cylindrical concrete shaft of the lighthouse a 20-sided polygonal steel shield has been rigidly installed in the waterline region. The steel shield provides twenty plane steel surfaces, each outfitted with a matrix of threaded holes for optional attachment of ice force panels. Thus, any flexibility for changing the position of the existing panels is provided, as well as the possibility to increase the number of panels up to a maximum of twenty.

From assessment of previous extreme ice force events at the lighthouse Norströmsgrund, a slight tendency could be detected at mid winter conditions for prevailing ice drift directions towards the north. Therefore, the ice force panels were installed in due south of the lighthouse as illustrated in Figure 5:2.

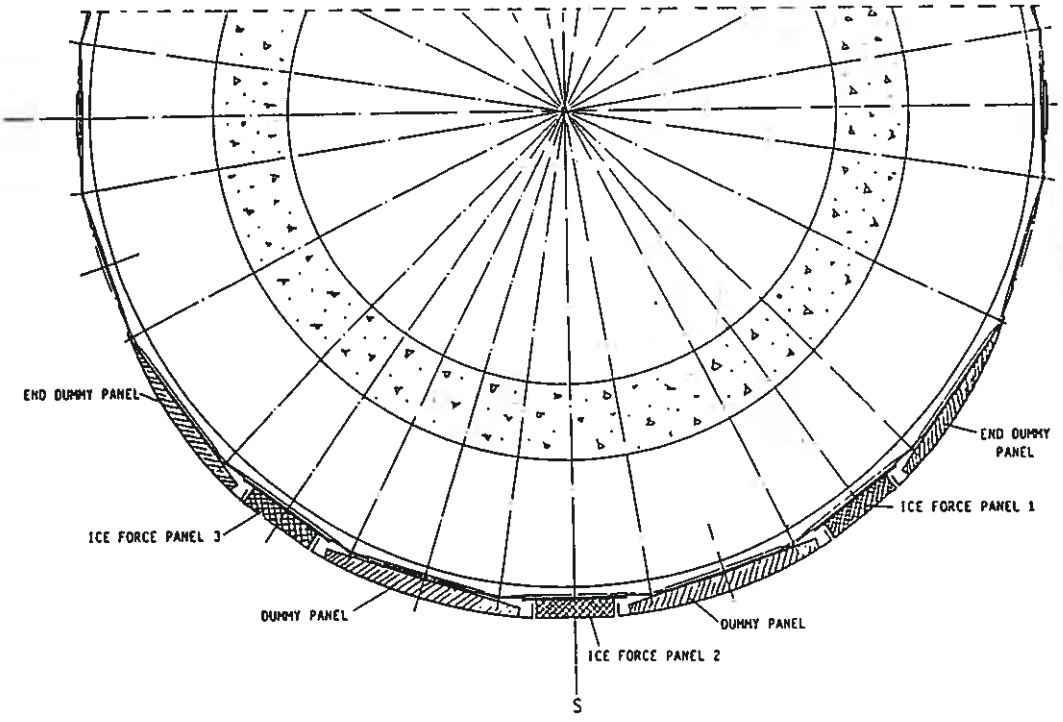

Figure 5:2
Panel arrangement

Three panels have been arranged such that they cover a 90°-sector together with two dummy panels to be installed between two sensing panels, in order to compensate for the projection of the panels. Correspondingly, two end-dummy panels have been installed in order to adjust the projection of the panels towards the actual curvature of the polygonal steel shield.

The sensing as well as the dummy panels are fixed towards the steel shield by clamping the top and the bottom part of the flanges by means of solid steel mounting bars.

5.4 Data acquisition system

Each of the three ice force panels is equipped with two biaxial and two uniaxial load cells. Therefore, there are six measuring channels per panel, and thus a total of 18 channels have to be simultaneously recorded by the data acquisition system. In order to be capable of identifying ice force peak values of short duration, the data sampling rate is about 30 Hz during dynamic ice load events.

In order to be able to automatically store as much data as possible, HSVA has developed a special "dynamic" data storage computer program; i.e. the measuring frequency will be constant at about 30 Hz, however, the measured data will only be stored for later data treatment if a certain relative change of data can be detected compared to the data measured immediately before ("dynamic threshold").

5.5 Measurements in winter 1988-89

The automatic operation of the data acquisition system for the three ice force sensing panels was started on the lighthouse Norströmsgrund in mid February 1989. Initially, due to the extreme mild winter and unfavourable ice drift directions, the ice force records were poor. The situation did not change remarkably for a period of about one month. Then, the general ice conditions in the study area altered and the major ice drift direction was towards the southern edge of the lighthouse, where the three ice force sensing panels had been installed. Thus, an almost continuous ice force recording was obtained over a period of about one month from March 24 until April 20, when the data tape was unloaded on occasion of a regular inspection trip to the lighthouse.

The analysis of the data and its results are discussed in Chapters 8 and 9.

6. MODIFIED PROCEDURE FOR TRANSFORMATION OF STRUCTURAL RESPONSE SIGNALS TO ICE FORCE TIME-HISTORIES

6.1 General

The previous studies led to the conclusion, that sequences of regular, fully developed steady-state resonance vibrations are decisive for most design purposes, in the case that the ice-structure conditions are likely to generate such vibrations. It was also concluded, that, in most cases, the conditional probability of fully developed resonance is rather high, once a structure is susceptible to ice-induced vibration. Thus, resonance is likely to occur within a broad range of ice conditions, including varying ice drift velocities.

Based on this conclusion, the analysis of global ice forces can now be focused merely on sequences of steady-state vibrations. For such sequences, the accuracy of the transformation between measured structural response and global ice force time-histories can then be improved in the following respects.

* All the modes of the structural vibrations can be considered, in the response functions as well as in the derivation of the relationships between the responses and the ice forces. (In the previous model the latter procedure was based on an approximation, neglecting other than the fundamental, predominant mode, notably the mode that governs the ice-structure interaction.)

* The transformation procedure becomes more straightforward and transparent, since several steps of the previous procedure can be omitted. Thus, the ice force functions can be derived directly from the acceleration signals, after Fourier-transformation. Step-wise integration of irregular signals is avoided. Integration errors need not be a concern as in the previous work.

* A FE-model, processed by means of a comprehensively tested commercial computer code, can be used for the mathematical processing of the signal transformation. The compliance between a measured accelerogram and the derived ice force time-history can then be demonstrated by applying the latter function as a load input to the FE-model.

As indicated above the novel procedure for transformation of measured responses to ice forces takes advantage of the fact that, during a sequence of steady-state resonance vibrations, a sine load generates a sine response with the same frequency. The components of free vibrations, with frequencies closely to the eigenfrequencies of the structure, are thus essentially damped out, when the vibrations stabilize into steady-state oscillations. Then, each sine component $F_n = F_{n\,max} \cdot \sin(\omega_n t + \Theta_n)$

of the load corresponds to a response component, e g acceleration, as follows:

$$\ddot{x}_n = \ddot{x}_{n\,max} \cdot \sin(\omega_n t + \phi_n)$$

Therefore, once the amplitude and phase relations between the load and the response have been determined by means of an accurate model of the ice-affected structure, these quantities can be used for transformation of any sinusoidal acceleration to the corresponding sine load.

Thus, two main tasks can be distinguished between. The first concerns the derivation of relationships between sinusoidal unit loads and responses for the particular structure, the responses of which are measured. This can be performed once and for all for a particular structure such as the NORSTRÖMSGRUND lighthouse. Secondly, each individual record of measured response signals have to be processed by Fourier analysis and transformed into ice force time-histories, employing the structure-specific relationssships between amplitudes and phases. The two phases of the work are described and illustrated by examples in the following.

6.2 Amplitude and phase relations between acceleration and ice force sine components

6.2.1 Calibration of the FE model

The FE-model, developed during Phase 1 of the ice force study, was adjusted (stiffnesses and masses) so that a reasonably good agreement was obtained between its modal frequencies and the eigenfrequencies of the lighthouse structure (Figure 6:1). The latter quantities can be identified in the power density spectra of the measured acceleration records. Most clearly, the modal frequencies can be distinguished in records of mainly free vibrations, but the peaks representing the eigenfrequencies are also visible in other records, as indicated in Subsection 6.2.3.

The following points are of major importance in the modelling of the structure:

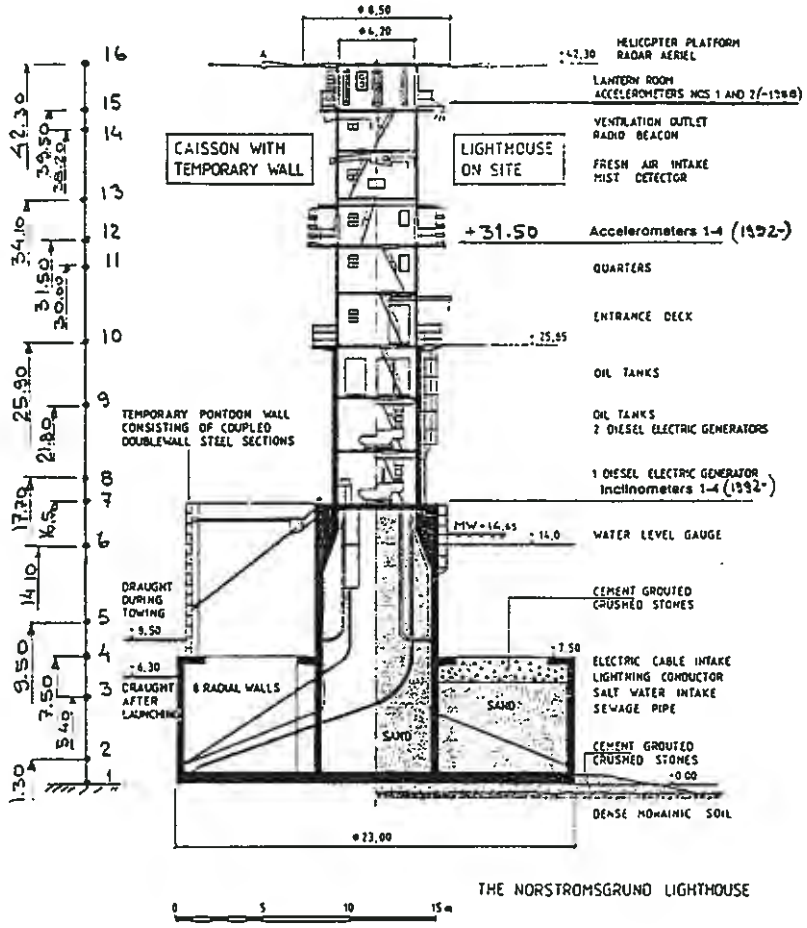

MODE 1 FREQ 2.3981 MODE 2 FREQ 6.0141 MODE 3 FREQ 11.377

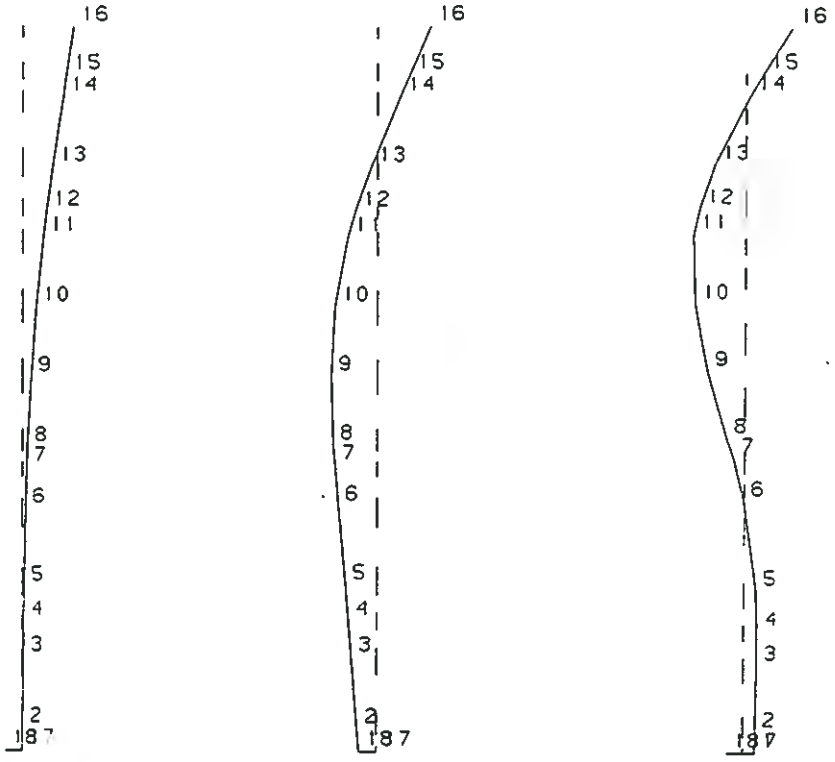

Figure 61

The FE-model and its significant modes of vibration

- The true modal frequencies and modal shapes, at least in the proximity of the measurement points, must be simulated with a very good accuracy. Since the fundamental eigenfrequency f_1 governs the frequencies f_n of all the load components, it is important primarily to obtain the correct ratios between each modal frequency f_k and f_1. A small deviation between the true f_1 value and that of the model can be tolerated only the ratios f_k/f_1 are correct.

  In our case we accepted f_1 = 2.40 Hz in the model, whereas the true frequency is normally around 2.35 Hz. This difference does not affect the derivation of amplitude and phase relations. Only, when demonstrating the ice-structure interaction by applying a derived load time-history to the model, this difference has to be accounted for by adjustment of the sine components of the load to fit f_1 = 2.40 Hz instead of the measured frequency 2.35 Hz.

- The modal damping, particularly that of the first mode, must also be determined with a good accuracy, since it strongly governs the amplitudes of the resonance vibrations and, though of less importance, the phases.

In principle, the modal damping can be determined for each mode that can be distinguished (by filtering) within the selected sequence(s) of free vibrations. Among other records of essentially free vibration, one of those displayed in Figure 6:2 (from March 28, 1988) may serve as an example.

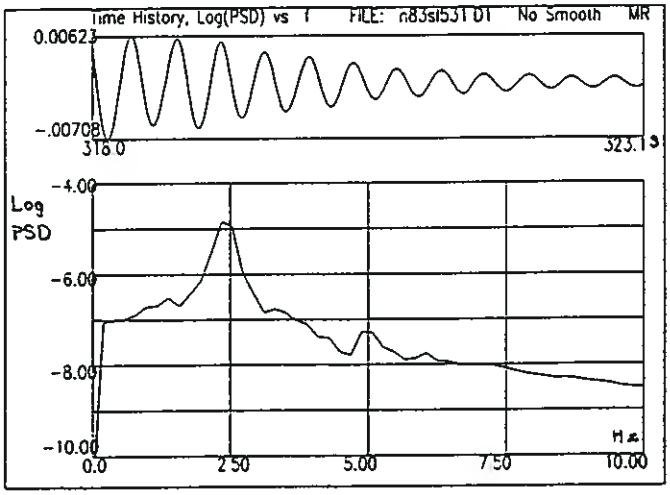

Figure 6:2

Displacement time-history from March 28, 1988, with sequences of essentially free vibrations

For the predominant **1st mode** the damping can be determined directly from the recorded accelerogram as follows:

$$c/c_{crit} = \frac{1}{2\pi} \cdot \ln \frac{m}{\Sigma \ddot{x}_i/\ddot{x}_{i-1}}$$

where m is the number of cycles and $\Sigma \ddot{x}_i/\ddot{x}_{i-1}$ is the sum of ratios between m consecutive amplitudes.

Thus, for the time period from 319 to 322 seconds, the average damping was obtained as follows.

$$m = 5: c/c_{crit} = \frac{1}{2\pi} \cdot \frac{1}{0{,}809} = 0{,}034$$

Previously, damping ratios between 0.036 and 0.050 have been observed. The most probable value is 0.040 ±0.005, possibly including some "ice damping", due to friction against broken fragments of ice, for instance.

6.2.2 Determination of acceleration amplitudes and phases for unit sine loads

The following instruction applies to the derivation of amplitude and phase relations.

(1) Apply unit sine loads to the FE-model

$F = 1 \cdot \sin n\omega_1 t$ with n = 1-5

(2) For each sine load determine the acceleration sine functions for steady state vibrations of modes 1, 2 and 3 individually and for all the modes vibrating together. 3 instrument levels are investigated. The response acceleration functions are defined by amplitude maxima and phase angles:

$a_{nk} = a_{nk\,max} \cdot \sin (n\omega_1 t + \varphi_{nk})$

n are load component numbers
k are mode numbers

$a_{nk\,max}$ and φ_n are thus determined for

n = 1-5 and
k = 1-3 and for Σk.

See Figure 6:3: Responses of the FE-model and its eigenmodes to unit sine loads n = 1-5.

The amplitude values $a_{n\,max}$ and phase angles φ_n for the common response of all the modes are listed in Table 6:1.

Sine load No n	Acceleration amplitude per 1 MN load amplitude (m/s^2)	Phase angle φ_n (radians)
1	4.30	1.511
2	1.04	6.261
3	0.57	3.318
4	0.13	3.274
5	0.07	3.419

Table 6:1

Responses to unit sine loads: Acceleration amplitudes and phase angles in node No. 14. Responses of all the nodes k = 1-3 taken together.

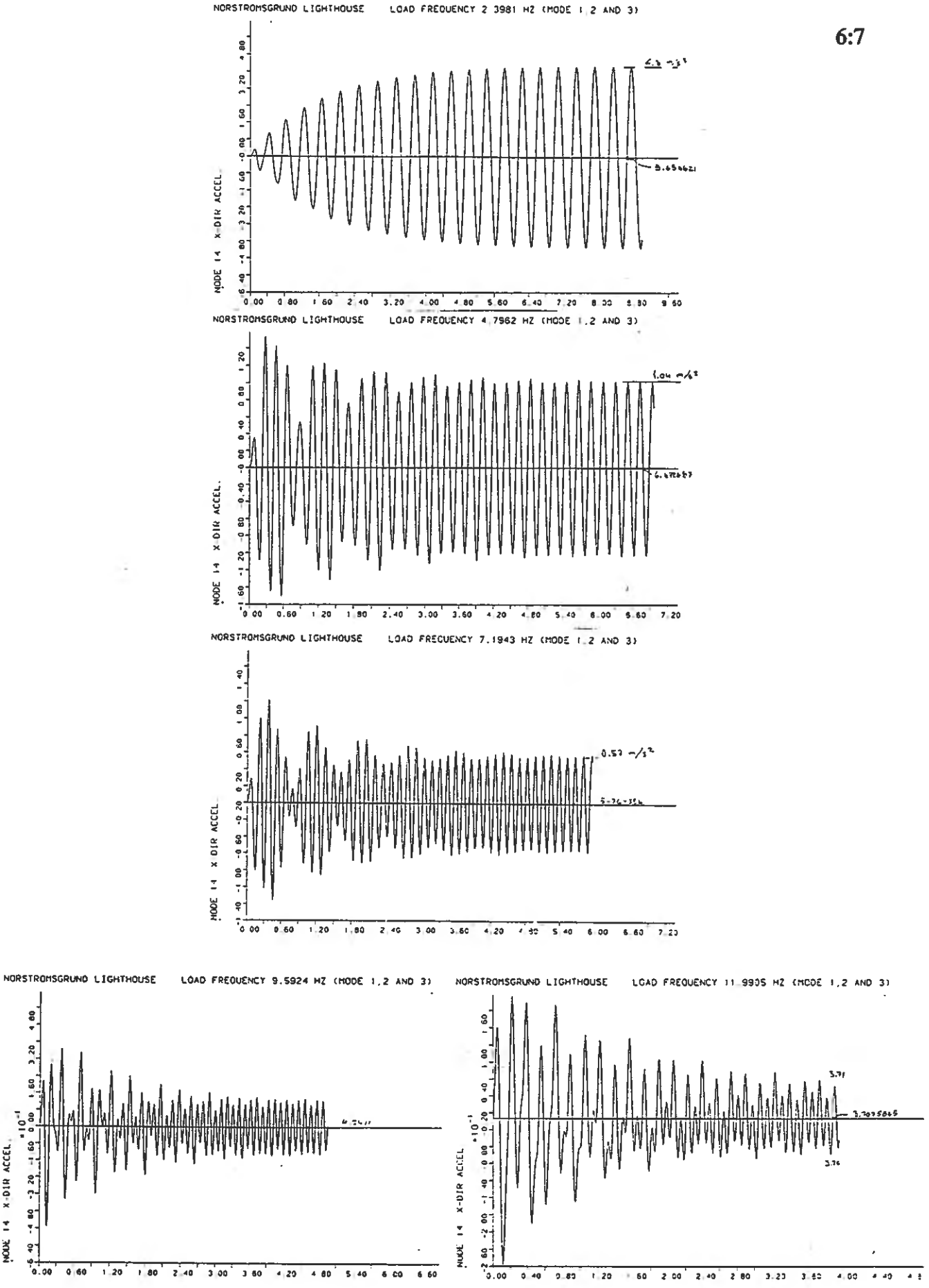

Figure 6:3

Responses of the FE-model to unit sine loads n = 1-5

6.2.3 Transformation of acceleration records to ice force time-histories

Based on an acceleration record from March 28, 1988 (File No. N83S-M051) the transformation procedure is here described step by step and illustrated by plotted outputs from the computer calculations.

(1) Input acceleration record

In Figure 6:4 the selected accelerometer signal No. 1 (Direction N-S) at level +39.5 (Model Node 14) is displayed together with its Power Density Spectrum.

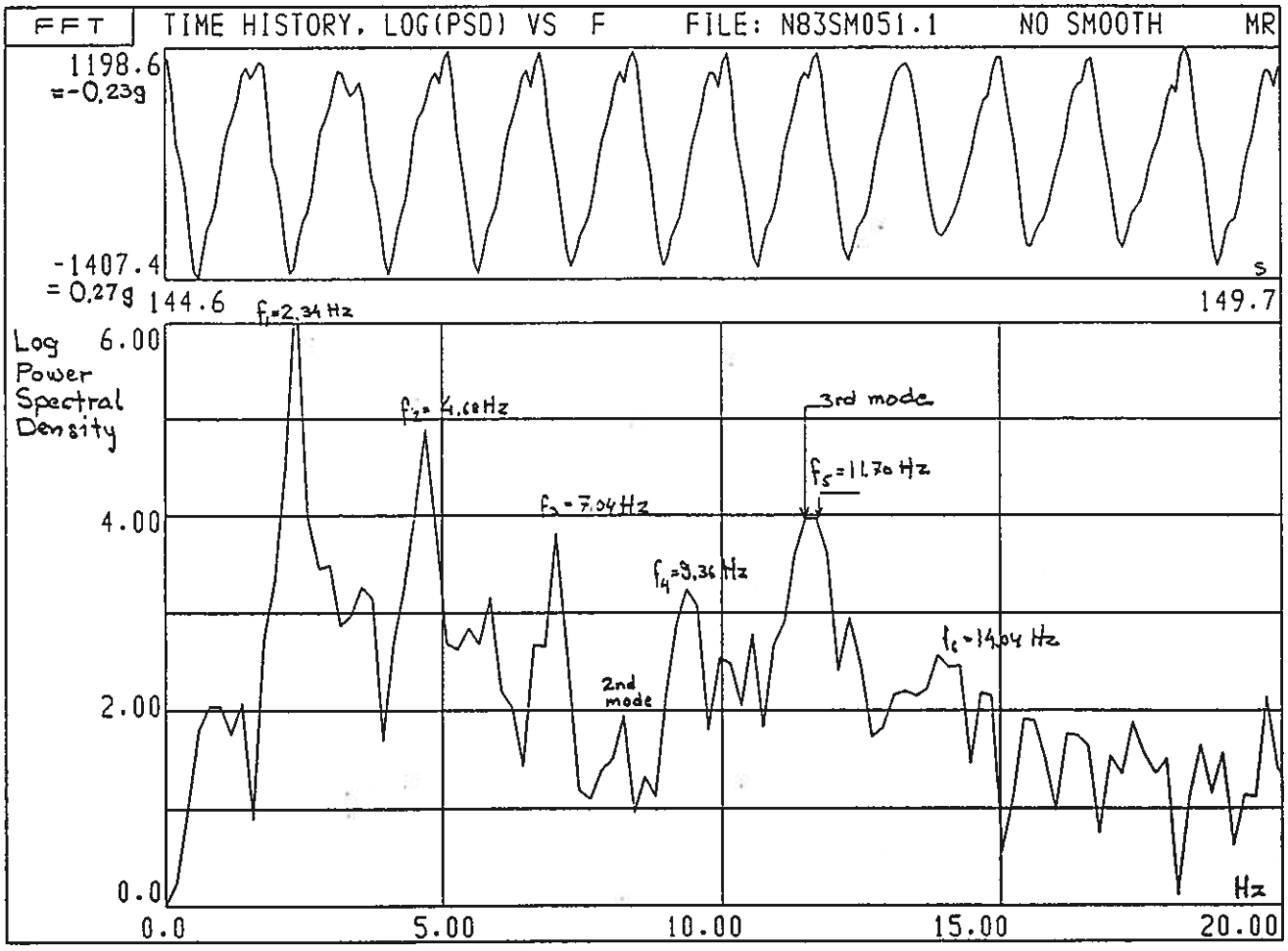

Figure 6:4

(2) Filtered acceleration signals

As illustrated in the logaritmic Power Density Spectrum (Figure 6:4), the vibration amplitudes are very much concentrated around the peaks representing the fundamental frequency and its multiples. Since the aim of the study is to define a generalized ice force time-history for resonance vibrations, the very small vibrations within the intermediate frequency ranges can be neglected which is also a condition for the validity of the transformation model.

Therefore, the first step of the signal processing is to filter the signals as illustrated in Figure 6:5. This can be done without any significant loss of vibration energy and it results in a "smoothed" accelerogram, composed of essentially sinusoidal components with frequencies corresponding to the fundamental eigenfrequency and its multiples (n = 1-6).

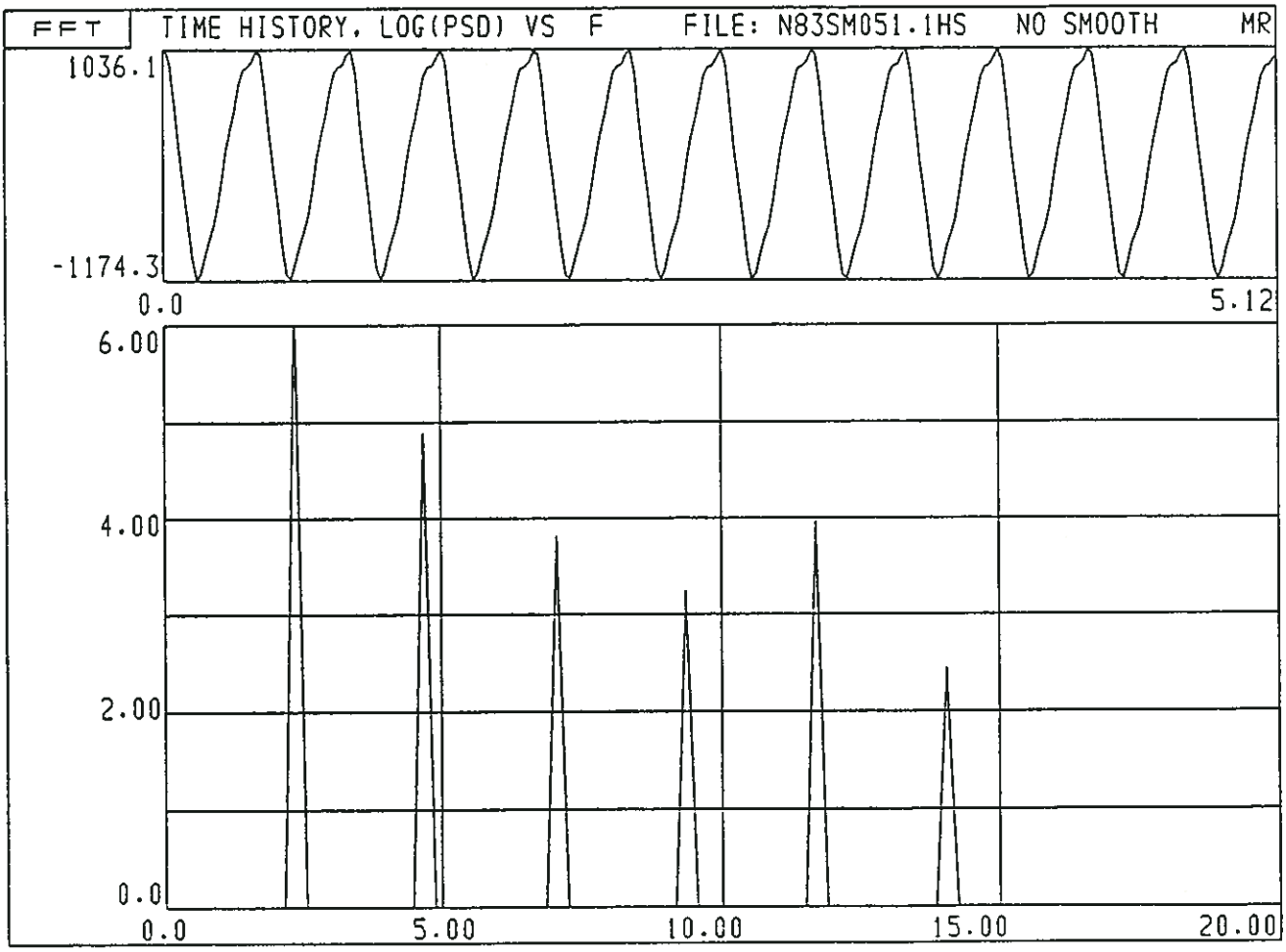

Figure 6:5

(3) Disintegration of the acceleration signals

The various components of the filtered signal shown in Figure 6:5 are displayed together with their Power Density Spectra in Figures 6:6 and 6:7. The lower frequency signals are very regular and sinusoidal, whereas the higher frequency signals are slightly irregular, depending partly on the limited resolution of the measurement frequency (50 Hz), However, without any significant loss of accuracy the various components can be treated as sine components in the transformation process:

$$\ddot{x}_n = \ddot{x}_{n\,max} \cdot \sin(\omega_n t + \phi_n)$$

The amplitudes $\ddot{x}_{n\,max}$ are given in "signal units" which are to be multiplied by -0.00191 (for Signal 1) to obtain the acceleration value in m/s^2 (+0.00191 for Signal 2).

The amplitudes and phase angles are as follows:

n	ϕ_n (rad.)	$\ddot{x}_{n\,max}$ (m/s^2)
1	2.0647	-1.960
2	0.6283	-0.3316
3	5.7002	-0.0966
4	1.2566	-0.0491
5	0	-0.1150
6	0.4485	-0.0199

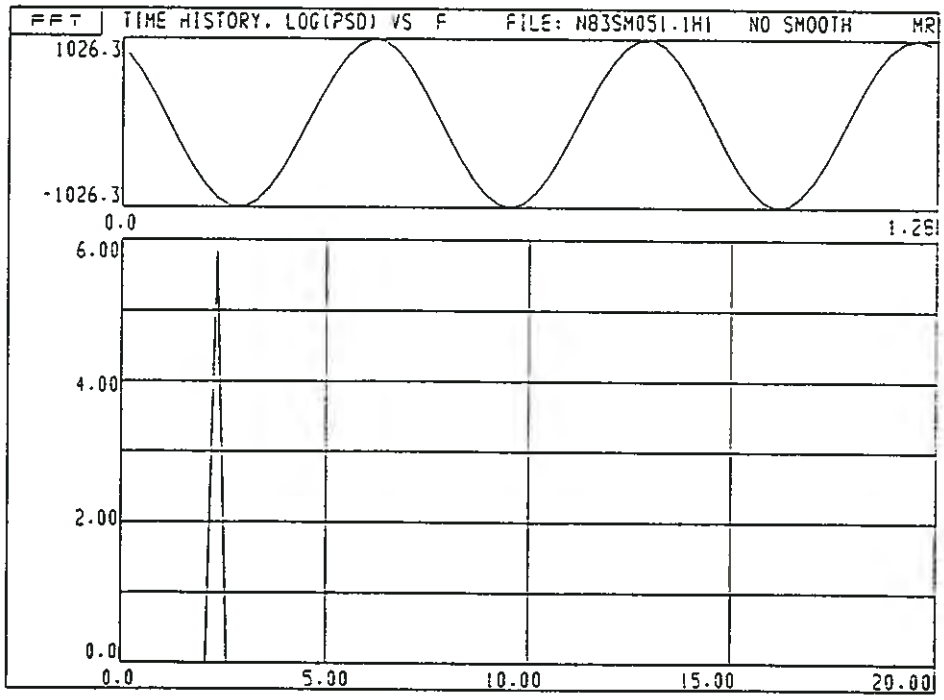

Figure 6:6

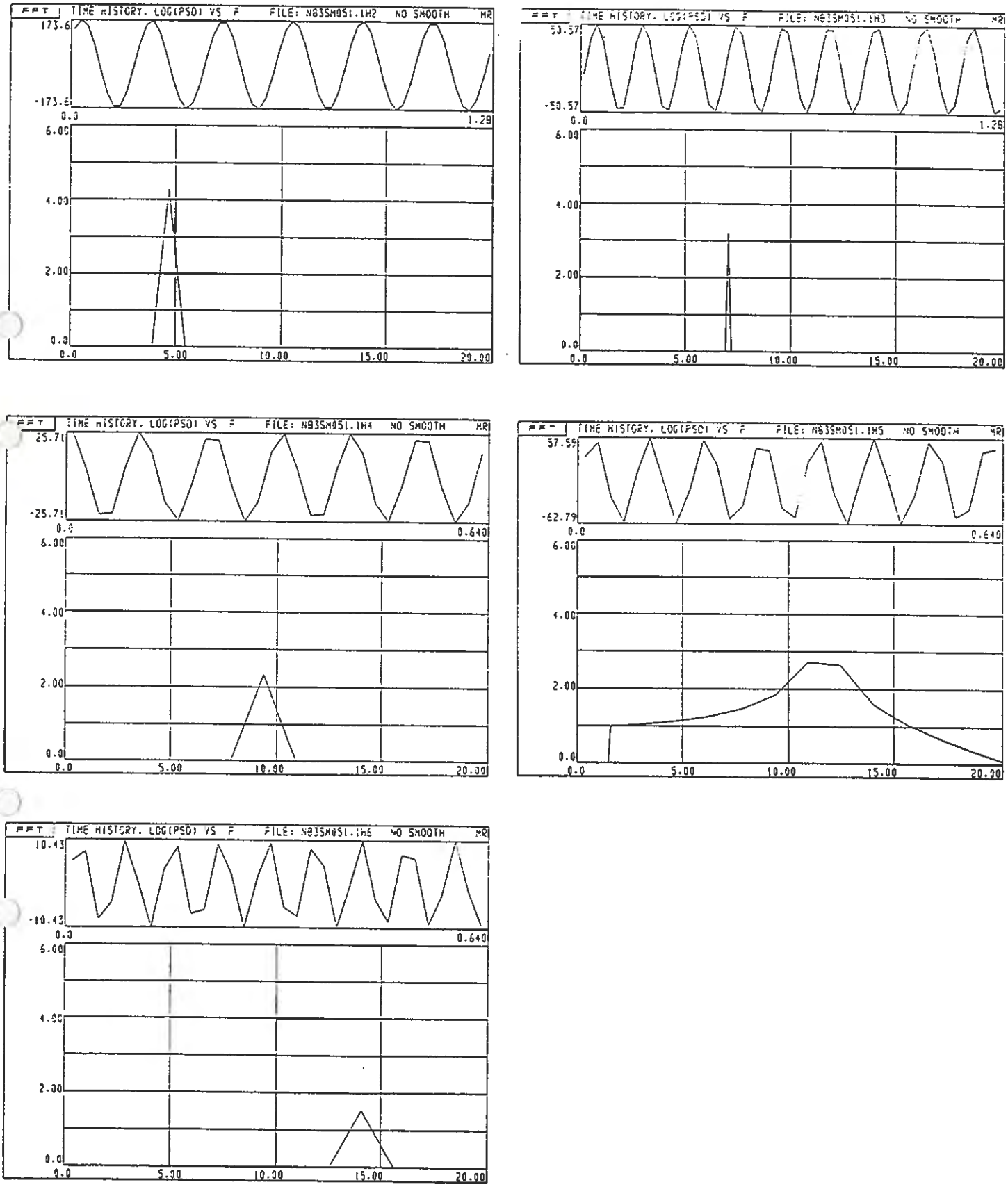
FFT TIME HISTORY. LOG(PSD) VS F FILE: N83SM05I.1H2 NO SMOOTH MR
173.6
-173.6
0.0
1.28
6.00
4.00
2.00
0.0
0.0
5.00
10.00
15.00
20.00
FFT TIME HISTORY. LOG(PSD) VS F FILE: N83SM05I.1H3 NO SMOOTH MR
50.57
-50.57
0.0
1.28
6.00
4.00
2.00
0.0
0.0
5.00
10.00
15.00
20.00
FFT TIME HISTORY. LOG(PSD) VS F FILE: N83SM05I.1H4 NO SMOOTH MR
25.71
-25.71
0.0
0.640
6.00
4.00
2.00
0.0
0.0
5.00
10.00
15.00
20.00
FFT TIME HISTORY. LOG(PSD) VS F FILE: N83SM05I.1H5 NO SMOOTH MR
57.59
-62.79
0.0
0.640
6.00
4.00
2.00
0.0
0.0
5.00
10.00
15.00
20.00
FFT TIME HISTORY. LOG(PSD) VS F FILE: N83SM05I.1H6 NO SMOOTH MR
10.43
-10.43
0.0
0.640
6.00
4.00
2.00
0.0
0.0
5.00
10.00
15.00
20.00

Figure 6:7

(4) Transformation of acceleration signals to ice force components

The ice force components

$$F_n = F_{n\,max} \cdot \sin(n\omega_1 t + \Theta_n)$$

are obtained from the acceleration functions derived under point (3) and the unit force response relations dealt with in Subsection 6.2.2 which give the following expressions for the amplitude and phase angle of each ice force component

$$\Theta_n = \phi_n - \varphi_n$$

$$F_{n\,max} = -\ddot{x}_{n\,max}/a_{n\,max}$$

The resulting ice force components for n = 1-3 are displayed in Figure 6:8

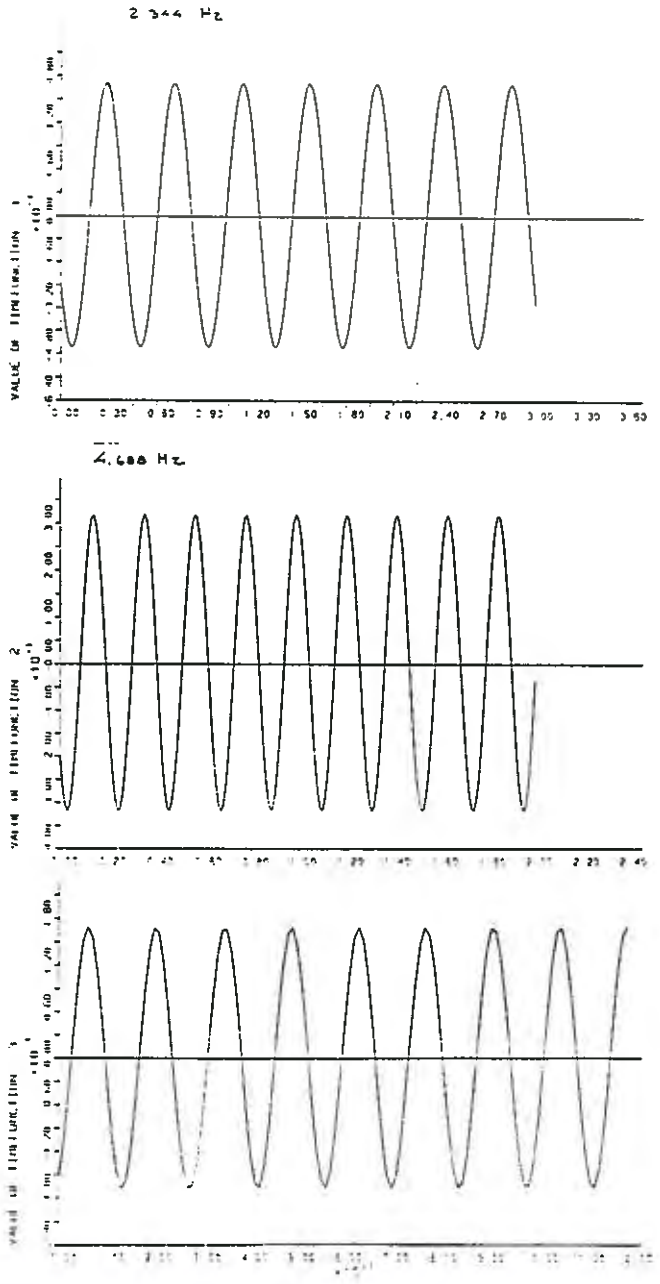

Figure 6:8

(5) Superposition of ice force sine components in Direction 1

The amplitudes and phase angles obtained by transformation of acceleration signals are as follows:

n	$F_{n\,max}$ (MN)	Θ_n (rad.)
1	-0.456	0.553
2	-0.319	0.650
3	-0.169	2.382
4	(-0.10)	4.266
5	(-0.10)	2.864

Negative amplitudes only indicate the direction of the ice force in the selected coordinate system. The sign is neglected in the graphs below. The amplitudes of the components 4-6 could only be roughly estimated due to a considerable uncertainty as regards the shape of the 3rd mode of vibration near to the measurement level.

The resulting sums of the ice force components
n = 1-3 and n = 1-5, respectively, are displayed in Figure 6:9. It appears, that the contributions of the 4th and 5th components still tend to be affected by a considerable uncertainty. At present, it is preferred only to rely on the components n = 1-3 to represent the "dynamic" part of the ice force time-history.

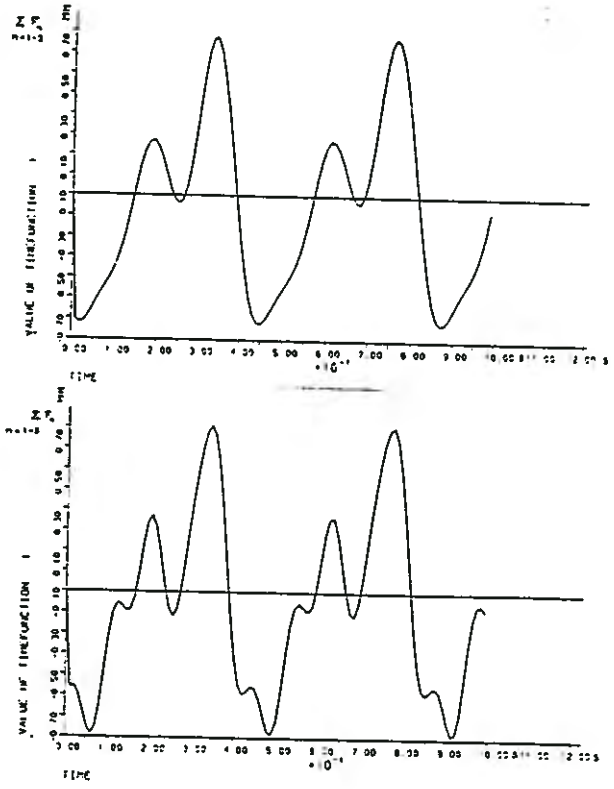

Figure 6:9

(6) Superposition of static and dynamic as well as directional components

The "dynamic" ice force time history in Direction 1 is to be added to the "low-frequency" or "static" ice force component, determined by inclinometer measurements as described in Section 4.

$$F(t) = F_o(t) + \Sigma F_{n\,max} \cdot \sin(n\omega_1 t + \Theta_n)$$

For the sequence studied the "static" ice force was almost constant: F_o = 1.98 MN.

Finally, the time-history of the resultant global ice force can be obtained by vector summation of the directional components at discrete points of time. Thus, the resultant of the components along Direction 1 and 2 for the selected sequence has been computed. The time-history is displayed in Figure 6:10. However, since the direction of the resultant varies, the unidirectional components along Direction 1 and 2 are preferred as a basis for generalization of ice load components.

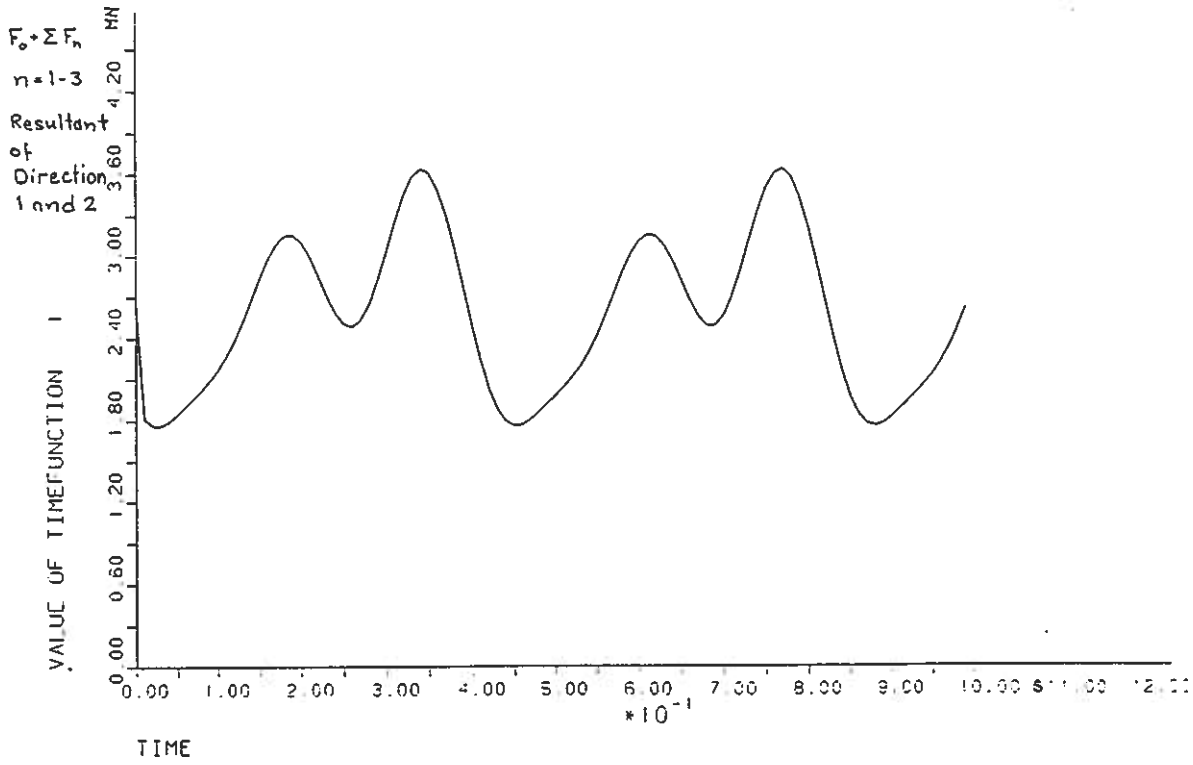

Figure 6:10

7. GLOBAL RESPONSE DATA

As mentioned in the introduction no additional ice force data could be acquired during the period 1990-94 due to the unusual persistence of the series of mild winters and the gradual falling off of the operability of the ice force sensing panel system. In accordance with the project plan, global ice force measurements were to be carried out only in combination with local ice force measurements, in order to concentrate the budget means on such coordinated measurements. Therefore, no efforts have been made to sample global data even during the present winter, although the ice conditions may have offered such opportunities at last.

However, our somewhat revised judgement is that, as regards the global ice force measurements, it is the quality of the data and not the quantity that is important. This is because we have found that the dynamic ice structure interaction can be modelled in a deterministic way. The need of data for probabilistic evaluation is not as strong as was presumed, when the Phase 1 program was outlined.

Therefore, in the work with refinement of the global ice force characterization, we have continued to use the same selection of data as was used in the Phase 1 study. This is a selection of the best data as regards fully developed resonance vibration of the structure, accuracy of acceleration as well as "static" deflection measurements and simultaneous observations of ice conditions. On the basis of these data a generalized ice force function has been derived as expressed in the preceding chapter. The function is anchored in the "static" ice force component which is in turn anchored in the "time-averaged effective ice pressure" as explained in Chapter 9. The latter parameter may, of course, be determined based on a probabilistic approach, since it is related to ice strength and ice thickness, etc.

8. LOCAL ICE FORCE DATA

As mentioned in Chapter 2 the aim of the program for sampling local ice pressure data by means of the panel system was to study the ice pressure distribution in space and time and to correlate time-histories of local pressure with those of global forces. In particular, the intention was to test the hypothesis presented as a result of the Phase 1 study, that this space-and-time distribution of the contact pressure is the prime explanation of the resonance phenomenon as well as, relating to the same mechanism, of the size dependence of observed "effective" ice pressures.

Since no data could be sampled after 1989, the only available basis for progress in the intended direction is the data collection from the March-April 1989, presented in HSVA's Report No 201/90 from March 1990 [Ref 3]. A considerable amount records of ice forces on the three panels was sampled during the period March 24 until April 20. The ice conditions had been investigated as late as on the 23rd of March, when the ice was already moving.

Unfortunately, the ice conditions were such, during the whole measurement period, that fully developed resonance vibrations did not occur. Furthermore, since springtime conditions were prevailing the ice was rather porous already in the beginning of the period and the ice conditions changed fairly much during the period. Therefore, the character of the ice force records is much more heterogeneous and diffuse than could be expected on the basis of experience from previously sampled global ice force records from periods of more homogenous conditions.

However, even this observation has a certain value and may be regarded as another manifestation of the randomness of the ice pressure.

Examples of records from 1989 are shown in Figures 8:1 - 8:3. The records shown in Figures 8:1 and 8:2 are typical for the most common situations when the ice is indented by a structure which does not move periodically. As pointed out in HSVA's report, the independence in time of the peak forces on the three panels is obvious.

However, although most of the records have this character and there are no records of typical resonance character, the records shown in Figure 8:3 indicate a tendency of resonance ice-structure interaction during a few seconds, with a predominant frequency around 2.3 Hz which is that of the fundamental mode of the lighthouse. In these records the peak forces on the two most affected panels are also more correlated in time than in other records, although the correlation only indicates a slight resonance.

Other conclusions can probably be drawn from this collection of local ice force records, but as regards the main objective of the present study,

we can only conclude that the indications mentioned above provide some additional support to the hypothesis regarding the space-and-time distribution of the ice pressure and its importance to the explanation of resonance and other phenomena. However, more data must be sampled, before any definite conclusions can be drawn.

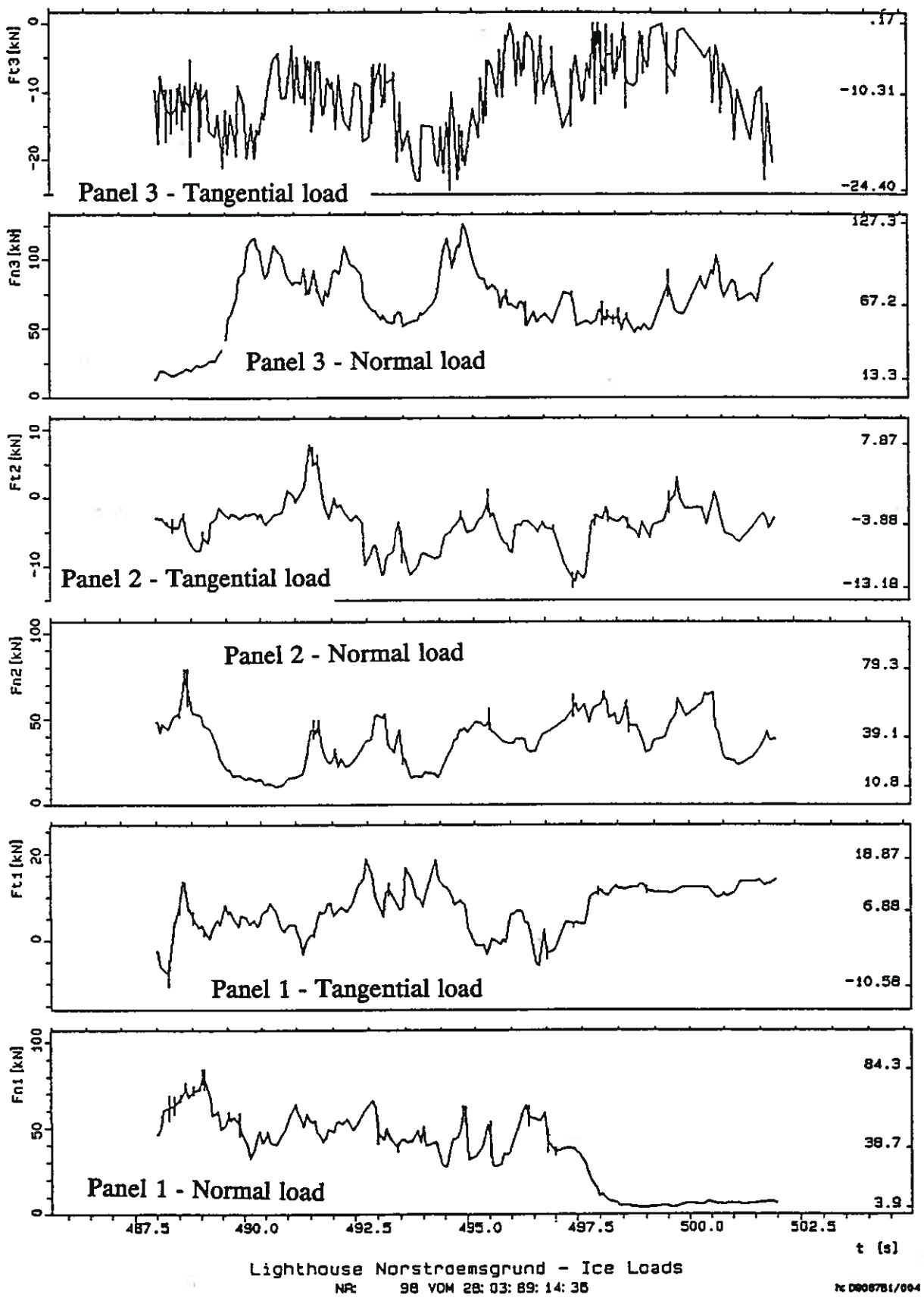

Figure 8:1
Ice force sensing panel records from March 28, 1989.

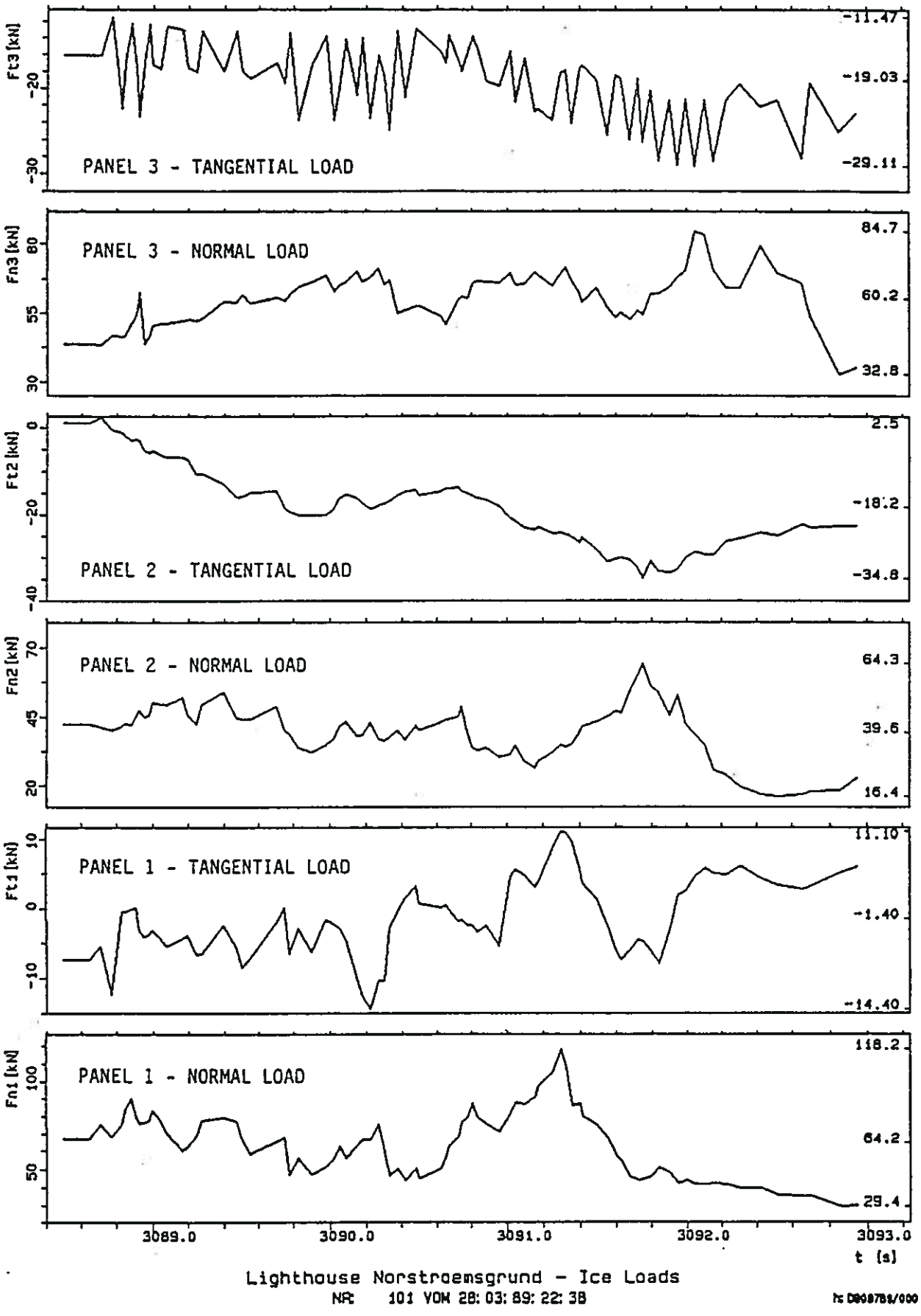

Figure 8:2
Ice force sensing panel records from March 28, 1989.

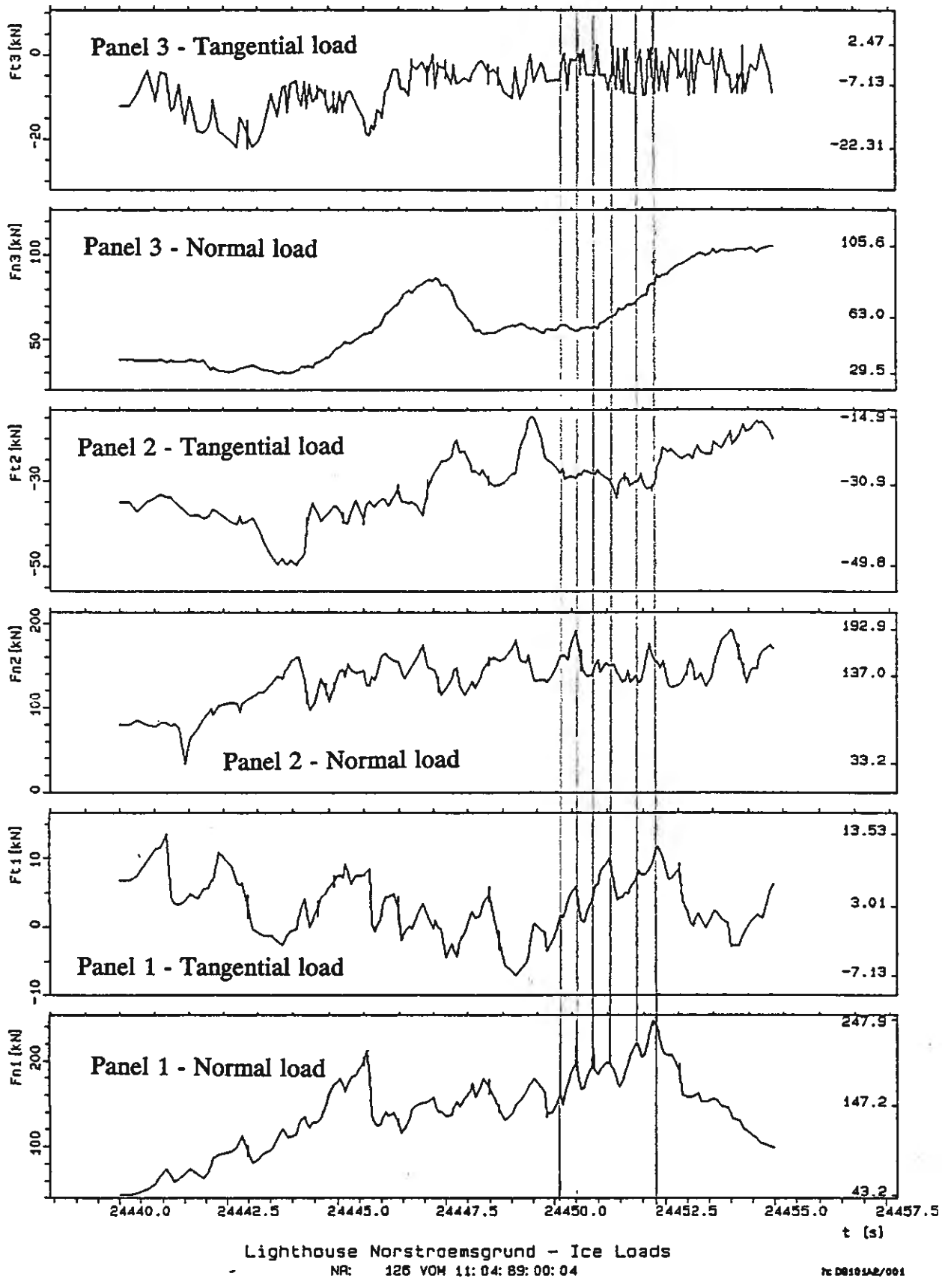

Figure 8:3
Ice force sensing panel records from April 4, 1989 with resonance features during a few seconds

9. AN IMPROVED MODEL FOR CHARACTERIZATION OF ICE FORCES ON OFFSHORE STRUCTURES

9.1 The generalized dynamic ice force function

Based on the results of the analysis described in Section 6 the previously suggested generalized ice force formula can now be adjusted, Thus, the improved accuracy of the process for transformation of response data is taken advantage of, resulting in a reduced uncertainty as regards the amplitudes of the dynamic components as well as the shape of the ice force time function.

Basically, the global ice force is still expressed by means of one "static" and a number of "dynamic" components:

$$F = F_o + \Sigma F_{n\,max} \cdot \sin (n\omega_1 t + \Theta_n)$$

As in the previous studies the amplitudes of the sine components can be normalized to the "static" or mean load which can then in turn be related to ice strength characteristics etc. The adjusted amplitude ratios and phase angles are:

n	$F_{n\,max}/F_o$	Θ_n (rad)
1	0.23	0.55
2	0.16	0,65
3	0.09	2.38
4	(0.05)	4.26
5	(0.05)	2.84

For most purposes it is likely to be sufficient to use only the three sine components n = 1-3. The resulting generalized ice force time-history is displayed in Figure 9:1. However, in the case that structures and equipment are sensitive to resonance at higher frequencies, load components with frequencies higher than 3 times the fundamental frequency should also be included as indicated in Chapter 6, in which case the increasing uncertainty as regards the amplitude values should be observed and accounted for by correspondingly increased safety factors.

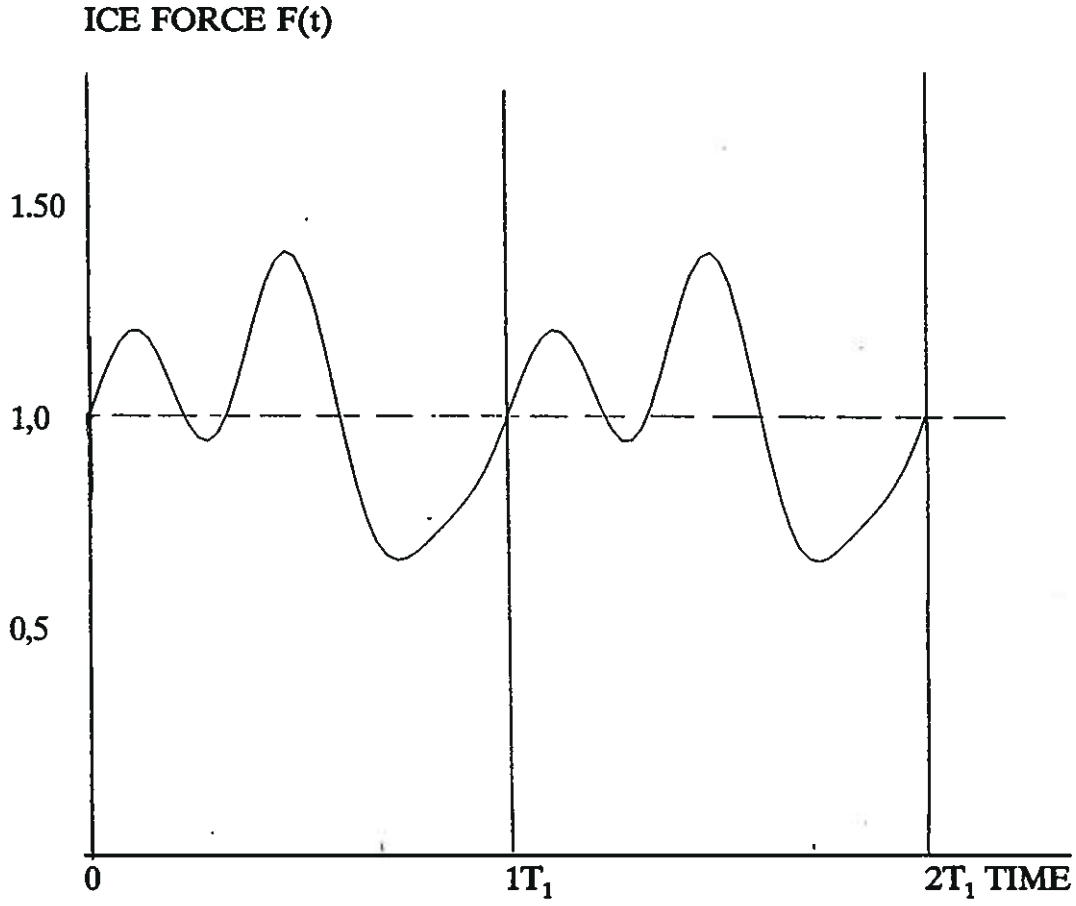

Figure 9:1

Generalized ice force time-history normalized to unit static ice force $F_o = 1$. T_1 is the predominant period of the natural vibrations of the structure with respect to displacement at the ice level. Fourier components n = 1, 2 and 3 are included

9.2 Calculated response of the Norströmsgrund lighthouse to the generalized dynamic ice load

The acceleration response of the Norströmsgrund lighthouse model at the accelerometer level (node 14) to the derived dynamic ice force (n = 1-3) was calculated in order to demonstrate the suggested response calculation procedure and also to check the appropriateness of the procedure for deriving the ice load by going backwards from load to response.

Thus, the dynamic load time-history shown in Figure 6:9 (n = 1-3) was applied as a load input to the FE model, the acceleration response of which was computed in accordance with the SOLVIA code. The computed acceleration time-history of node 14 is displayed in Figure 9:2. This time-history may be compared with the recorded accelerogram

displayed in Figure 6:4. The values of the calculated acceleration amplitudes stabilize at about 0.22 g which is well in agreement with the average of the measured acceleration amplitudes. As expected, there are some peaks, even up to 0.27 g, in the record. Allowance for such occasional effects can be made within the frame of the safety-factoring of the design load.

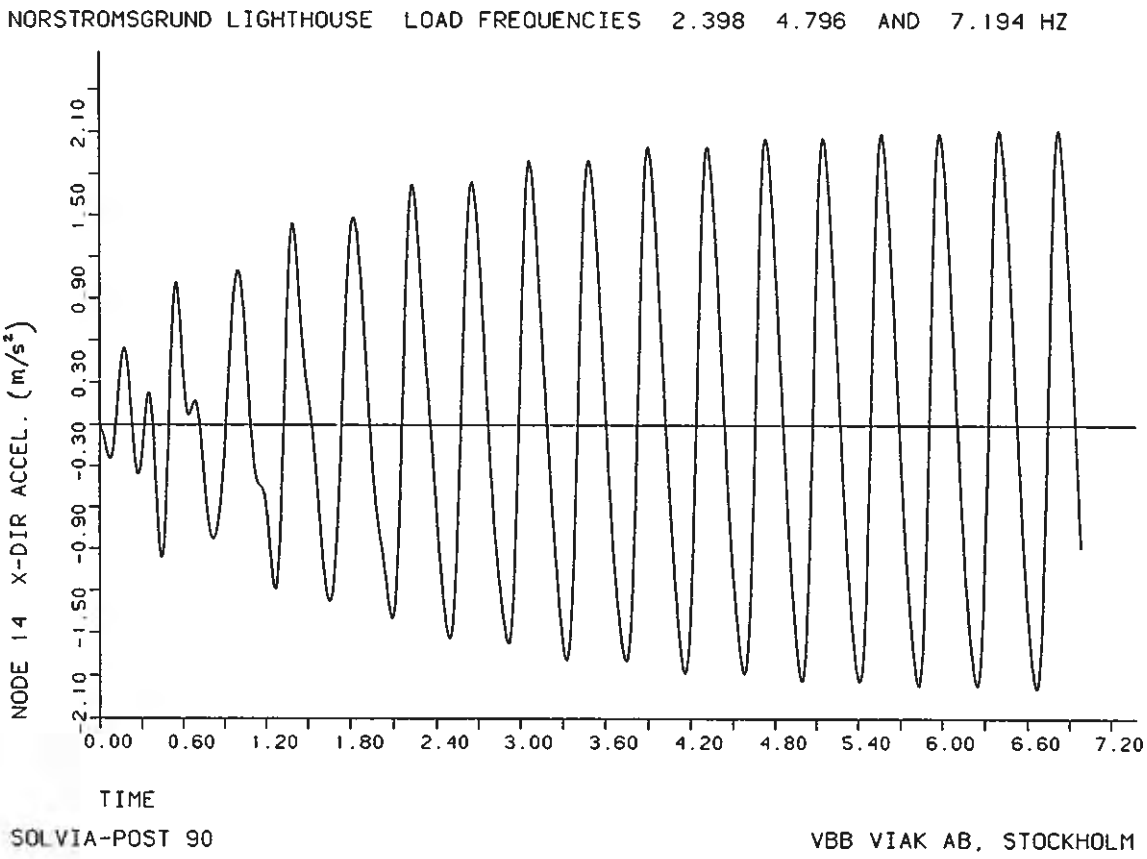

Figure 9:2

Computed acceleration response of the lighthouse model when subjected to the load time-history derived based on the measured response of the lighthouse.

9.3 Quantification of the ice force function based on ice parameters

The anchor parameter for the generalized dynamic ice force function is the "static" ice force component F_o which is obtained by averageing the fluctuating ice force during a time period of sufficient length not to give rise to any dynamic response of the affected structure.

This average force may also be written as the product between the "effective ice pressure" and the "gross contact area":

$$F_o = p_{eff} \cdot A_g$$

Since the net contact area could hardly be quantified in generalized terms, it is the "effective pressure over the gross area" that has to be related to the specific ice conditions, for which the ice force is to be predicted. Then, by analogy with the definition of the static ice force F_o, the effective ice pressure should be defined as the mean ice pressure over the gross contact area, averaged during a time period of sufficient length to obtain a smooth time-history, not affected by the fluctuations caused by local pressure increase followed by brittle failure. In mathematical terms this component of the pressure may also be expressed by one or several of those low-frequency Fourier-components of the load which have lower frequencies than the components reflecting the fluctuations associated with local ice failures.

This "time-averaged effective ice pressure" can be related to the various ice strength parameters, the size of the contact area, the ice thickness, etc. as described in Chapter 2.

From the observations of ice forces acting on the ice force sensing panels, as summarized in Chapter 8, we can draw the conclusion, that the effective ice pressure, defined as above, will be less sensitive to the geometry of the contact area than peak pressures. By superposition of simultaneous time-histories from two or three panels we can see, that the peak values of the effective pressure vary considerably with the size of the total contact area.

Considering the mechanism of more or less random local failures over the cross contact area, this is what can be expected, but little attention has been paid to this condition when observations and derivations of ice forces have been discussed in literature.

In summary, the work during Phase 2 of the study has resulted in a refined model for characterization of ice force time-histories as well as improved understanding of the coupling between the load characteristics and the failure mechanism of the ice. This has been achieved mainly by an extended analysis of data from Phase 1, since the extreme series of mild winters in Northern Europe has precluded sampling of additional data.

REFERENCES

1. A. Engelbrektson:
An ice-structure interaction model based on observations in the Gulf of Bothnia.
Report to POAC 89.

2. E. Wessels, P. Jochmann, L. Hoffmann:
First results of ice force measurements with TIP-panels at Norströmsgrund lighthouse. Report to POAC 89

3. J. Schwartz, E. Wessels: Ice force measurements with TIP-panels at Norströmsgrund Lighthouse in Winter 1988/89.
HSVA-Report No. 201/90. March 1990.

VBB VIAK

APPENDIX 1

ICE FORCE STUDIES IN THE BOTHNIAN BAY Phase 2

DATA ACQUISITION SYSTEMS

DATA ACQUISITION SYSTEMS

1. Overview

The following instrument systems were developed and tested during Phase 1:

Instruments	Measured quantities	Derived quantities
Accelerometer system	Accelerations over the whole frequency range of interest	Dynamic ice forces (poor resolution for low-frequency accelerations)
Inclinometer system	Accelerations, (focused on low-frequencies)	Tilt angles and low-frequency ("static") ice forces
Pendulum system	Differential displacement between pendulum mass and refe-rence point of lighthouse	Inclination and lateral displacements of the structure. Static and dynamic ice forces.

In principle, each system has a potential for measuring all the parameters needed for evaluating static and dynamic ice forces. There are, however, limitations which are basically associated with the problem of measuring static or nearly static and dynamic deflections at the same time and then separating the effects. This calls for a certain diversification in setting the measuring range, the resolution and the triggering levels for each system. After the introduction of the Fourier transformation technique for the processing of response data, it became evident that the inclinometer records had to be used for the low-frequency components of the responses. Since these records did not cover all the larger amplitudes of high-frequency accelerations, the accelerometer records had to be used for the high-frequency components of the accelerations.

In addition to the response measurement systems the instrumentation includes video camera systems and monitoring systems.

In the summer 1987 three ice force measurement panels were also installed on NORSTRÖMSGRUND. This system is described separately.

5.2 Accelerometer and inclinometer systems

As indicated above there is no distinct difference between the functions of the so called accelerometers and inclinometers and moreover, the pendulum system has a typical inclinometer function. However, we hope that a strict application of the nomenclature introduced above will prevent confusion.

The instruments are both operating as inertial instruments. (See Figure A1:1) An eccentrically supported mass exerts a torsional moment around the supporting axis and this moment is taken as a measurement of the inertia force and thus the acceleration of the instrument. If the instrument is tilted, the corresponding fraction of gravity force affects the mass and is consequently superimposed on the inertia force due to horizontal acceleration, if any. The most important difference between the instruments in the actual application is that the "inclinometers" (Manufacturer's nomenclature) can measure the tilt angle with a resolution of 0.5×10^{-6} radians as a minimum.

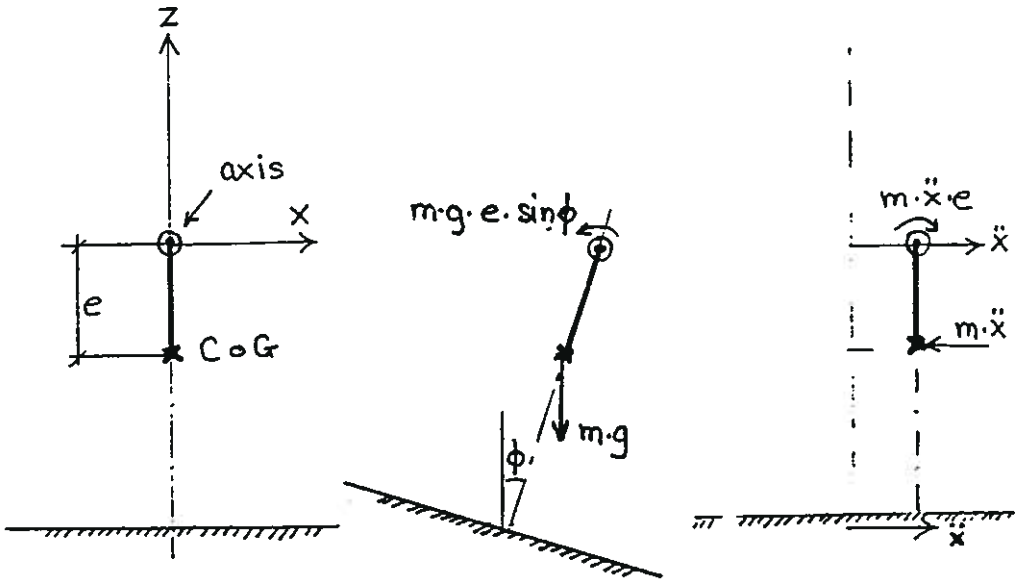

Figure A1:1

The moment turning around the instrument axis is $M = m \cdot e \cdot (\ddot{x} - g \sin\phi)$ where $\ddot{x}$ is the horizontal acceleration of the axis and $g \cdot \sin\phi$ is the gravity component as a function of the tilt angle.

The manufacturer's description of the instruments are attached to this appendix.

The normal data collection frequency is 50 readings per second.

Two of the accelerometers have been in operation on NORSTRÖMSGRUND since 1972. Whereas the signals were previously recorded in analogous form they are now digitized directly, which eliminates low-frequency disturbances.

The new data processing system was installed on NORSTRÖMSGRUND in the beginning of March 1986.

At each measurement point the acceleration components are measured in two orthogonal directions.

Descriptions of the entire accelerometer systems including manufacturer's specifications are given at the end of this section.

The pendulum system (Figure A1:2) was tested during springtime 1986 and the following observations and experiences were made during these tests.

The pendulum mass consists of two iron discs (10 kg each) separated by an adjustable rod. The mass was suspended from a slab in the lighthouse superstructure by a piano wire of 7.58 m length giving a natural period of about 5.5 seconds. To reduce effects of air flow disturbances on the wire it was run through a steel tube.

The position of the pendulum was measured by a two dimensional optical system which allowed a touchless measurement of the position in a plane.

The position measurement device was composed of a bar code reader and a bar pattern which was engraved on a plate attached underneath the pendulum. The resolution of the system was about 0.2 mm and maximum measurement range 5 cm.

The pendulum system was developed and tested in parallel with the installation and testing of the inclinometer system. Since the latter proved to perform satisfactorily, no further efforts were made with the development of the less mature pendulum system.

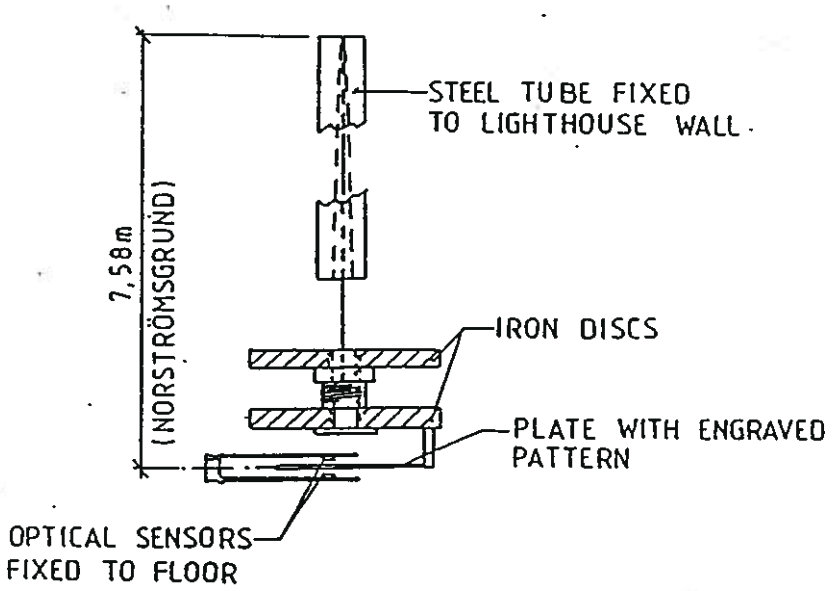

Figure A1:2

The pendulum system

3. Video camera system

Three video cameras were installed during Phase 1 on the superstructures of each of the lighthouses NORSTRÖMSGRUND and FARSTUGRUND. In 1992 the cameras on the latter lighthouse were moved to NORSTRÖMSGRUND.

The cameras are enclosed in protecting casings which are heated to keep the front glasses free from condensation. The cameras are provided with automatical iris adjustment devices, to make them adapt to different light conditions. They are not sensitive enough, however, to give good quality pictures during nighttime, so additional spotlights are arranged to improve the ordinary floodlights from the lighthouses.

The cameras are of mark KOYO with high sensitivity new-vicon tube 8 mm optics with F1.4 2/3" aperture. They are permanently connected to the power supply of the lighthouse.

A switching device connects the cameras sequentially to Video Cassette Recorders (VCR).

The switching device is synchronized with the accelerometer and inclinometer system, whereby the pictures can be correlated to the vibration measurements with a timing accuracy of 20 ms.

Absolute date and time information is also recorded on the audio channel to the VCR.

The VCR is a Panasonic G10 with a modified remote control unit connected to the accelerometer system which controls the start and stop of the recording.

4. Remote monitoring

Remote control and monitoring is arranged between the lighthouse and a Central Monitor in Norrköping (CMN). Communication is established via a radiolink path to Luleå Pilot Station and then to the CMN over dialled-up telephone connections. The pilot station is provided with an automatic dialling equipment which dials the CMN in case of an alarm condition on the lighthouses. At present the remote control equipment is capable of transferring 7 maneuvres to the lighthouse and 14 indications from it. A number of these indications and maneuvres are already used for the operation of the lighthouse. One maneuvre is, however, used to start the accelerometer recording system and one indication is used to indicate the proper functioning of that maneuvre. When the accelerometer system starts recording, this indication is also sent to the CMN as an alarm to alert the personnel that there are indications of ice movements. The control personnel at the CMN are instructed to relay this information to people concerned so that proper actions can be taken.

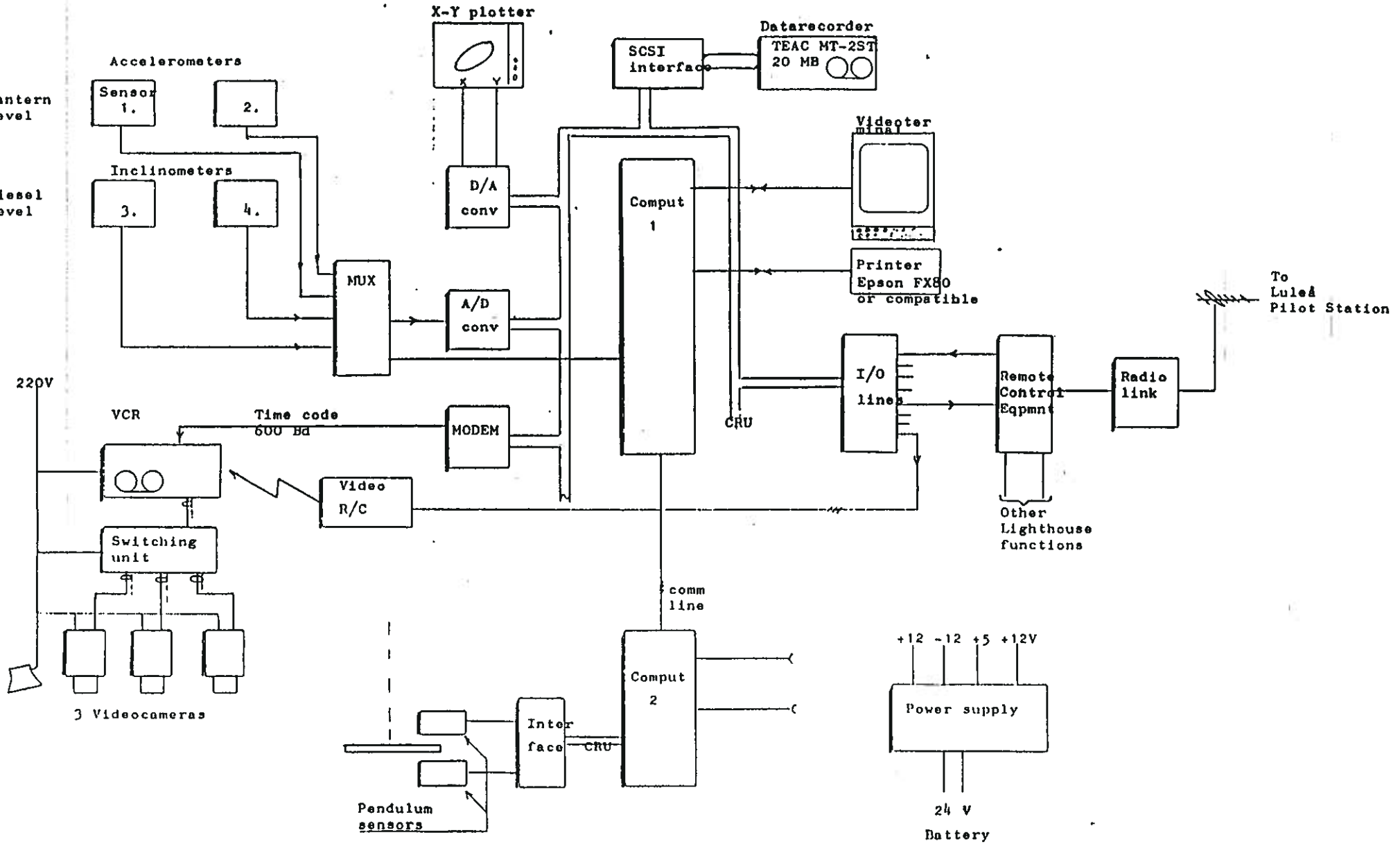

APPENDIX 1:6

Block schematic
Ice Force Measurement Arrangement at
Norströmo Grund

LINEAR AND ANGULAR SERVO ACCELEROMETERS

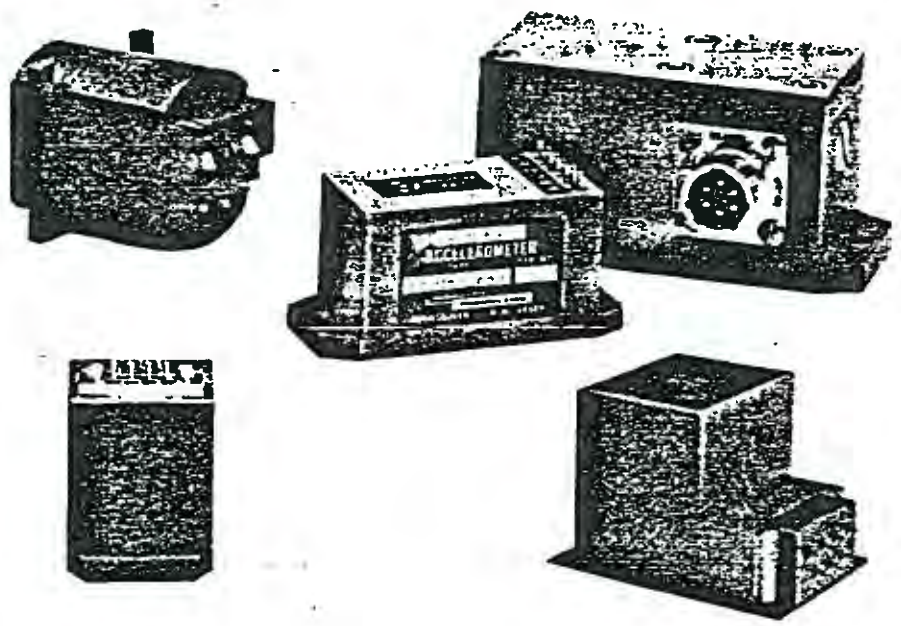

- DC Input — DC Output
- Small Size — Light Weight
- Electrical Self-test Feature
- High Reliability
- TSO Qualified Units
- MIL Qualified Units

Schaevitz servo accelerometers are DC-operated closed-loop force balance transducers for the measurement of acceleration. They are more stable and accurate than open-loop accelerometers by several orders of magnitude. Undesirable characteristics inherent in open-loop accelerometers such as sensitivity to supply voltage, non-linearity in the acceleration-to-position pickoff, and high thermal coefficients of scale factor and zero shift are negligible in closed-loop force balance accelerometers.

Typical applications of Schaevitz servo accelerometers are in high reliability guidance systems for missiles, torpedoes, or related military devices; stable platforms for spacecraft and shipboard requirements; monitoring and controlling deceleration in mass transit systems; and in roadbed analysis and fault detection equipment for high speed railways. Low range instruments can be used to level gun platforms, monitor the angle-of-elevation of naval guns or field artillery, and check slope and grade in earthmoving or paving operations.

Many Schaevitz servo accelerometers have been MIL-qualified for use in a broad variety of weapons systems. Schaevitz also offers servo accelerometers that have been TSO-qualified by the FAA for flight avionics. For nearly twenty years, high reliability for such critical applications has been a significant feature of Schaevitz inertial products. Depending on the application, the MTBF for Schaevitz servo accelerometers ranges between 25,000 and 100,000 hours.

In addition to the instruments offered in this catalog, Schaevitz Engineering designs and produces servo accelerometers specifically for a customer's particular application. These custom-designed units can be manufactured and tested in conformity with current military standards, utilizing the quality assurance procedures described in MIL-Q-9858A or MIL-Q-45208A.

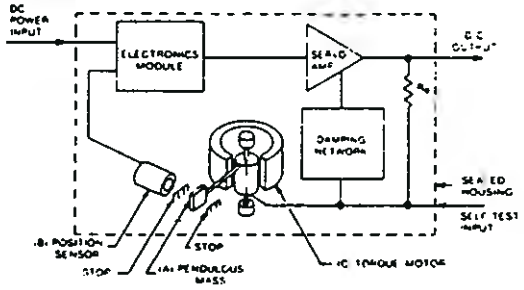

A Schaevitz servo accelerometer is a closed-loop torque balance system. In the illustration above, pendulous mass (A) develops a torque proportional to the product of its mass unbalance and the applied acceleration. Motion of mass (A) is detected by position sensor (B) whose output signal is applied to an electronic amplifier. The output current from the servo amplifier is applied to torque motor (C), which then develops a torque exactly equal to, but directly opposed to, the initial torque from the pendulous mass (A). Thus mass (A) stops moving, assuming a position minutely differing from its original position before acceleration. The current through the torque motor is accurately proportional to input acceleration, and when passed through a stable resistor (Ro), an accurately proportional output voltage is developed. The instrument can be checked for proper servo operation (self-test) by applying an independent current input to the torque motor. By adjusting the parameters of the servo amplifier and related electronic networks, the operating characteristics of a servo accelerometer can be changed or modified to suit a particular application. This same flexibility gives rise to a variety of optional features in some models.

SB Series

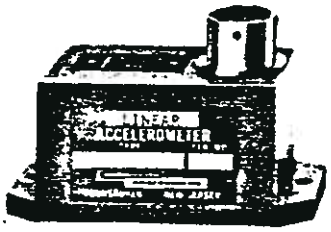

SB series accelerometers are intended for general use in the measurement of acceleration, guidance control systems, vehicle ride analysis, and a variety of other applications. A durable pivot-and-jewel sensor and miniature electronic module are integrated within a common housing, leaving space for several optional electronic circuits including telemetry output, output bias around a non-zero level, unipolar output, output limiting, bipolar output with a single supply voltage, and low impedance output. Pin or connector terminations are available.

Specifications at 20°C

LSB Linear

Range g	Nominal Natural Frequency Hz	Nominal Output Impedance kilohms
± 0.25	50	20
± 0.5	70	10
± 1.0	100	5
± 2.0	140	2.5
± 5.0	125	5
±10.0	140	2.5
±20.0	160	5
±50.0	200	5

Input Voltage	±15V DC nominal
Input Current	10 mA DC maximum (6mA DC average)
Full-Range Open-Circuit Output Voltage	±5.0V DC
Damping Ratio	0.6 typical (0.3 to 1.0 on request)
Linearity (Notes 1 & 2)	±0.05% of full scale output to 10 g, ±0.1% of full scale output over 10 g
Hysteresis (Note 2)	0.02% of full scale
Resolution (Note 2)	0.0005% of full scale
Cross-Axis Sensitivity (Note 3)	±0.002 g per g up to ±10 g range, inclusive ±0.005 g per g over ±10 g range
Bias	Less than 0.1% of full scale
Sensitive Axis to Case Alignment	±1°
Noise Output	5mV rms maximum
Operating Temperature	−55°C to +95°C
Storage Temperature	−65°C to +105°C
Thermal Coefficient of Sensitivity	0.02% per °C
Thermal Coefficient of Bias	0.002% per °C
Shock Survival	100 g — 11 ms
Weight	3 oz.
Options (Note 4)	1-g bias (or any bias) Unipolar output 28 VDC input, 0.2-4.8 VDC Telemetry output 28 VDC input, bipolar, non-isolated output Low output impedance

INCLINOMETERS DC-OPERATED GRAVITY-REFERENCED TILT SENSORS

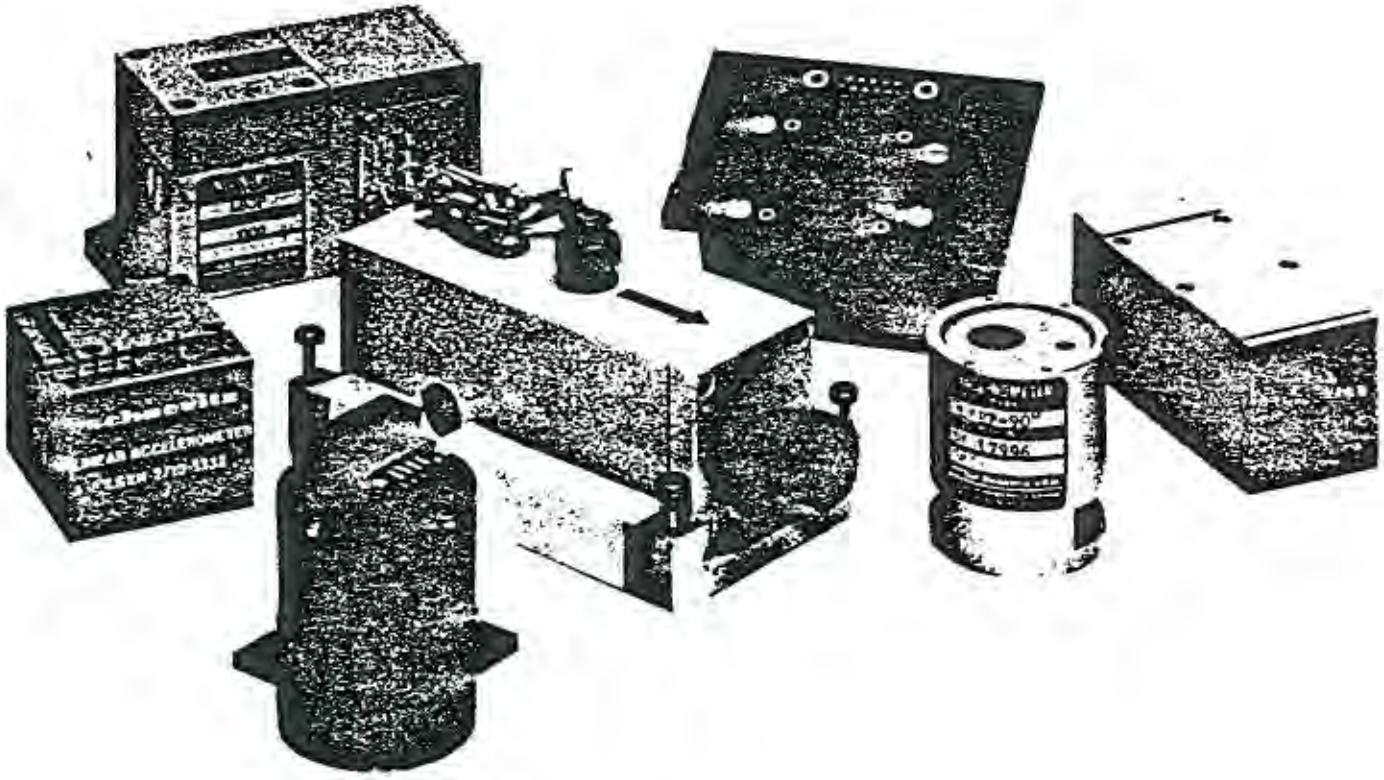

APPLICATIONS

- Borehole mapping, dam and rock shifts, and other geophysical, seismic, and civil engineering studies
- Ballast transfer systems for offshore barges, ships, and other marine applications
- Gunsight level control and calibration, weapons platforms, missile launchers
- Pipeline leveling, setting tilt of grading machines, crane overturning-moment alarms, and other heavy construction control requirements
- Large machinery installation, and other electronic level applications

FEATURES

- Units are fully self-contained. Connect to a DC power source and a readout or control device for a complete operating system
- High-level DC output signal proportional to sine of the angle of tilt from as little as ±1° full scale to ±90° full scale
- Responds to changes of slope as small as 0.000006"/ft, and changes in angle as small as 0.1 second of arc
- Hysteresis less than 0.0005% of full range output
- Vibration rectification less than 10 arc seconds/g^2

U.S. Route 130 & Union Ave., Pennsauken, New Jersey • Phone: (609) 662-8000

DESCRIPTION

The Schaevitz inclinometer is an extremely sensitive transducer that measures horizontal angle or vertical deviation with virtually infinite resolution. Rugged enough to withstand severe shock and vibration, its "all weather" construction makes it ideally suited for use in the construction industry for setting tilt of road grading and paving machines; in the geophysics field for tilt and strong motion studies; in the civil engineering field for evaluation of tilt of supporting walls in dams and other structures; and other applications where high-accuracy measurement of tilt is required.

The Schaevitz inclinometer is fully self-contained and designed to operate from a standard DC power source. Its output is an analog DC signal directly proportional to the sine of the angle of tilt. In level (horizontal) position, the DC output is zero. When tilted in one direction, the inclinometer output is 0 to +5V DC. When tilted in the opposite direction, the output is 0 to −5V DC.

The inclinometer operates as a closed-loop torque balance servo system (Figure 1). The heart of this gravity-referenced angle detector is a torsional flexure-supported moving mass system that is rugged enough to withstand severe shock and vibrations and still maintain excellent precision and accuracy. The servo system electronics, torque motor, and feedback sensor are all enclosed within an environmentally sealed housing, permitting operation under hostile conditions without degrading performance.

PRINCIPLES OF OPERATION (Refer to Figure 1)

The Schaevitz inclinometer is a precision inertial instrument (accelerometer) that responds to the normal component of the gravitational acceleration vector (gravity). Pendulous mass (A) is attached to the torsionally suspended armature of torque motor (C). Stops on either side of the mass (A) limit its travel when the device is not powered. When the power is applied, the pendulous mass (A) automatically moves to its "zero" position.

As the inclinometer is tilted through some angle (Θ) along its sensitive axis, mass (A) tries to move in the direction of tilt as a result of a force (torque) applied to the mass by the normal component of gravitation acceleration. The resulting change in position of mass (A) is detected by position sensor (B), which produces an error signal output. This DC error signal is fed to a servo amplifier whose output is a DC current coupled to the armature of torque motor (C) through R_o. Current applied to the torque motor armature produces a torque that opposes the gravitational force acting on the mass (A) and moves it back toward its original position. When the torque developed by the servo system output current just balances the torque developed by the gravity vector component acting on pendulous mass (A), the mass no longer moves and is at rest almost in its original position, being displaced by some minute amount that produces the required error signal from position sensor (B). Because the gravity component's force is exactly equal in magnitude to the torque motor's output, which, in turn, is directly proportional to the applied current, this current, passed through R_o generates a voltage across R_o that is proportional to the normal component of the gravity vector. The normal component is the product of the essentially constant gravity vector times the sine of angle (Θ). Therefore, the output voltage, E_o x across R_o is proportional to the sine of the tilt angle Θ.

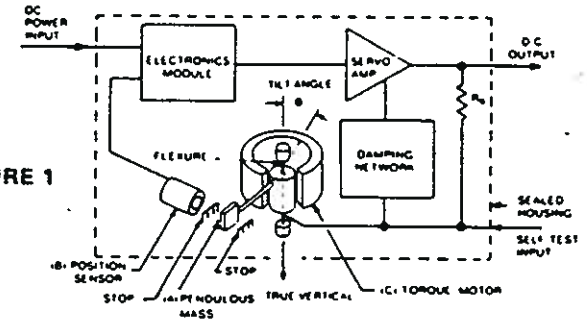

FIGURE 1

GENERAL OPERATING CHARACTERISTICS @ 20°C

Range	±1°	±3°	±14.5°	±30°	±90°
Input Voltage, V DC (Note 1)	±12 to ±18	±12 to ±18	±12 to ±18	±12 to ±18	±12 to ±18
Input Current, mA (nominal)	±15	±15	±15	±15	±15
Full Range Output (FRO) VDC (Note 2)	−5to +5	−5to +5	−5to +5	−5to +5	−5to +5
Output Standardization, % FRO	±1	±1	±1	±1	±1
Output Impedance, Ohms	15k	5k	16k	8k	4k
Output Noise, Vrms (Nominal)	0.002	0.002	0.002	0.002	0.002
Non-linearity, % FRO (Note 3)	0.05	0.02	0.02	0.02	0.02
Non-repeatability and Hysteresis, % FRO (maximum)	0.02	0.01	0.002	0.001	0.0005
Resolution, arc seconds	0.1	0.1	0.1	0.1	0.1
-3dB Frequency, Hz (typical)	0.5	1	15	20	40
Sensitive Axis-to-Case Misalignment, ° (maximum)	±0.1	±0.15	±0.25	±0.5	±1.0
Cross-axis Sensitivity, g/g cross (Note 4)	0.001	0.001	0.001	0.001	0.001
Output Offset at Zero Case Tilt, VDC (maximum) (Note 5)	±0.1	±0.04	±0.02	±0.02	±0.02
Vibration Rectification, arc seconds/g² (maximum)	10	10	10	10	10
Zero Tilt Offset Thermal Sensitivity, % FRO/°C	0.05	0.03	0.01	0.005	0.003
Scale Factor Thermal Sensitivity, % Reading/°C	0.02	0.01	0.003	0.003	0.003

ENVIRONMENTAL CHARACTERISTICS

Operating Temperature Range	−18°C to +71°C
Survival Temperature Range	−40°C to +75°C
Constant Acceleration Overload	50g
Shock Survival	1500g
Vibration Endurance-Sinusoidal	50g peak
Vibration Endurance-Random	35g rms, 20Hz to 2000Hz
Environmental Sealing	MIL-STD 202, Method 112

NOTES:

1) Units can be easily adapted to operate from single-ended, floating power supplies of 24 to 36 Volts DC.
2) Full Range is defined "from negative full input angle to positive full input angle".
3) Non-linearity is specified as deviation of output referenced to theoretical sine function value.
4) Cross-axis sensitivity is specified as the inclinometer output with a 1-g acceleration applied perpendicular to the sensitive axis, independent of case alignment errors.
5) Zero tilt offset is specified under static conditions with no vibration inputs; it represents the combination of mechanical bias, electrical bias, and axis-to-case alignment errors.

VBB VIAK

APPENDIX 2

ICE FORCE STUDIES IN THE BOTHNIAN BAY Phase 2

PROCESSING OF RESPONSE DATA DURING PHASE 1

PROCESSING OF RESPONSE DATA DURING PHASE 1

1. General

Three alternative procedures were developed during Phase 1 for the analysis of recorded accelerograms, as described in this Appendix. The methods are, in principle, applicable to high-frequency as well as low-frequency signals. Hence, the general notations are used instead of dashed symbols indicating low-frequent signals, although the procedures are primarily applied only to these, since the high-frequent signals can be processed with simpler procedures, as described in Chapter 4.

The recorded acceleration is composed of two components, the true horizontal acceleration $\ddot{x}$ and the "tilt acceleration $\ddot{x}_\phi$ due to the inclination of the structure and the attached inclinometer as explained in the description of the instruments, Appendix 1. (1)

$$\ddot{x}_R = \ddot{x} - \ddot{x}_\phi$$

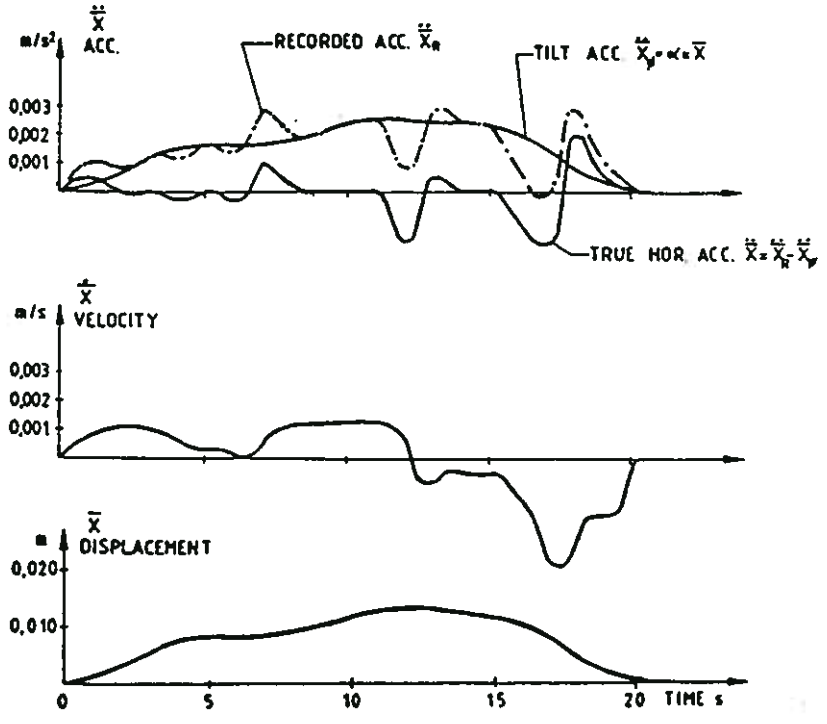

Figure A2:1

Separation of true horizontal and tilt components of measured accelerations

The three alternative procedures developed during Phase 1 are described in Section 2, 3 and 4, respectively. The first method was based on stepwise integration of the accelerograms, in order to determine the deflection of the structure and thereby identify the tilt angle. Like other methods based on integration, the accuracy of the results depends strongly on the resolution of measured quantities which limited the practical use of the method. The second method was developed in order to avoid this sensitivity of the resolution. However, when Fourier transformation was introduced, the particular relationships between acceleration and deflection of a sinusoidal motion time-history could be taken advantage of. The separation of the horizontal and gravity components of the measured acceleration could be made in the frequency domain with a very good accuracy.

Therefore, the third method, described in Section 4 of this appendix, was preferred already during the end of Phase 1 and has been used without exception during Phase 2.

2. Separation of tilt and true acceleration components by integration of recorded accelerations at one level

The "tilt acceleration" is proportional to the true displacement x.

$$\ddot{x}_\phi = \alpha \cdot x \qquad (2)$$

Consequently the true horizontal acceleration can be expressed

$$\ddot{x} = \ddot{x}_R + \ddot{x}_\phi = \ddot{x}_R + \alpha \cdot x \qquad (3)$$

The true velocity $\dot{x}$ and displacement x can thus be computed by a stepwise integration of

$$\ddot{x}_R + \alpha \cdot x$$

For the time increment $\Delta t = t_{i+1} - t_i$
the following quantities are known:

$\ddot{x}_{Ri}$, $\ddot{x}_{Ri+1}$, $\dot{x}_i$ and x_i

The true velocity can be expressed:

$$\dot{x}_{i+1} = \dot{x}_i + \Delta\dot{x} = \dot{x}_i + \ddot{x}_{mean} \cdot \Delta t = \dot{x}_i + \frac{\ddot{x}_i + \ddot{x}_{i+1}}{2} \cdot \Delta t =$$

$$= \dot{x}_i + \frac{\ddot{x}_{Ri} + \ddot{x}_{Ri+1}}{2} \cdot \Delta t + \alpha \cdot \frac{x_i + x_{i+1}}{2} \cdot \Delta t \qquad (4)$$

The true displacement can be expressed:

$$x_{i+1} = x_i + \Delta x = x_i + \dot{x}_{mean} \cdot \Delta t =$$
$$= x_i + \frac{\dot{x}_i + \dot{x}_{i+1}}{2} \cdot \Delta t =$$

$$= \dot{x}_i + \dot{x}_i \cdot \Delta t + \frac{\ddot{x}_{Ri} + \ddot{x}R_{i+1}}{4} \cdot \Delta t^2 + \alpha \cdot \frac{x_i + x_{i+1}}{4} \cdot \Delta t^2 \quad (5)$$

i.e.

$$x_{i+1} = \frac{x_i + \dot{x}_i \cdot \Delta t + \frac{\ddot{x}_{Ri} + \ddot{x}_{Ri+1}}{4} \cdot \Delta t^2 + \frac{\alpha \cdot x_i}{4} \cdot \Delta t^2}{1 - \frac{\alpha \cdot \Delta t^2}{4}}$$

$\dot{x}_{i+1}$ is obtained from Eq. (4) and

$\ddot{x}_{i+1}$ from Eq. (3)

The tilt angle

$$\phi_i = \frac{\ddot{x}_{\phi i}}{g} = \frac{\ddot{x}_i - \ddot{x}_{Ri}}{g} \quad (7)$$

The static ice force

$$F = \frac{K\phi}{Z_F} \cdot \phi \quad (8)$$

where K_ϕ is obtained from the static mode of the "transfer model's" deflection.

According to Eq. (2):

$$\alpha = \frac{\ddot{x}_\phi}{x} = \frac{\phi \cdot g}{x} \quad (9)$$

This factor varies with the level referred to and with the mode of deflection (static or dynamic). Therefore the "static" inclination of the structure must be evaluated after separating the "static" response function from the "dynamic".

For the two accelerometer levels at NORSTRÖMSGRUND and for static loads the following values can be used:

$$\alpha_1 = \alpha_2 = \frac{0.784 \cdot 10^{-3} g}{0.032} = 0.240$$

$$\alpha_3 = \alpha_4 = \frac{0.784 \cdot 10^{-3} g}{0.015} = 0.513$$

The accuracy of these preliminary α-values have been checked by test loading of the structures.

One implication of the integration procedure described above is that the accuracy of the result is extremely dependent on the accuracy of the initial boundary condition as well as the recorded acceleration values introduced during the integration process. Since errors increase exponentially with time, the process should only be applied to limited time intervals, starting from boundary conditions where the tilt or the horizontal acceleration can be assessed with a very good accuracy. Such boundary conditions may be identified and quantified using the procedure described in the following section.

3. Determination of the inclination from acceleration records at two levels

The tilt component $\ddot{x}_\phi$ of the recorded acceleration $\ddot{x}_R$ can be separated from the true horizontal acceleration $\ddot{x}$ by taking advantage of simultaneous acceleration measurements at the upper and lower points of measurements and the following relations:

From Eq. 1:

$$\ddot{x}_1 = \ddot{x}_{R1} + \ddot{x}_{\phi 1} \tag{10}$$

$$\ddot{x}_3 = \ddot{x}_{R3} + \ddot{x}_{\phi 3} \tag{11}$$

where the indices 1 and 3 refer to the upper and lower acceleration values, respectively, measured in the same horizontal direction. (The perpendicular components shall of course be accounted for in the same manner).

Provided that the lighthouse structure behaves elastically, the ratio between the upper and lower horizontal displacements is constant and so is the corresponding ratios between the true horizontal acceleration values:

$$x_1/x_3 = \ddot{x}_1/\ddot{x}_3 = \text{Const.} \tag{12}$$

Furthermore, since the inertia contributions are negligible for the low-frequency modes of deflections, the tilt angle is essentially the same for the upper as for the lower measurement point, both points being located above the level of ice action:

$$\ddot{x}_{\phi 1} = \ddot{x}_{\phi 3} = \ddot{x}_\phi \tag{13}$$

The tilt component $\ddot{x}_\phi = \phi \cdot g$ can thus be derived from the following set of equations:

$$\ddot{x}_1 = \ddot{x}_{R1} + \ddot{x}_\phi \tag{14}$$

$$\ddot{x}_3 = \ddot{x}_{R3} + \ddot{x}_\phi \tag{15}$$

$$\ddot{x}_1/\ddot{x}_3 = x_1/x_3 = \text{Const.} \tag{16}$$

As a result the tilt acceleration can be expressed:

$$\ddot{x}_\phi = \phi \cdot g = \frac{1}{x_1/x_3-1} \cdot \ddot{x}_{R1} - \frac{x_1/x_3}{x_1/x_3-1} \cdot \ddot{x}_{R3} \tag{17}$$

Finally the static ice force components are obtained using Eq. 8.

The ratios x_1/x_3 and x_2/x_4 are obtained from the transfer model. For the NORSTRÖMSGRUND transfer model the preliminary numerical value is:

$$x_1/x_3 = x_2/x_4 = 2.133$$

(Since $\alpha = \frac{\phi \cdot g}{x}$ and $\phi_1 = \phi_3$ the ratios

$\frac{\alpha_3}{\alpha_1} = \frac{\alpha_4}{\alpha_2}$ = have the same value as x_1/x_3 etc.)

The following expression for the tilt angle at NORSTRÖMSGRUND was obtained:

$$\phi = \frac{1}{g} (0.883 \cdot \ddot{x}_{R1} - 1.883 \cdot \ddot{x}_{R3}) \tag{18}$$

It is obvious that, if the horizontal acceleration is large compared with the "tilt acceleration",the tilt will be derived as a small difference between large numbers, which may impair the accuracy significantly. The tilt angle should therefore preferably be derived for situations where the true horizontal acceleration is comparatively small. This is indicated, for instance, by the appearance of sequences of <u>linear</u> time functions of the recorded acceleration $\ddot{x}_R$, particularly such sequences where the acceleration is constant. Under most circumstances, this indicates that the horizontal acceleration is close to zero and that the true deflection velocity is zero or constant, i.e. the ice force and the spring forces of the structure are in equilibrium.

This also justifies the assumption that the "static" mode of deflection is predominant.

4. Determination of the inclination by transformation of accelerograms into the frequency domain

A recorded acceleration time-history $\ddot{x}_R(t)$ can be represented by Fourier component sinusoids. The amplitude $\ddot{x}_{Rf}$ of a component wave representing the frequency interval $fi \pm \Delta f/2$ in the recorded accelerogram represents the difference between the true horizontal acceleration component $\ddot{x}_f$ and the tilt component $\ddot{x}_\phi$ (See Section 5.2 of the main report):

$$\ddot{x}_{Rf} = \ddot{x}_f - \ddot{x}_{\phi f} = \ddot{x}_f - \alpha_f \cdot x_f \qquad (19)$$

Since the component waves are sinusoidal, the relationship between the horizontal displacement x_f and the corresponding acceleration $\ddot{x}_f$ can be expressed:

$$x_f = -\ddot{x}_f/\omega^2 \qquad (20)$$

Hence

$$\ddot{x}_{Rf} = \ddot{x}_f + \alpha_f \cdot \frac{\ddot{x}_f}{\omega^2}$$

For each component wave of the recorded accelerogram the true horizontal acceleration and the tilt components can thus be separated:

$$\ddot{x}_f = \frac{\omega^2}{\omega^2 + \alpha f} \cdot \ddot{x}_{Rf} \qquad (21)$$

$$\ddot{x}_{\phi f} = \phi \cdot g = \frac{-\alpha_f}{\omega^2 + \alpha_f} \cdot \ddot{x}_{Rf} \qquad (22)$$

$$\alpha_f = \frac{\phi \cdot g}{x_f}$$

expresses the relationship between the tilt angle and the horizontal displacement at the instrument level and is frequency dependent. It can be determined from the transfer model.

Example:

- For f = 1 Hz; α_f= 0.5:
  $\ddot{x}_{\phi f} = -0.0125\ \ddot{x}_{Rf}$
  $\ddot{x}_f = 0.9875\ \ddot{x}_{Rf}$

- For f = 0.2 Hz; α_f= 0.5:
  $\ddot{x}_{\phi f} = -0.285\ \ddot{x}_{Rf}$
  $\ddot{x}_f = 0.715\ \ddot{x}_{Rf}$

- For f = 0.1 Hz; α_f= 0.5:
  $\ddot{x}_{\phi f} = -0.559\ \ddot{x}_{Rf}$
  $\ddot{x}_f = 0.441\ \ddot{x}_{Rf}$

- For f = 0.01 Hz; α_f= 0.5:
  $\ddot{x}_{\phi f} = -0.9922\ \ddot{x}_{Rf}$
  $\ddot{x}_f = 0.0078\ \ddot{x}_{Rf}$

VBB

APPENDIX 3

AN ICE-STRUCTURE INTERACTION MODEL BASED ON OBSERVATIONS IN THE GULF OF BOTHNIA

By Alf Engelbrektson
VBB Consulting Ltd

Report to the 10th Conference on
Port and Ocean Engineering under Arctic Conditions - POAC 89,
Luleå, Sweden, June 12-16, 1989

MEMBER OF SVVECO

VBB · ENGINEERS · ARCHITECTS · ECONOMISTS · MEMBERS OF THE SWEDISH ASSOCIATION OF CONSULTING ENGINEERS

Postal address	Office address	Telephone	Telegram address	Telex	Bank
P.O. Box 5038	2, Linnégatan	+46 8 782 70 00	VATTEN	10477 VATTEN S.	Skandinaviska Enskilda Banken
S-102 41 STOCKHOLM, SWEDEN			Stockholm		

AN ICE-STRUCTURE INTERACTION MODEL BASED ON OBSERVATIONS IN THE GULF OF BOTHNIA

Alf Engelbrektson

VBB-SWECO
Box 5038
S-102 41 STOCKHOLM
SWEDEN

ABSTRACT

On the basis of experiences from studies of ice-structure interaction in the Gulf of Bothnia a model has been outlined for the characterization of periodic ice forces associated with resonant structural vibrations. A generalized ice force time-history is proposed to be used for engineering purposes, and the model is discussed in terms of ice mechanics. It appears that the basic features of the model are of a generic character and that the suggested ice force equations are relevant, in principle, to cases of static as well as of dynamic structural response.

1. LONG-TERM STUDIES OF ICE-STRUCTURE INTERACTION

For about 30 years ice action on offshore lighthouse structures in the Gulf of Bothnia has been increasingly studied. Largely, each decade represents a specific stage of development.

During the 1960's the studies were quite unsophisticated: simply a follow-up of the performance of the structures when affected by drifting ice, ice-piling, icing etc. On the basis of the rather poor knowledge of ice action at that stage and, apparently, a portion of good intuition, ice forces were predicted rather closely to the optimum risk level. A few cases of damage gave fairly clear indications as regards particular ice conditions, requiring adjustments of the design loads.

During the 70's the problem of ice-induced vibrations was realized and the most strongly affected structure was instrumented. Vibration records sampled during that decade, together with the continued follow-up and analysis of a few cases of static and dynamic overloading of Finnish and Swedish lighthouses, improved the understanding of ice-structure interaction considerably.

During the 80's the studies have been expanded appreciably, quantitatively as well as qualitatively. Taking advantage of the Gulf of Bothnia as a convenient facility for Arctic research, several independent ice study projects with international participation have been conducted and some are in progress. The product is a continuous inflow of parametrically well-defined data and subsequent improvements of the bases for ice-force predictions for Arctic areas, whereever the fundamental ice parameters can be quantified and where ice conditions are not essentially different from those prevailing in the Gulf of Bothnia.

2. RECENT STUDIES

In 1985 the studies of ice-structure interaction were intensified in that a joint study project was agreed between Arco, Exxon and Mobil (USA), Norwegian Contractors, Canadian Coast Guard, Mitsubishi, the Swedish National Industrial Board, Hamburgische Schiffbau-Versuchsanstalt and VBB. The latter two companies, cooperating with the Swedish Administration of Shipping and Navigation and with the University of Luleå obtained financial and advisory support for a comprehensively extended field study of ice-structure interaction, by employing some large lighthouses in the Bothnian Bay as objects for data sampling and other abservations.

The instrumentation of the lighthouses was improved and during a three years' period the database was greatly enlarged, and suitable analysis methods were developed for transformation of measured structural response to ice forces. Since the instrumented lighthouse structures serve, in principle, as full-scale elastic obstacles and measurement devices with calibrated constitutive properties, static as well as dynamic relations between the structural response and the ice forces can be determined within uncertainty ranges that are judged to be quite acceptable from an engineering viewpoint.

Two years of development, including trial operations and refinements, resulted in an elaborate system for data acquisition and processing, based on the following elements:

* Accelerometer and inclinometer systems including computers, filters, tape recorders, etc, for sampling of response data in the form of records of acceleration and inclination (in principle two types of accelerograms).

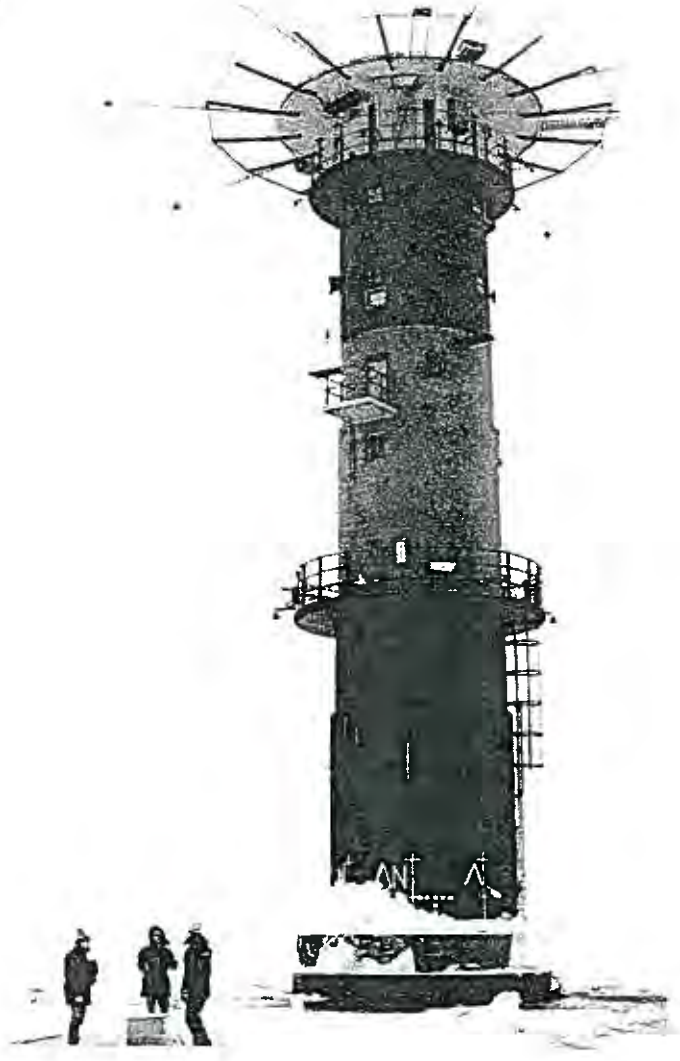

Figure 1. Sampling of ice data in connection with an event of indentation

* Video camera systems, coordinated with the above systems, for observation of ice movements etc.

* Signal processing procedures especially developed for the analysis of the rather complex data records, involving separation of signals in respect of frequencies as well as directions. (The lack of reference points on the open sea and the strongly vibrational character of the structural response necessitate that very small gravity related signals must be distinguished in the inclinometer records, containing predominantly signals caused by horizontal inertia due to the strong vibrations.)

* Constitutive models of the lighthouses, calibrated by pull tests etc, for transformation of response data to ice force time-histories.

* Field sampling and laboratory investigation of ice data (Figure 1).

3. ICE FORCE TIME-HISTORIES DERIVED FROM RECORDS OF OBSERVED STRUCTURAL RESPONSE

The records of structural response data and the corresponding ice force time-histories studied so far present a fairly clear picture of the mechanism of ice-structure interaction from the mechanical point of view. On the basis of these data the mechanism can be modelled mathematically in terms of ice force and response time-histories. By selecting simple characteristics, such as the maximum and minimum ice forces as key parameters, the relationships can be normalized, resulting in a set of ice force expressions for engineering applications.

Obviously, the type of ice-structure interaction that involves dynamic structural response and, particularly, resonant vibrations is a more complex manifestation of ice action than stationary ice pressure or steady-state indentation. This presentation will still originate from the dynamic type of ice structure interaction and it will be demonstrated, that the various types of ice action are closely related. By way of introduction some ice force records from a large offshore lighthouse in the Bothnian Bay are shown. The diameter of the cylindrical structure is 7.2 m (Figure 1).

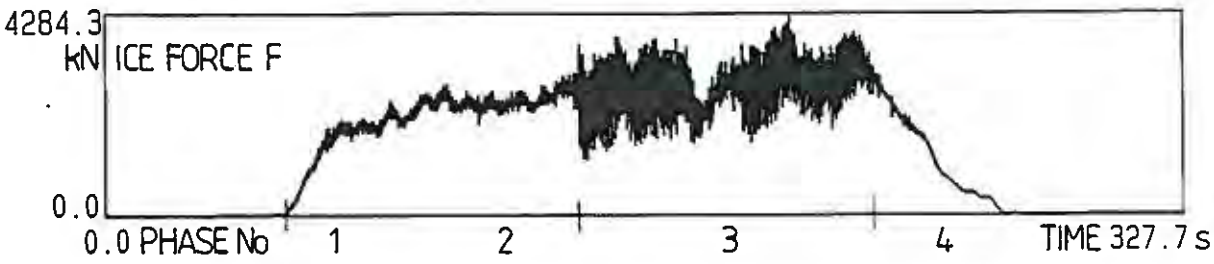

Figure 2. Condensed ice force time-history from an event of indentation through an ice floe drifting with a speed of 0.04-0.06 m/s. Four different phases are observed: Initial indentation with increasing interface width, steady-state indentation without major structural dynamics, indentation associated with a greatly fluctuating ice force and, finally, a phase of load decay.

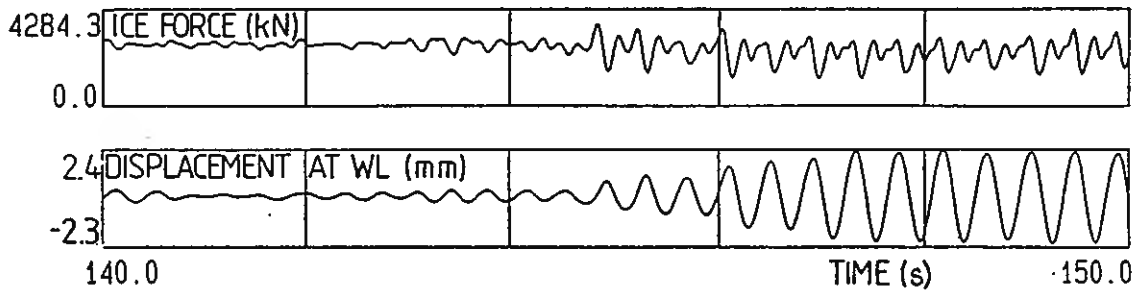

Figure 3. The sequence 140-150 s from the above record displayed in an extended time scale together with the corresponding time-history of structural displacement at the ice force level. (Positive for displacement in the ice force direction.)

During this short sequence the ice-structure interaction changes from an almost "static" mode to a mode associated with periodic fluctuation of the ice force as well as the structural displacement. The latter phase is initiated by a sudden load peak followed by a load drop. The corresponding amplitude of the structural response motion is sufficient for starting the periodic phase of the ice-structure interaction, associated with increasing amplitudes of structural deflection until energy equilibrium is reached. The frequency of vibration is very close to the fundamental natural frequency of the structure and the vibrations are of a typically resonant character.

The study of numerous records of strong vibrations and associated periodic ice forces has provided unambiguous evidence on the following points:

* When an ice cover is being indented by a flexible structure and fails mainly in a crushing mode, so-called self-induced vibrations occur frequently. The resonant vibrations are coupled to a periodic fluctuation of the resultant ice force.

* If the drift speed is not much lower than the maximum velocity of the structural vibrations, the frequency of the predominant structural oscillations determines the frequency of the load fluctuations. Obviously, the structural vibration induces the periodicity of the ice force, that in turn amplifies the vibration and so on, until the energy consumption due to damping becomes equal to the energy input from the resonant load.

* When the vibration amplitudes are below the threshold, where the periodic interaction becomes significant, the resultant ice load also fluctuates, but the amplitudes are comparatively small and the fluctuations are more irregular. The character of the load is almost the same for a rigid structure as for a flexible one and the deflection of the latter is essentially static. Whereas a distinction is made betwen static and dynamic structural response during indentation, it should be kept in mind that the ice force during indentation is always more or less dynamic.

* The most important feature of the ice force time-history during periodic indentation associated with resonant vibrations is the sudden drop of the resultant force after reaching the peak of each load cycle. Another important observation is that the time-averaged resultant ice force appears to be essentially equal to the ice force during non-periodic indentation of the same ice-floe. The maximum, mean and minimum ice forces (F_{max}, F_0, F_{min}) are therefore suitable key parameters for characterization of a sequence of periodic as well as non-periodic ice-structure interaction.

* The periodic ice force can be characterized in a spectral form, by means of Fourier analysis, i.e. by breaking down the force time-history into component sine waves, the amplitudes and phases of which can be represented in a spectral form. In Figure 4 the power density spectrum of the sequence previously displayed in Figure 2 is shown as an example. The spectrum clear-

ly demonstrates the strong coupling between the structural oscillations and the ice force fluctuations. The component waves of the ice force time-history have their frequencies predominantly concentrated at the fundamental structural frequency 2.34 Hz and its multiples, an observation that will be further referred to, when generalizing the ice force time-history for design purposes.

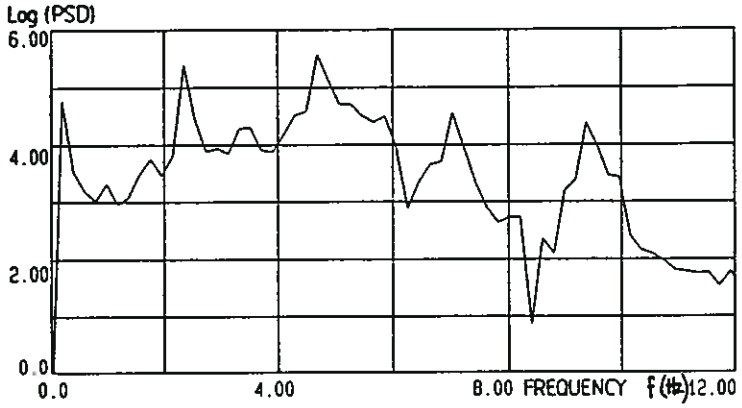

Figure 4. Typical power density spectrum of ice forces associated with resonant structural vibrations.

2. OBSERVED BEHAVIOUR OF DRIFTING ICE DURING INDENTATION

The following observations are based mainly on studies of video records from events of strong ice action associated with continuous as well as periodic indentation of ice-sheets with thicknesses of 0.5-1.0 m. Occasional direct visual observations are also referred to.

* The load limiting mode of ice failure is crushing. Occasionally, the load limit is set by splitting, associated with more or less radial cracks (seen from the centre of the structure). However, splitting does not occur continuously and can therefore not be relied upon for design purposes. Consequently, crushing across the whole width of the structure can be regarded as the ultimate load limiting mechanism, at least when dealing with conditions similar to those prevailing in the Bothnian Bay. In waters where there are multiyear ice ridges the utlimate loads exerted by such ridges are sometimes limited by other failure modes than crushing, but in other respects the Bothnian Bay conditions are broadly representative for Arctic areas.

* The crack propagation and crushing take place within a short distance from the ice-structure interface. Normally, it has the character of pulverisation of the ice. From laboratory experiments we have learned that such a pulverisation is the final phase in a course of initial fracture growth, progressive cracking and final collapse of the ice structure.

* Obviously the cracking and pulverisation are more or less outspread in space and time, which is associated with a corresponding limitation and variation of the interface contact. At a certain instant the contact is concentrated at limited spots or zones. At each zone the ice is stressed to a condition between ductile strain and cracking, and the phases are more or less different from one zone to another. This phase difference or non-simultaneous failure is a key feature in our following considerations.

* Basically, the large scale mode of ice failure appears to be that of crushing in case of static structural response as well as in case of strong vibrations. The non-uniform distribution of failure zones has sometimes been discerned in the video records, but the resolution is, of course, not sufficient for allowing details such as the periodicity of the crushing and the local phase difference to be distinguished.

5. A GENERIC MODEL OF ICE-STRUCTURE INTERACTION

It is particularly in the light of recent experiences from the field studies in the Bothnian Bay that all the findings seem to converge towards basically one single mode of ice-structure interaction during indentation. Based on a few variants of that mode, simple explanations can be found for various forms of interaction such as steady-state indentation, periodic indentation associated with strong structural vibrations and even interaction with unbroken ice to some extent.

A generic model of ice-structure interaction is therefore proposed, with reference to the following categories of supporting material.

* The above-mentioned observations of the mode of ice failure and the observations of structural response and ice force time-histories, enabling a mathematical characterization of "static and dynamic" ice forces against structures in the Bothnian Bay.

* Current knowledge regarding relations between ice strength, strain and strain-rate as well as reported observations concerning apparent relations between ice forces and the size of the interface area, the aspect ratio etc.

* Observations and qualitative explanations, admittedly hypothetical to some extent, regarding the details of the transient ice stress and failure conditions close to the interface.

The model has the following basic features:

* During the course of indentation the contact between the ice and the structure is predominantly concentrated at local zones, the location of which vary with time.

* At each temporary contact zone the ice undergoes at least one cycle of transient conditions, from increasing stress associated with ductile behaviour to cracking and pulverisation. The load cycles at different contact zones are more or less out of phase.

One extreme is a random phase distribution (although there is, most likely, a certain coupling between adjacent contact zones due to interactive stress conditions). The opposite extreme is synchronized load cycles at the various contact zones.

* During a course of steady-state indentation (when the indentor does not oscillate) the local zones are consecutively undergoing their individual stress cycles, the rate being determined by the ice drift velocity. This parameter also determines the strain-rate and, therefore, it probably influences the ice strength and the amplitude of the contact forces. Since the time distribution of the load impulses, represented by the local contact forces, has a random feature, the global load on a large interface area will be rather uniform and correspond to the average contact force. In case of a smaller interface and only a few contact zones, the majority of the contact forces may be in phase occasionally and the global force is likely to be fluctuating irregularly. The maximum effective contact pressure will exceed the pressure associated with a large area. For otherwise homogeneous ice conditions the maximum value will be determined by

the ice drift velocity and the random phasing, thus by the duration of the indentation.

The widely observed size effect on the effective pressure may thus be explained by the phase distribution of local contact forces. However, for narrow indentors the effect of confinement due to unstressed ice adjacent to the interface should not be neglected. There are strong indications pointing at confinement effects in some cases of over-loading when narrow structures have been damaged. The aspect ratios have, however, not exceeded the order of 4 in those cases.

* During a course of periodic rate of indentation the vibrating indentor influences the local load pulses largely. The structural movements affect the strain-rate and coordinate the local pulses, as illustrated in Figures 5 and 6.

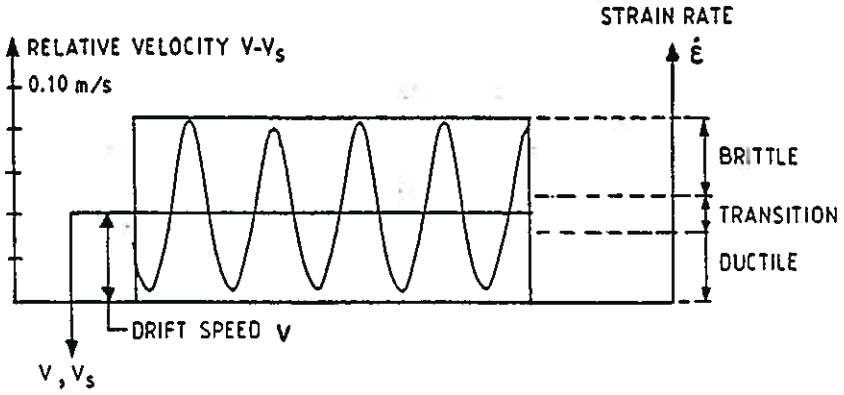

Figure 5. During each cycle of structural oscillation the relative velocity and the strain-rate (as well as the strain) passes to and fro over the ranges corresponding to ductile deformation, fracture growth and brittle failure.

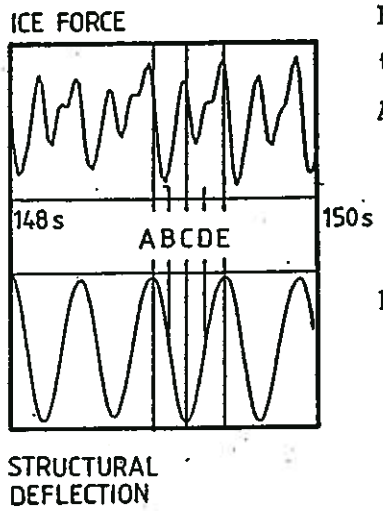

Figure 6. Various phases of ice-structure interaction during a cycle of oscillation:

A-B: The structure moves backwards after the preceding coordinated ice failure. The strain-rate is high, the contact reduced and the ice force passes its minimum.

B-D: The structure slows down and then turns, the strain-rate decreases and the contact pressure increases to a peak before the forward velocity increases and the structure tends to move ahead from the ice.

D-E: The structure decelerates, the contact pressure increases once more in a ductile manner until a sudden coordinated failure occurs, when the ice strength is being exceeded.

The global peak load is therefore composed of relatively well-coordinated local pulses. The peaks of the individual load cycles may reach the limit corresponding to the maximum strength of the ice almost simultaneously. During the phase when the structure moves in the ice drift direction the onloading is soft and the strain-rate is initially rather low. Therefore, the ice strength may come close to its optimum before the coordinated failure, and the peak load may reach the same order as in case of any initial failure over a smooth interface. Actually, no cases have yet been observed, where such an initial peak has exceeded the peaks during subsequent resonant vibrations.

Beside the build-up of the peak load the sudden stress drop following the peak is the most important feature as regards the periodic ice-structure interaction. This stress drop occurs almost simultaneously at various contact zones and is the strongest coordinating factor. The mechanism of coordination is quite understandable, considering the brittleness of the ice after the fracture nucleation, leading to progressive cracking not only within the induvidual fractured zones but also leading to progressive collapses when the load at one collapsed zone is overtaken by adjacent zones.

The obvious lower limit of the minimum force, locally and globally, is zero. However, our observations indicate, that the global load drop is normally

of the order of 50 per cent of the peak load in case of strong resonant vibrations, and that 75 per cent of the peak load is an extreme value.

6. GENERALIZED CHARACTERIZATION OF ICE FORCE TIME-HISTORIES FOR ENGINEERING PURPOSES

In respect of the choice of key parameters the development of ice force formulae for engineering purposes can be approached in two steps:

* Characterization of a generalized load time-history normalized to the key ice force parameters F_{max}, F_0, F_{min} or the corresponding "effective pressure" parameters p_{max}, p_0, p_{min}.

* Formulation of relationships between the above load parameters and fundamental parameters for characterization of ice conditions.

It is recognized that a more or less probabilistic approach must be considered, for the latter step in particular. However, generalized relationships may very well be formulated deterministically, assessing approximate uncertainty ranges for the parameters until sufficient data have been acquired for enabling a refined probabilistic approach.

With reference to the Fourier analyses of ice force time-histories and the example of an ice force spectrum given in Figure 4, the following simple expression has been chosen for characterization of a generalized time-history of the effective ice pressure:

$$p(t) = p_0 + \sum p_n \cdot \cos(n \omega_1 t + \theta_n) \qquad (1)$$

The loading function can thus be represented by a constant and a number of sine waves with n = 1, 2, 3, 4 etc., the angular frequencies $n \omega_1$ of which are multiples of the fundamental structural frequency ω_1.

For most engineering purposes four sine waves are sufficient for obtaining a realistic generalization of the loading function, as demonstrated in Figure 7.

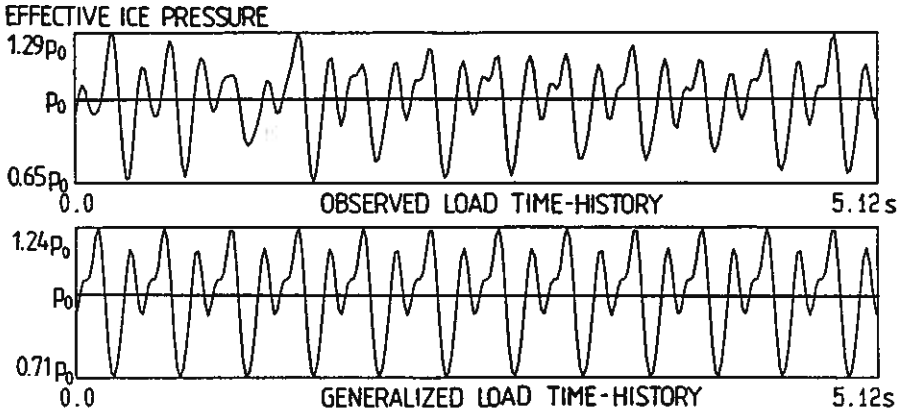

Figure 7. Comparison of an ice pressure sequence from the record shown in Figure 3 and the corresponding generalized function (below), composed of a constant pressure and four sine waves. The normalized constants are $p_0/p_{max} = 0.78$, $p_1/p_{max} = 0.110$, $p_2/p_{max} = 0.165$, $p_3/p_{max} = 0.050$, $p_4/p_{max} = 0.040$ and the phase angles are 5.38, 2.24, 4.62 and 3.66 radians respectively, for n = 1-4.

Equation (1) can be applied to ice-structure interaction associated with dynamic as well as static structural response. Steady-state indentation is represented by the first term and in case of resonant vibrations the sine terms are to be included. The use of the maximum effective pressure as a normalizing parameter is motivated by its close relation to the maximum ice strength before fracturing.

The next problem is to establish a reliable relationship between the effective pressure and a well-defined ice strength parameter. We may refer to the classical Korzhavins formula and set

$$p = k_S \cdot k_I \cdot k_C \cdot f_{um} \qquad (2)$$

where f_{um} is the uniaxial compressive ice strength averaged over the thickness.

For relatively large cylindrical structures as those referred to above the effects of shape (k_S) and of lateral confinement (k_I) need not be assessed explicitly and the relationship can simply be expressed by one factor $k = p/f_{um}$. In case of invariable interface area and ice strength the time function of k is obtained from Eq. 1:

$$k(t) = k_0 + \Sigma k_n \cdot \cos(n \omega_1 t + \theta_n) \qquad (3)$$

It follows from the above that the factor k varies strongly with the mode of ice-structure interaction. Typical maximum and mean values during sequences of saturated resonant vibrations are 0.6 and 0.4, respectively.

7. CONCLUSIONS AND OUTLOOKS

Previous experiences and future objectives of the ongoing ice force studies in the Gulf of Bothnia may be briefly summed-up as follows:

* The model outlined in Sections 5 and 6 for the characterization of static and dynamic ice structure interaction, including the proposed generalized ice force equations, is intended to provide engineers with an improved basis for the design of offshore structures including installed equipment. A simplified spectral presentation of the ice force function has been chosen. This is for practical reasons and for allowing transperancy, but a more complete spectral presentation, including higher-frequency components if needed, might be incorporated in the future work.

* In addition to the observation that a generalized ice force function can be expressed in terms of a few key parameters, such as the maximum, mean and minimum ice forces during a sequence of periodic interaction, it is important to note that the basic features of the function can be explained in terms of ice mechanics. Key elements are the interactive cycling of the interface pressure, the variation of the constitutive properties of the ice during each load cycle, the synchronism of ice failures at local zones, the strain-rate dependence etc. Further investigations of these relations will be performed by means of a system of ice force sensing panels, enabling separation of local pressures in time and space.

* In the first approach the ice force relationships have been expressed mainly in a deterministic manner, the probabilistic aspects covered only by indicating fairly broad ranges of uncertainty and expected spread. These ranges are based on the long-term experiences from the Gulf of Bothnia. The experiences are, however, sufficient only for very rough probabilistic quantifications. Acquisition of more data, for improved probabilistic considerations is therefore programmed to become an important part of future activities.

BIBLIOGRAPHY

The present report contains selected highlights from a series of reports, produced within the scope of the joint industry research project "ICE FORCES AGAINST OFFSHORE STRUCTURES". Detailed descriptions of methods and means for data sampling and analyses, as well as reviews of data records and analysis results, are compiled in those project reports.

For general "state-of-the-art" information concerning static and dynamic ice-structure interaction, reference is made to publications such as Bernard Michel's: Ice Mechanics (1978) and T.J.O. Sandersons's: Ice Mechanics-Risk to Offshore Structures (1988).

The problem of ice-induced structural vibrations has been addressed at several conferences on cold regions research during the last years, not least at the POAC conferences since 1977, when ice-induced resonant vibrations were tentatively analysed in papers by M. Määttänen and A. Engelbrektson.

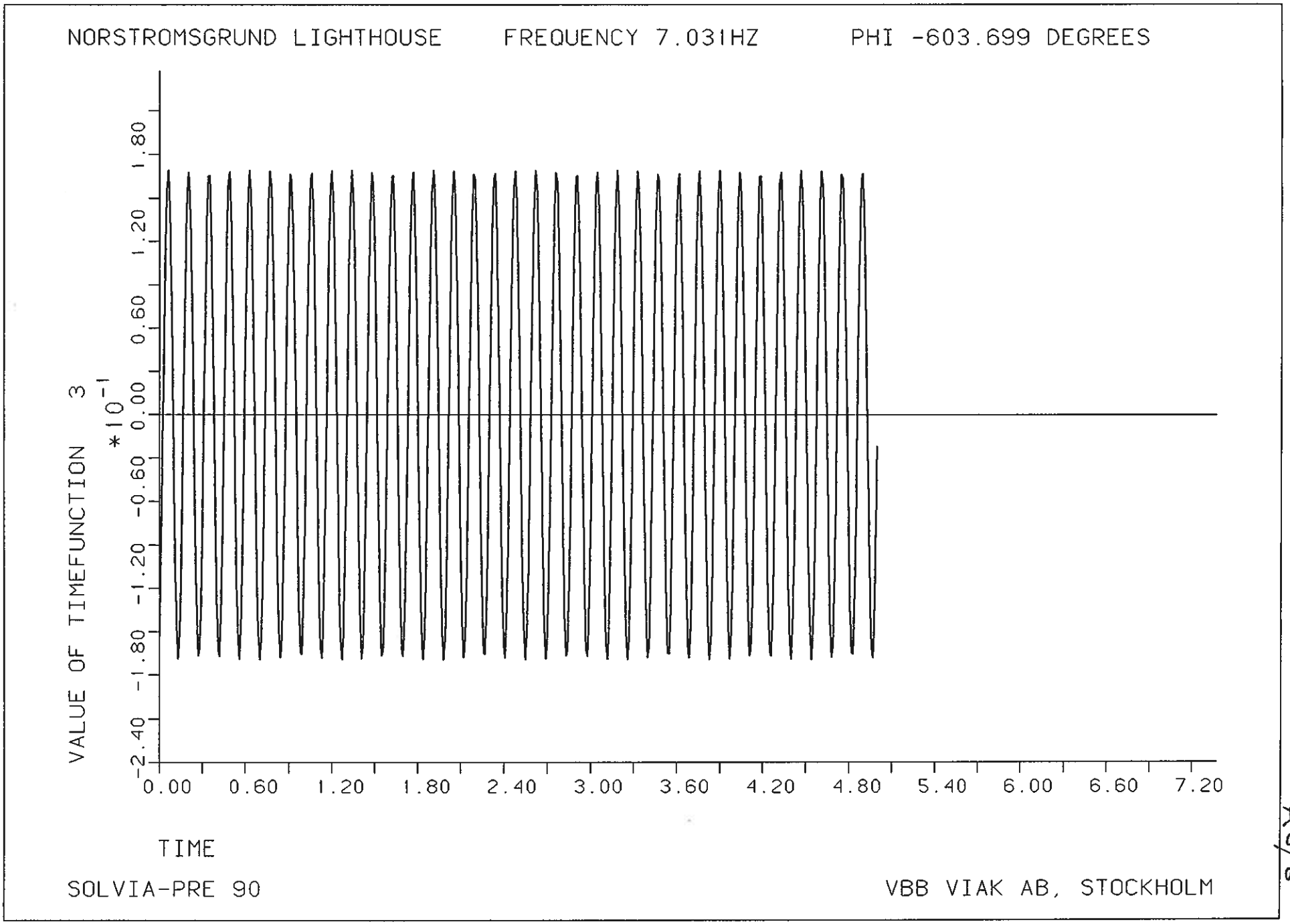
NORSTROMSGRUND LIGHTHOUSE
FREQUENCY 7.031HZ
PHI -603.699 DEGREES
VALUE OF TIMEFUNCTION 3
*10^-1
1.80
1.20
0.60
0.00
-0.60
-1.20
-1.80
-2.40
0.00
0.60
1.20
1.80
2.40
3.00
3.60
4.20
4.80
5.40
6.00
6.60
7.20
TIME
SOLVIA-PRE 90
VBB VIAK AB, STOCKHOLM

A6/6

```
   *** WELCOME TO SOLVIA-POST 90.2G
   *** COPYRIGHT SOLVIA ENGINEERING AB, 1987-1991
   *** THIS COPY IS LICENSED TO VBB VIAK AB, STOCKHOLM
   *** NO 'set.post' FILE FOUND.
post: post: post: post: SET ERRORLIMIT=100
DATABASE CREATE
   *** READING SOLVIA PORTHOLE FILE

NORSTROMSGRUND LIGHTHOUSE    LOAD FREQUENCY 7.1943 HZ (MODE 1,2 AND 3)

   *** IN DATABASE:  NODAL AND ELEMENT INPUT DATA
   ***IN DATABASE:  INITIAL CONDITIONS AT TIME  0.00000000E+00
   ***IN DATABASE:   595    NODAL RESULTS TIME 1.00000000E-02 TO  5.9500000
   ***IN DATABASE:   595  ELEMENT RESULTS TIME 1.00000000E-02 TO  5.9500000

*DATABASE OPEN
*SSSSSSSSSSSSSSSSSSSSSSSSSSSSSSSSSSSSSSSSSSSSSSSSSSSSSSSSSSSSSSSSSSSSSSSSSSS
*  SCANNING
*****************************************
NHIST 14 1 K=A O=L TST=5.5 TE=5.9
```

TIME HISTORY FOR NODE 14 DYNAMIC ANALYSIS

A6/8

OUTPUT RESULTS ARE MEASURED IN GLOBAL COORDINATE SYSTEM

TIME	X-DIR ACCEL.
5.500	2.97521E-01
5.510	4.75112E-01
5.520	5.55585E-01
5.530	5.22816E-01
5.540	3.83557E-01
5.550	1.66057E-01
5.560	-8.56520E-02
5.570	-3.20647E-01
5.580	-4.91386E-01
5.590	-5.63297E-01
5.600	-5.21753E-01
5.610	-3.75023E-01
5.620	-1.52606E-01
5.630	1.00705E-01
5.640	3.33859E-01
5.650	4.99831E-01
5.660	5.65114E-01
5.670	5.16481E-01
5.680	3.63673E-01
5.690	1.37455E-01
5.700	-1.16564E-01
5.710	-3.47109E-01
5.720	-5.07561E-01
5.730	-5.65365E-01
5.740	-5.08602E-01
5.750	-3.48428E-01
5.760	-1.16862E-01
5.770	1.39625E-01
5.780	3.69438E-01
5.790	5.26228E-01
5.800	5.78224E-01
5.810	5.14647E-01
5.820	3.47914E-01

TIME HISTORY FOR NODE 14 DYNAMIC ANALYSIS

A6/9

OUTPUT RESULTS ARE MEASURED IN GLOBAL COORDINATE SYSTEM

TIME	X-DIR ACCEL.
5.830	1.11178E-01
5.840	-1.48289E-01
5.850	-3.78571E-01
5.860	-5.33520E-01
5.870	-5.82022E-01
5.880	-5.14261E-01
5.890	-3.43714E-01
5.900	-1.04469E-01

NHIST 11 1 K=A O=L TST=5.5 TE=5.9

TIME HISTORY FOR NODE 11 DYNAMIC ANALYSIS

A6/10

OUTPUT RESULTS ARE MEASURED IN GLOBAL COORDINATE SYSTEM

TIME	X-DIR ACCEL.
5.500	-7.16949E-01
5.510	-1.19736E+00
5.520	-1.43645E+00
5.530	-1.38631E+00
5.540	-1.05726E+00
5.550	-5.15759E-01
5.560	1.29023E-01
5.570	7.47156E-01
5.580	1.21413E+00
5.590	1.43591E+00
5.600	1.36785E+00
5.610	1.02371E+00
5.620	4.72835E-01
5.630	-1.73751E-01
5.640	-7.85727E-01
5.650	-1.23969E+00
5.660	-1.44402E+00
5.670	-1.35732E+00
5.680	-9.96771E-01
5.690	-4.34720E-01
5.700	2.15862E-01
5.710	8.24087E-01
5.720	1.26748E+00
5.730	1.45661E+00
5.740	1.35315E+00
5.750	9.77554E-01
5.760	4.05060E-01
5.770	-2.49436E-01
5.780	-8.54437E-01
5.790	-1.28826E+00
5.800	-1.46352E+00
5.810	-1.34471E+00
5.820	-9.55374E-01

TIME HISTORY FOR NODE 11 DYNAMIC ANALYSIS

OUTPUT RESULTS ARE MEASURED IN GLOBAL COORDINATE SYSTEM

TIME	X-DIR ACCEL.
5.830	-3.73444E-01
5.840	2.84380E-01
5.850	8.86040E-01
5.860	1.31063E+00
5.870	1.47269E+00
5.880	1.33939E+00
5.890	9.37156E-01
5.900	3.46407E-01

NHIST 7 1 K=A O=L TST=5.5 TE=5.9

TIME HISTORY FOR NODE 7 DYNAMIC ANALYSIS

OUTPUT RESULTS ARE MEASURED IN GLOBAL COORDINATE SYSTEM

TIME	X-DIR ACCEL.
5.500	-9.12584E-01
5.510	-1.51577E+00
5.520	-1.81286E+00
5.530	-1.74433E+00
5.540	-1.32427E+00
5.550	-6.37593E-01
5.560	1.77186E-01
5.570	9.55797E-01
5.580	1.54131E+00
5.590	1.81575E+00
5.600	1.72380E+00
5.610	1.28399E+00
5.620	5.84927E-01
5.630	-2.32534E-01
5.640	-1.00363E+00
5.650	-1.57289E+00
5.660	-1.82540E+00
5.670	-1.71002E+00
5.680	-1.24965E+00
5.690	-5.36725E-01
5.700	2.85410E-01
5.710	1.05128E+00
5.720	1.60657E+00
5.730	1.83922E+00
5.740	1.70196E+00
5.750	1.22193E+00
5.760	4.95233E-01
5.770	-3.32271E-01
5.780	-1.09430E+00
5.790	-1.63753E+00
5.800	-1.85246E+00
5.810	-1.69543E+00
5.820	-1.19750E+00

TIME HISTORY FOR NODE 7 DYNAMIC ANALYSIS

OUTPUT RESULTS ARE MEASURED IN GLOBAL COORDINATE SYSTEM

TIME	X-DIR ACCEL.
5.830	-4.58225E-01
5.840	3.74217E-01
5.850	1.13279E+00
5.860	1.66512E+00
5.870	1.86410E+00
5.880	1.68942E+00
5.890	1.17573E+00
5.900	4.25741E-01

END

*** EXIT FROM SOLVIA-POST 90.2G

VBB VIAK

APPENDIX 5

ICE FORCE STUDIES IN THE BOTHNIAN BAY Phase 2

WORK PLANS PREPARED DURING PHASE 2

March 25, 1991
R4816-000
R4819-000
Project ICE FORCES AGAINST
OFFSHORE STRUCTURES,
PHASE 2

Preliminary work plan

Task A: GLOBAL ICE FORCE STUDY

A3.1 Inspection and repair of existing accelerometer, inclinometer and video systems onboard Norströmsgrund Lighthouse (NASAN).

A3.2 Installation of equipment from Farstugrund onboard Norströmsgrund (for supplementary measurements and redundancy). (NASAN)

A3.3 Periodic checking of the operation. (NASAN)

A3.4 Instrumental data aquisition during the winter 91-92.

A3.5 Data analysis and reporting. (VBB)

Task B: ICE FORCE DISTRIBUTION STUDY

B2.1 Reinstallation of Ice Force Sensing Panels.

2.1.1 **Inspection** of Norströmsgrund lighthouse. Investigation of the conditions of panels, dummy panels, attachements, instrumentation etc. (NASAN)

2.1.2 **Fabrication** of equipment for replacement of damaged parts. (HSVA)

2.1.3 **Reinstallation** of the panels, electrical cable system etc. (NASAN, HSVA)

2.1.4 **Testing** of the operation of the entire panel system (HSVA, NASAN)

2.1.5 Supplementary installation work, if necessary. (HSVA, NASAN)

2.1.6 **Retesting** of the panel system periodically. (NASAN)

B2.2 Ice force measurements during the winter 91-92 incl. sampling of ice strength data etc. (HSVA).

B2.3 Data analysis and reporting. (HSVA)

Task C. GENERAL PROJECT WORK

C2.1 Project coordination, general activities (meetings, general arrangements for transportation etc.) (VBB)

C2.2 Maintenance and operation of the diesel power supply system (NASAN).

C2.3 Summary report including coordination of analysis results. (VBB)

April 27, 1992
R4816, R4819

Appendix to letter
April 27, 1992

Project ICE FORCES AGAINST OFFSHORE STRUCTURES
- PHASE 2

WORK PLAN

(1) **Preparatory work**

(1.1) Dismounting of accelerometers, computers, cameras and other sensitive equipment
(Spring -92).

(1.2) Inspection and testing of the ice force sensing panels.
(Late summer -92)

(1.3) Reinstallation of measurement and observation systems (after service and repair) and overhaul and refueling of the diesel generators and heating system.
(Late fall -92)

(1.4) Starting up expedition including checking of the operation of involved systems.
(Dec. 92 to early Jan. -93.)

2. **Field activities, viz manning of the lighthouse for surveillance of the measurements and for sampling of ice data**
(during one or more periods of ice drift in January to early April -93)

3. **Data analysis, reporting and coordination work**
(Mid -93)

4. Unprogrammed repair work

Most likely the need of repair and replacement of equipment will be moderate and the expenses will not exceed the budget. However, in the worst case malfunctions of the ice force sensing panels may call for unprogrammed work which could range from repair on site to removal, workshop repair and reinstallation of one or more panels.
(Late fall -92)

VBB VIAK

APPENDIX 6

ICE FORCE STUDIES IN THE BOTHNIAN BAY Phase 2

EXTRACT from

A SUMMARY OF ICE SEASON AND ICE BREAKING ACTIVITIES 1992/93

published by

the Swedish Meteorological and Hydrological Institute
pp. 35-45

Vintersjöfartsforskning

Vintersjöfartsforskning bedrivs i samarbete mellan Sverige och Finland. Styrelsen för Vintersjöfarts-forskning som är sammansatt av representanter från Sjöfartsverket i Sverige och Sjöfartsstyrelsen i Finland, fördelar i samarbete medel till forskningsprojekt.

För svenskt vidkommande har medel bl a gått till SMHI som bedrivit vintersjöfartsforskning koncentrerad till ismodellering och fjärranalys.

Inom projektet ismodellering har en modell för samkörning av isdrifts- och havsmiljödata utvecklats. Med hjälp av denna modell, och med underlag i form av aktuella väderprognoser, avses förmodad isdrift med vallbildning respektive öppna råkar som följd kunna presenteras. Modellkoden har utvecklats av Finska Havsforskningsinstitutet. På SMHI har modellen utvidgats till att gälla hela Östersjön och dessutom har den kopplats till en vädermodell som tidigare utvecklats vid SMHI. Modellen har under 1992 testats och verifierats samt under 1993 körts i operativt bruk.

Inom fjärranalysen har verksamheten varit helt koncentrerad till mottagning, bearbetning, tolkning och distribution av radarsatellitbildsdata. Ett system för distribution av bilder till isbrytarledningen och isbrytarna i nära real tid har byggts upp. Ett demonstrationsprojekt för operativ användning av radarsatellitbilder på en isbrytare (Atle) genomfördes under 1993.

Ombord på isbrytarna presenteras de digitalt överförda radarbilderna, övriga satellitbilder och plott-information i applikationen ICEPLOTT. Detta program har det gångna verksamhetsåret försetts med ett tillägg för att kunna framställa ritade iskartor för presentation på isbrytarledningen och isbrytarna.

Utöver ovanstående pågår arbete med att utvärdera nyttan av isbrytaren Oden:s vattensmörjsystem. Projektet som ej har slutförts p g a de senaste mildra vintrarna, genomförs av Bureau Oden icebreaker design AB.

Under 1993 har ytterligare två projekt inletts. Ett arbete syftar till att beskriva vilka parametrar som påverkar ett fartygs framkomlighet i is. Chalmers Tekniska Högskola har erhållit medel för att inleda en förstudie i ämnet. I en förlängning eftersträvas dock ett samarbete mellan högskolorna i Helsingfors och Göteborg.

Det andra projektet avser en studie av framkomligheten i arktisk is. Denna studie planeras att vara ett samarbetsprojekt mellan Styrelsen för Vintersjöfarts-forskning samt US Coast Guard och Canadian Coast Guard.

Winter navigation research

Winter navigation research is carried on in co-operation between Sweden and Finland. Funds for research projects are allocated by the Winter Navigation Research Board, which is made up of representatives of the National Swedish Administration of Shipping and Navigation (SjöV) and its Finnish counterpart the Finnish Board of Shipping and Navigation.
On the Swedish side, research funds went to, among others, the Swedish Meteorological and Hydrological Institute (SMHI) to conduct winter navigation research focusing on ice-modeling and remote analysis techniques.

Within the ice-modeling project, a model of joint running of ice-drift and marine environment data was developed. Using the model and based on current weather forecasts, presumed ice-drift patterns resulting in either ridging or open leads can be presented. The model code has been developed by the Finnish Marine Research Institute. At the SMHI, the model was extended to cover the whole of the Baltic and was also linked up with a weather model previously developed by the SMHI. The model was tested and verified in 1992, and during 1993 was run in operative use.

Remote analysis work was completely focused on the reception, processing, interpretation and distribution of radar satellite image data. A near real-time system for distributing images to the ice-breakers and the Ice-Breaking Service was built up. A demonstration project for the operative use of radar satellite images on board an ice-breaker (the Atle) was implemented during 1993.

On board the ice-breakers, the digitally transferred radar imagages, other satellite images and plotted information were presented in the ICEPLOTT application. During the year under review, this program was provided with a supplemental part to enable it to draw ice-charts for presentation to the Ice-Breaking Service and on board the ice-breakers.

In addition to the above activities, work is going on to evaluate the usefulness of the water lubrication system installed on the ice-breaker "Oden". This project is run by the company Bureau Oden Ice-Breaker Design AB, but it has not been possible to finalize it due to the mild winters in recent years.

Two further projects were initiated during 1993, one of which aims to describe what parameters have an influence on a vessel's navigability in ice. The Chalmers Institute of Technology has been granted funds to launch a pilot study on the subject. In an extension, the aim is to establish a co-operation between the institutes of technology in Helsinki and Gothenburg.

MAXIMALA ISUTBREDNINGEN 1985/86-1992/93

Isvintrarna indelas i "lindriga", "normala" och "stränga". Den grundläggande faktorn vid bedömning av en isvinters totala svårighetsgrad är havsisens utbredning. Även andra förhållanden som inverkat på sjöfarten tas dock också i beaktande. Dit hör isperiodens längd, istäckets framkomlighet under inverkan av vind- och strömförhållanden m m. Inom begränsade områden kan svårighetsgraden avvika från den totala svårighetsgraden. Under en isvinter som betecknas som lindrig kan t.ex. isarna i Bottenviken uppvisa en utbredning och framkomlighet som kännetecknar en normal isvinter.

MAXIMUM ICEEXTENT 1985/86 - 1992/93

The ice winters are classified as easy, normal and strong. The ice extent is the main factor when judging the degree of difficulty. Other conditions which have influenced the navigation are also taken into account, i.e. the length of the ice period, the navigability due to winds and currents. Local variations may of course occur. During an ice winter classified as easy ice conditions in the bay of Bothnia may have been normal.

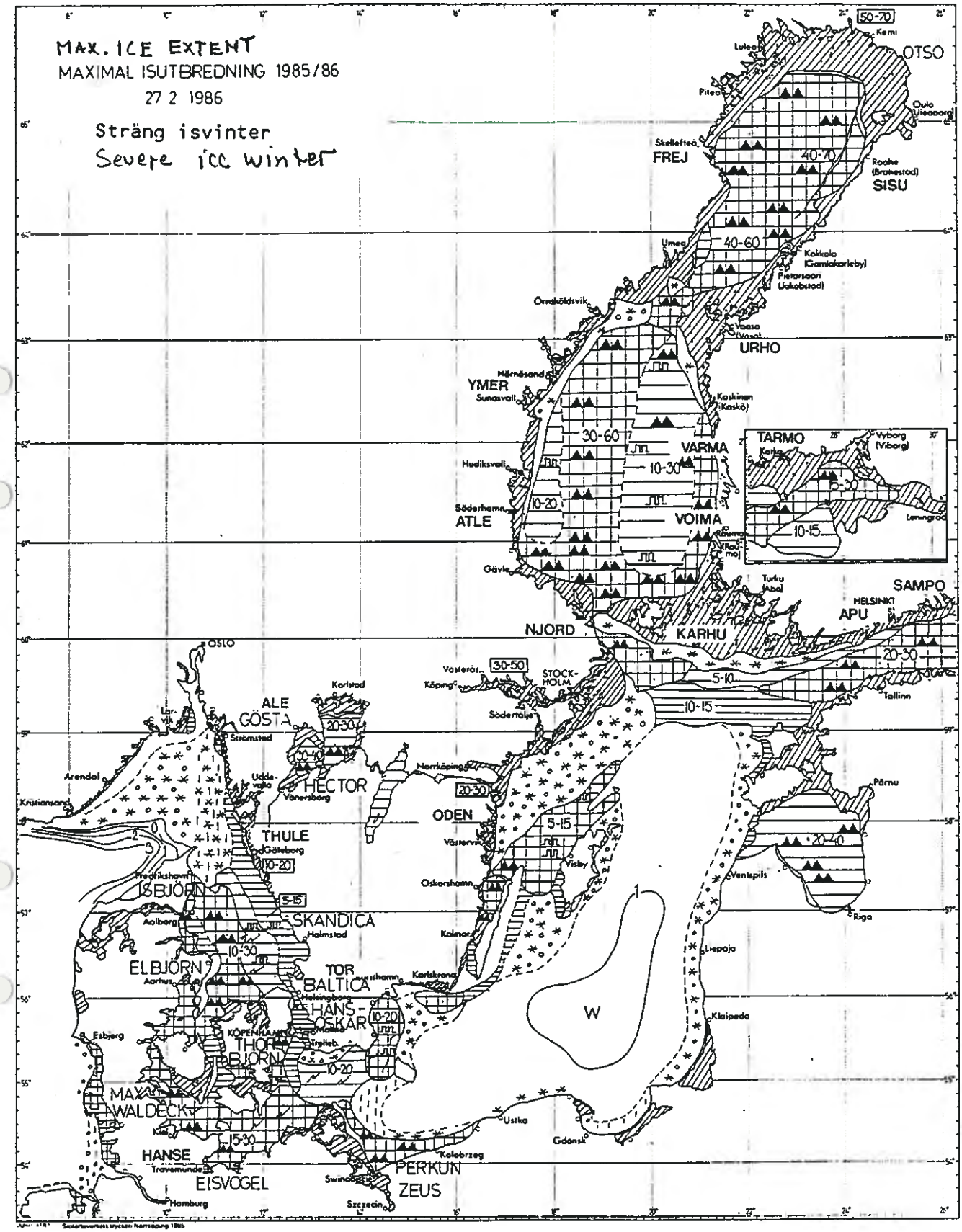
MAX. ICE EXTENT
MAXIMAL ISUTBREDNING 1985/86
27 2 1986
Sträng isvinter
Severe ice winter
50-70
OTSO
FREJ
40-70
SISU
40-60
URHO
YMER
30-60
VARMA
10-30
ATLE
10-20
VOIMA
TARMO
5-10
10-15
SAMPO
APU
NJORD
KARHU
30-50
20-30
ALE
GÖSTA
HECTOR
ODEN
THULE
ISBJÖRN
SKANDICA
ELBJÖRN
TOR
BALTICA
HANS-OSKAR
THOR
BJÖRN
MAX
WALDECK
HANSE
EISVOGEL
PERKUN
ZEUS
W
OSLO
Stockholm
Helsinki
Tallinn
Riga
Gdańsk
Hamburg
Szczecin

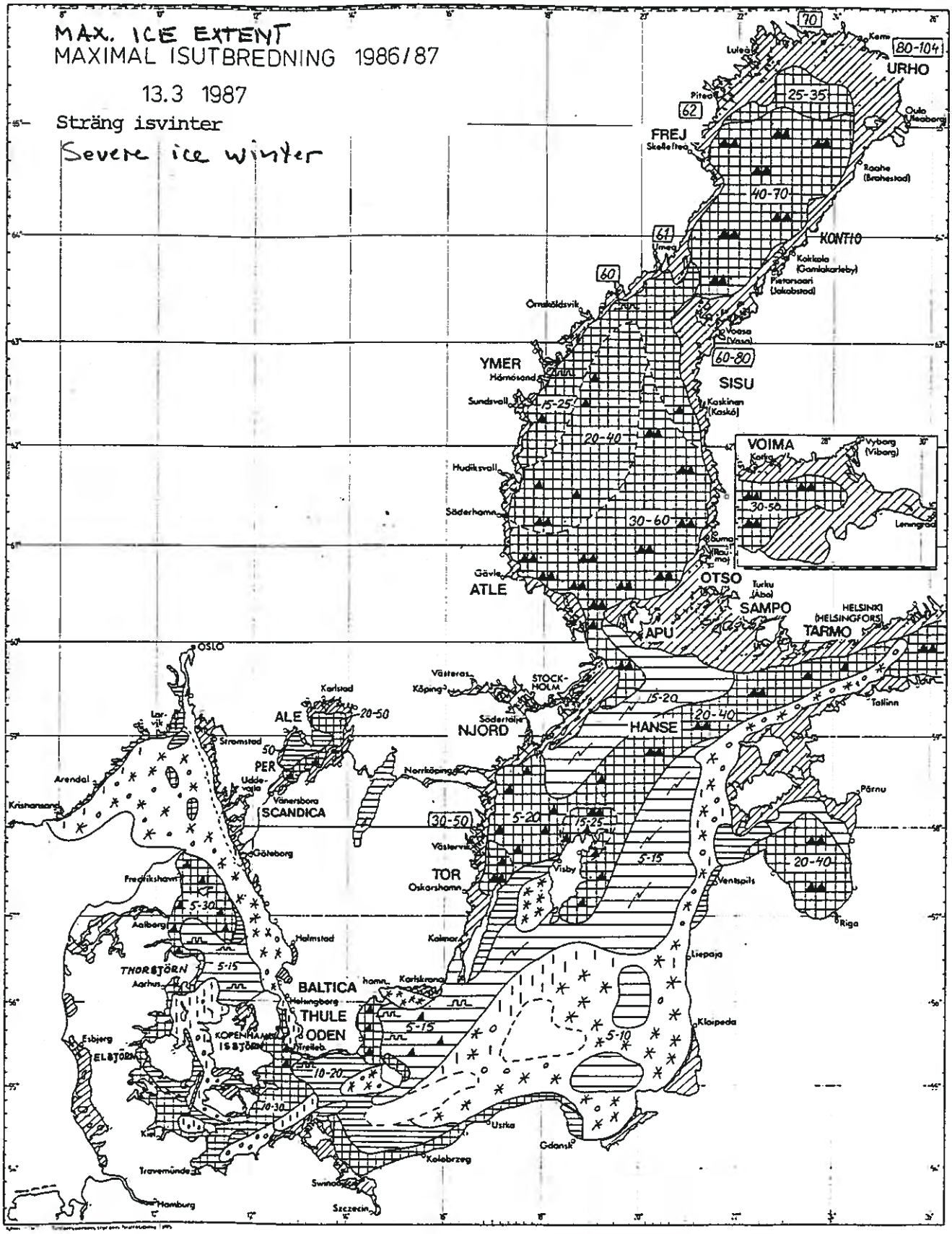
MAX. ICE EXTENT
MAXIMAL ISUTBREDNING 1986/87
13.3 1987
Sträng isvinter
Severe ice winter
70
80-104
URHO
25-35
62
FREJ
40-70
61
KONTIO
60
60-80
SISU
YMER
15-25
20-40
VOIMA
30-50
30-60
OTSO
ATLE
SAMPO
APU
TARMO
HELSINKI (HELSINGFORS)
OSLO
ALE
20-50
NJORD
HANSE
15-20
20-40
PER
SCANDICA
30-50
5-20
15-25
TOR
5-15
20-40
5-30
THORSTÖRN
5-15
BALTICA
THULE
ODEN
ISBJÖRN
ELBJÖRN
10-20
10-30
5-10
Riga
Tallinn
Pärnu
Liepaja
Klaipeda
Gdansk
Kolobrzeg
Szczecin
Hamburg
Travemünde
Kiel
Esbjerg
Aarhus
Aalborg
Göteborg
Strömstad
Arendal
Kristiansand
Fredrikshavn
Helsingborg
Halmstad
Kalmar
Visby
Stockholm
Västerås
Norrköping
Södertälje
Gävle
Sundsvall
Härnösand
Örnsköldsvik
Vasa
Uleåborg
Kemi
Luleå
Piteå
Skellefteå
Umeå
Raahe (Brahestad)
Oulu (Uleaborg)
Kokkola (Gamlakarleby)
Pietarsaari (Jakobstad)
Kaskinen (Kaskö)
Hudiksvall
Söderhamn
Kotka
Vyborg (Viborg)
Leningrad
Turku (Åbo)
Tallinn
Ventspils

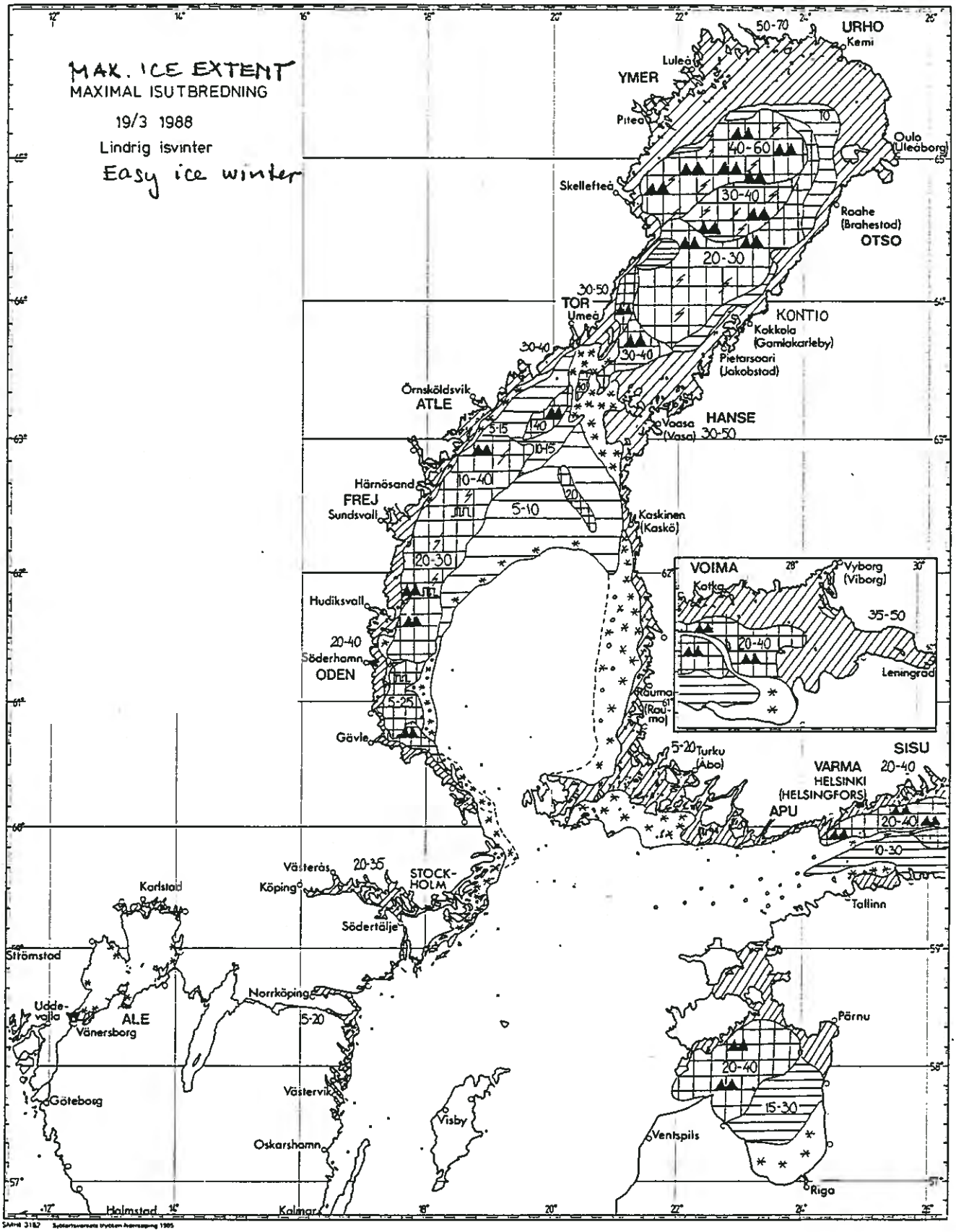
MAK. ICE EXTENT
MAXIMAL ISUTBREDNING
19/3 1988
Lindrig isvinter
Easy ice winter
URHO
Kemi
Luleå
YMER
Piteå
Oulo (Uleåborg)
Skellefteå
Raahe (Brahestad)
OTSO
TOR
Umeå
KONTIO
Kokkola (Gamlakarleby)
Pietarsaari (Jakobstad)
Örnsköldsvik
ATLE
Vaasa (Vasa)
HANSE
Härnösand
FREJ
Sundsvall
Kaskinen (Kaskö)
Hudiksvall
Söderhamn
ODEN
Gävle
VOIMA
Kotka
Vyborg (Viborg)
Leningrad
Raumo (Rauma)
Turku (Åbo)
SISU
VARMA
HELSINKI (HELSINGFORS)
APU
Tallinn
Västerås
STOCK-HOLM
Köping
Karlstad
Södertälje
Strömstad
Norrköping
Udde-valla
ALE
Vänersborg
Göteborg
Västervik
Oskarshamn
Visby
Pärnu
Ventspils
Riga
Kalmar
Halmstad

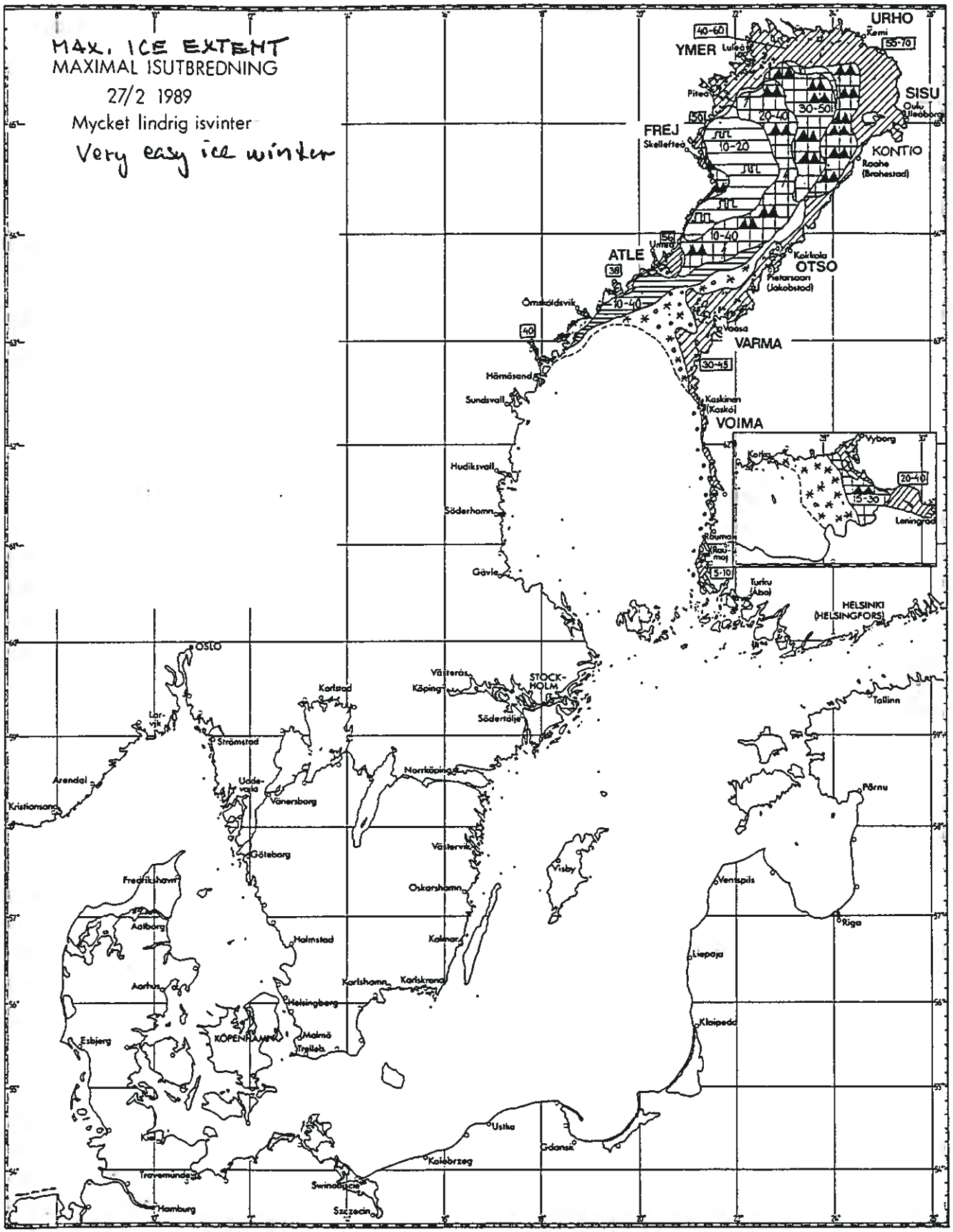
MAX. ICE EXTENT
MAXIMAL ISUTBREDNING
27/2 1989
Mycket lindrig isvinter
Very easy ice winter
URHO
YMER
SISU
FREJ
KONTIO
ATLE
OTSO
VARMA
VOIMA
40-60
55-70
30-50
20-40
10-20
10-40
30-45
5-10
15-30
OSLO
STOCK-
HOLM
HELSINKI
(HELSINGFORS)
Tallinn
Pärnu
Riga
Liepaja
Klaipeda
Ventspils
Visby
Gdansk
Ustka
Kolobrzeg
Swinoujscie
Szczecin
Hamburg
Travemünde
Kiel
Esbjerg
Aalborg
Aarhus
Fredrikshavn
Kristiansand
Arendal
Larvik
Strömstad
Uddevalla
Vänersborg
Göteborg
Karlstad
Hudiksvall
Sundsvall
Hämösand
Gävle
Söderhamn
Västerås
Köping
Södertälje
Norrköping
Västervik
Oskarshamn
Kalmar
Karlshamn
Karlskrona
Helsingborg
Malmö
Trelleb.
Vaasa
Oulu
Raahe
(Brahestad)
Kemi
Luleå
Piteå
Skellefteå
Umeå
Kaskinen
(Kaskö)
Pietarsaari
(Jakobstad)
Ömskoldsvik
Turku
(Åbo)
Raumo
Rauma
Kotka
Vyborg
Leningrad

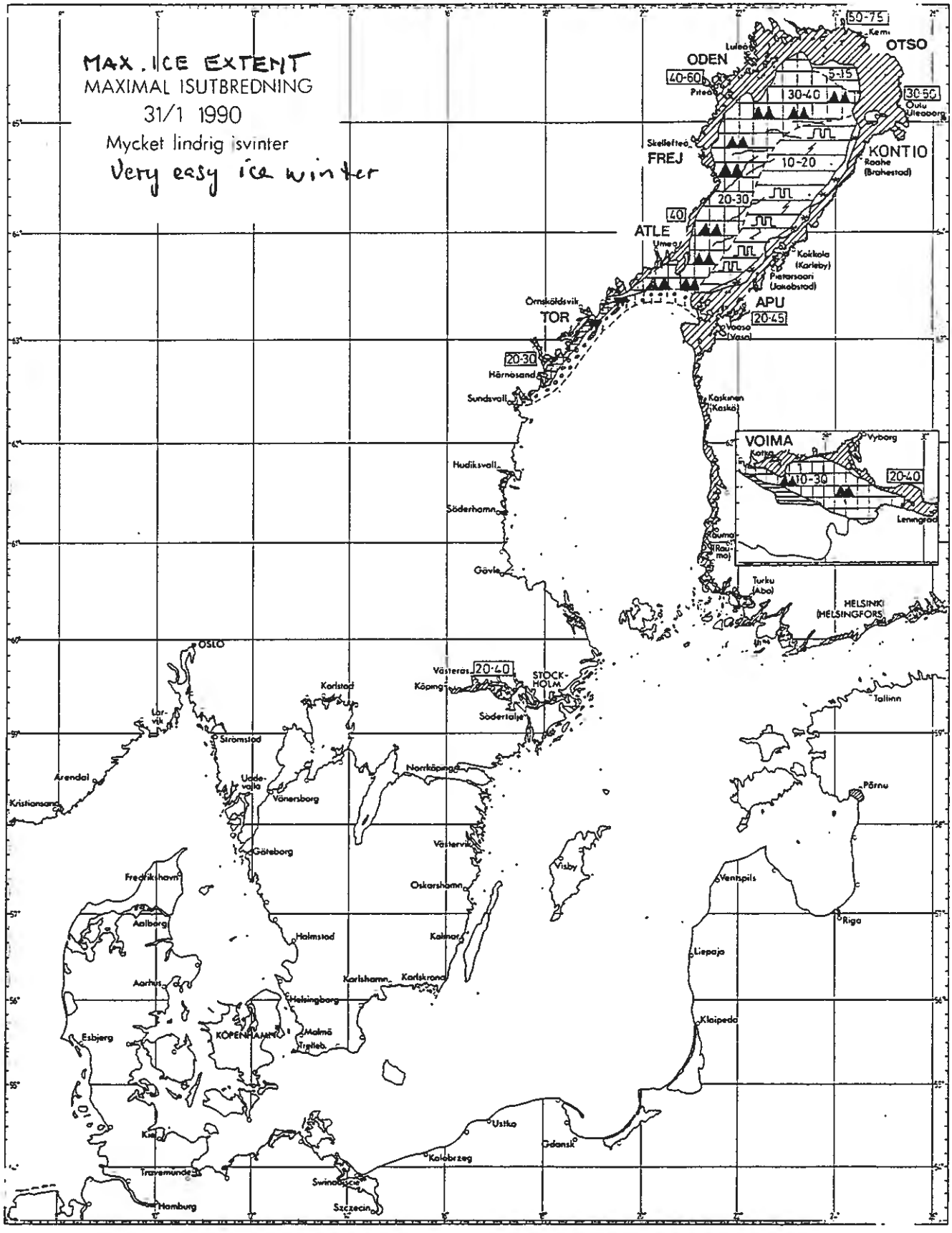
MAX. ICE EXTENT
MAXIMAL ISUTBREDNING
31/1 1990
Mycket lindrig isvinter
Very easy ice winter
ODEN
40-60
OTSO
50-75
5-15
30-40
30-50
FREJ
10-20
KONTIO
20-30
40
ATLE
APU
20-45
TOR
20-30
VOIMA
10-30
20-40
20-40
OSLO
STOCK-
HOLM
HELSINKI
(HELSINGFORS)
KØBENHAVN
Tallinn
Pärnu
Riga
Liepaja
Klaipeda
Ustka
Gdansk
Kolobrzeg
Swinoujscie
Szczecin
Hamburg
Travemünde
Kiel
Esbjerg
Aarhus
Aalborg
Frederikshavn
Kristiansand
Arendal
Strömstad
Lysekil
Karlstad
Uddevalla
Vänersborg
Göteborg
Halmstad
Helsingborg
Malmö
Trelleb.
Karlshamn
Karlskrona
Kalmar
Oskarshamn
Visby
Västervik
Norrköping
Västerås
Köping
Södertälje
Gävle
Hudiksvall
Söderhamn
Sundsvall
Härnösand
Örnsköldsvik
Umeå
Skellefteå
Luleå
Kemi
Oulu
Uleaborg
Raahe
(Brahestad)
Kokkola
(Karleby)
Pietarsaari
(Jakobstad)
Vaasa
(Vasa)
Kaskinen
(Kaskö)
Raumo
(Raumo)
Turku
(Abo)
Vyborg
Leningrad

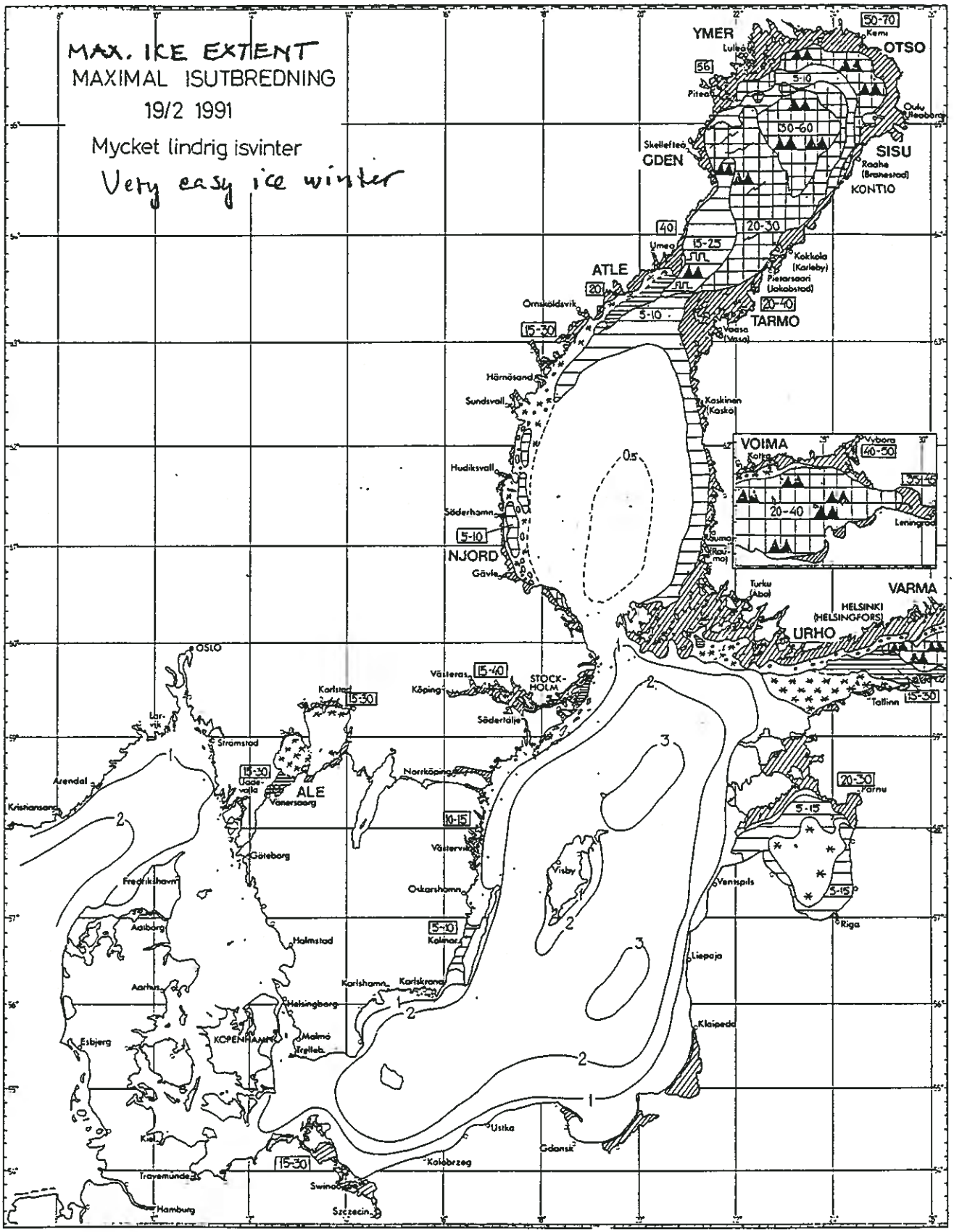
MAX. ICE EXTENT
MAXIMAL ISUTBREDNING
19/2 1991
Mycket lindrig isvinter
Very easy ice winter
YMER
OTSO
SISU
GDEN
KONTIO
ATLE
TARMO
VOIMA
NJORD
VARMA
URHO
ALE
OSLO
STOCK-
HOLM
HELSINKI
(HELSINGFORS)
50-70
56
5-10
30-60
40
20-30
15-25
20
20-40
15-30
0.5
40-50
20-40
5-10
10-15
5-15
20-30
Kemi
Luleå
Piteå
Skellefteå
Umeå
Kokkola
(Karleby)
Pietarsaari
(Jakobstad)
Oulu
(Uleåborg)
Raahe
(Brahestad)
Vaasa
(Vasa)
Örnsköldsvik
Härnösand
Sundsvall
Hudiksvall
Söderhamn
Gävle
Kaskinen
(Kaskö)
Kotka
Vyborg
Leningrad
Sumor
(Rauma)
Turku
(Åbo)
Tallinn
Pärnu
Västerås
Köping
Södertälje
Karlstad
Lar-
vik
Strömstad
Arendal
Krishansand
Jäde-
valla
Vänersborg
Norrtälje
Västervik
Oskarshamn
Visby
Ventspils
Riga
Liepaja
Klaipeda
Kalmar
Karlshamn
Karlskrona
Helsingborg
Halmstad
Göteborg
Fredrikshavn
Aalborg
Aarhus
Esbjerg
KOPENHAMN
Malmö
Ystad
Kiel
Travemünde
Hamburg
Swinoujscie
Szczecin
Kolobrzeg
Gdansk
Ustka

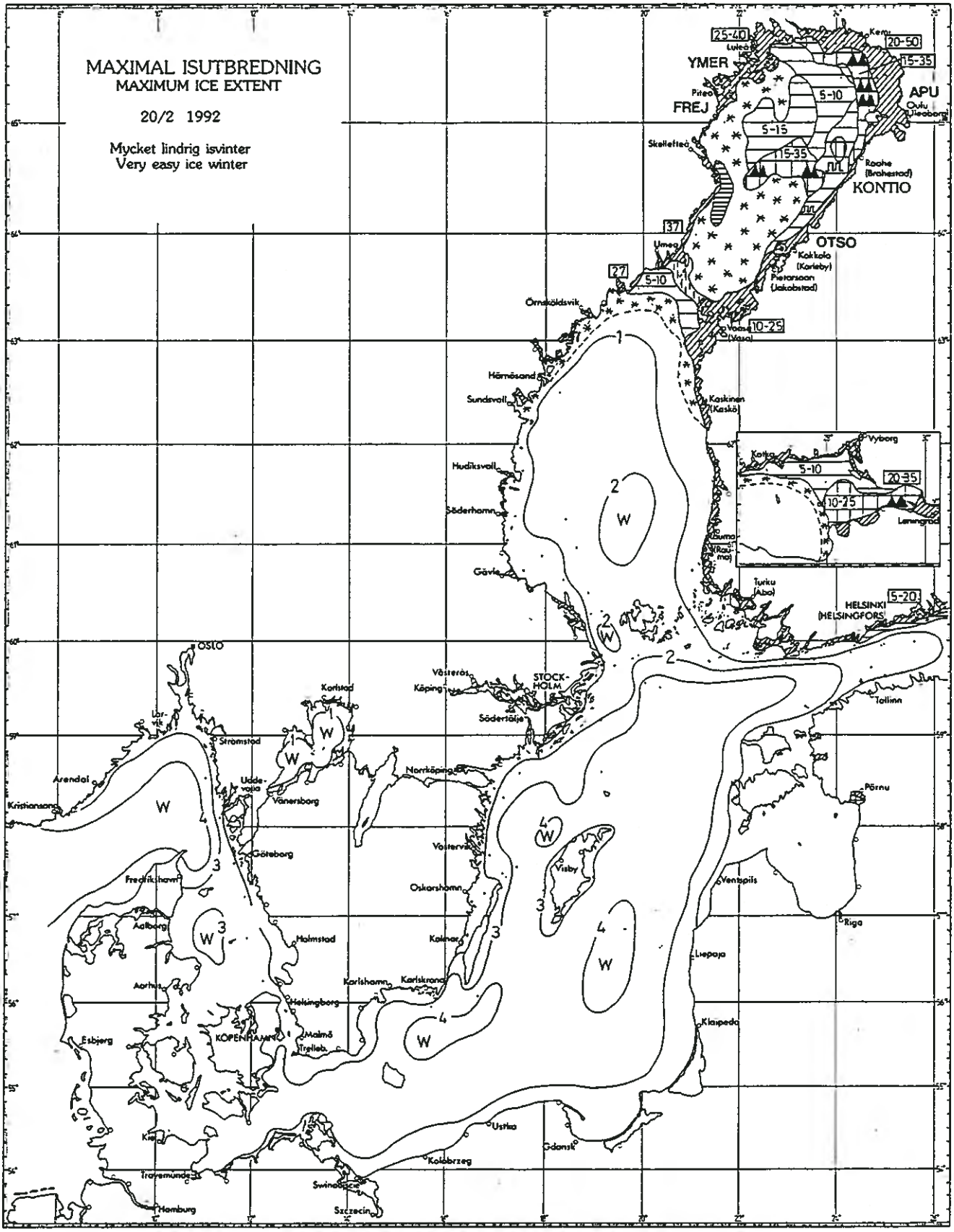
MAXIMAL ISUTBREDNING
MAXIMUM ICE EXTENT
20/2 1992
Mycket lindrig isvinter
Very easy ice winter
YMER
FREJ
APU
KONTIO
OTSO
25-40
20-50
15-35
5-10
5-15
10-25
20-35
5-20
37
27
HELSINKI
(HELSINGFORS)
STOCK-
HOLM
OSLO
KØBENHAVN
Tallinn
Riga
Pärnu
Ventspils
Liepaja
Klaipeda
Gdansk
Ustka
Kolobrzeg
Szczecin
Swinoujscie
Hamburg
Travemünde
Kiel
Esbjerg
Aarhus
Aalborg
Frederikshavn
Kristiansand
Arendal
Larvik
Strömstad
Uddevalla
Vänersborg
Göteborg
Karlstad
Köping
Västerås
Södertälje
Norrköping
Västervik
Oskarshamn
Kalmar
Karlskrona
Helsingborg
Malmö
Trelleb.
Halmstad
Visby
Hudiksvall
Söderhamn
Gävle
Sundsvall
Härnösand
Örnsköldsvik
Umeå
Skellefteå
Piteå
Luleå
Kemi
Oulu
(Uleaborg)
Raahe
(Brahestad)
Kokkola
(Karleby)
Pietarsaari
(Jakobstad)
Vaasa
(Vasa)
Kaskinen
(Kaskö)
Turku
(Åbo)
Raumo
(Rauma)
Pori
(Björneborg)
Hanko
(Hangö)
Vyborg
Leningrad
W
1
2
3
4

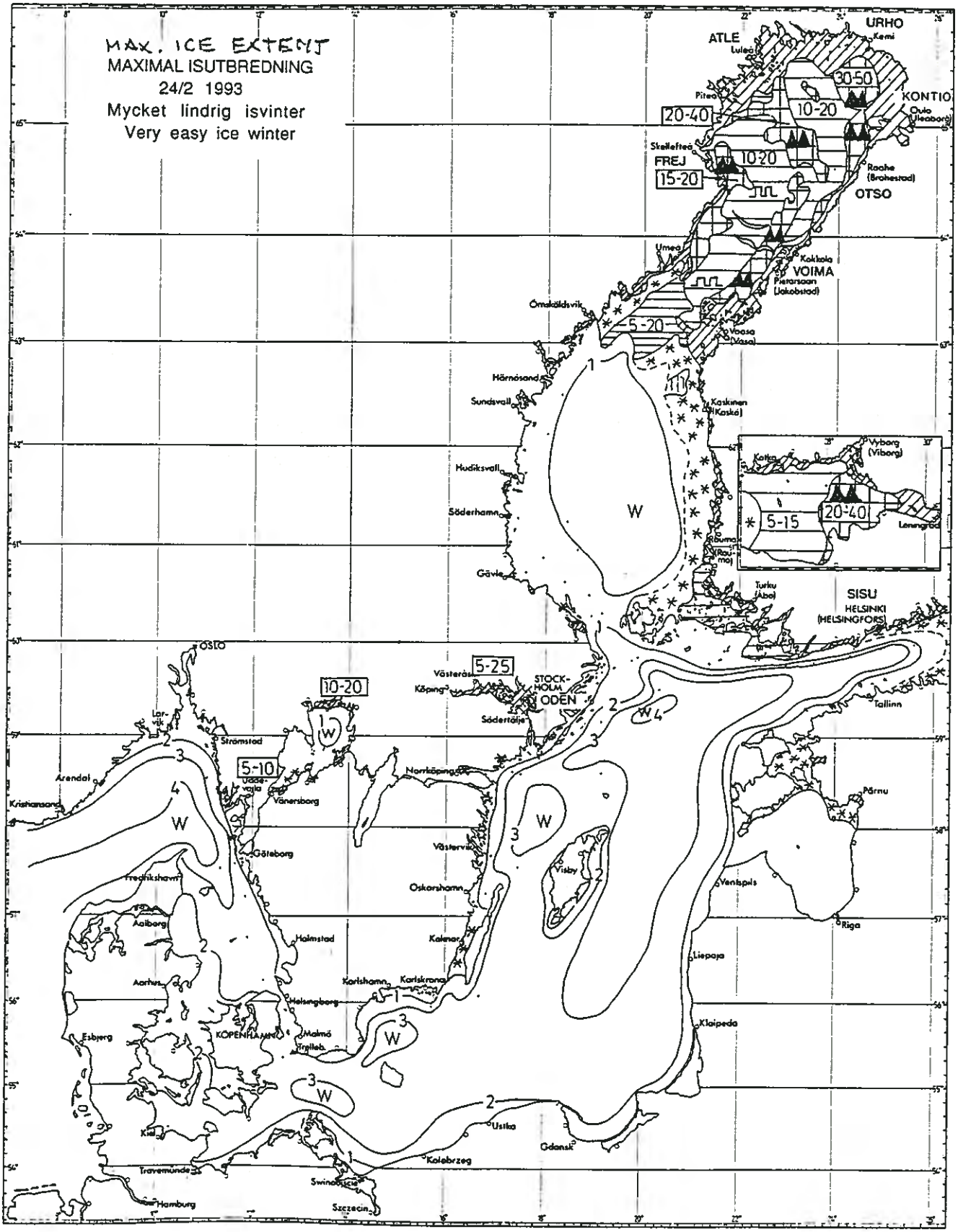
MAX. ICE EXTENT
MAXIMAL ISUTBREDNING
24/2 1993
Mycket lindrig isvinter
Very easy ice winter
URHO
ATLE
KONTIO
FREJ
OTSO
VOIMA
SISU
ODEN
STOCK-HOLM
HELSINKI (HELSINGFORS)
30-50
10-20
20-40
10-20
15-20
5-20
5-15
20-40
5-25
10-20
5-10
W
1
2
3
4

Kommentar till figur över vintrarnas svårighetsgrad.

Temperaturfunktionen tar indirekt hänsyn till havets lagrade värmemängd. Den kan i viss mån jämföras med en köldsumma. Den är dock mermer eftersläpande och utjämnande för extrema lufttemperaurer under kort tid. Vinden har endast en indirekt påverkan på funktionen genom att dygnsmedeltemperaturen utgör ingångsdata för funktionen. Metoden visar mycket god överensstämmelse med totala isutbredningen, men också ett mått på istjockleken. Genom att vinden inte är representerad direkt, ger den inte ett mått på isens svårighetsgrad eller framkomlighet.

Staplarna kring axeln motsvarar normala isvintrar, medan staplarna ovanpå axeln motsvarar lindriga eller mycket lindriga och de undre stränga eller mycket stränga isvintrar.

Rödrasterade staplar visar milda vintrar, ofyllda normala och blå svåra. Som syns, av fig. är samtliga värden på temperaturfunktion under 0 grader i Bottenviken, vilket är ett mått på att Bottenviken varje år täcks med is, även en mild vinter. Däremot ligger normalvärdet på södra Östersjön och på Västkusten kring 0 grader eller t.o.m. över. Det är m.a.o. mer normalt med isfritt än med is.

Notes on the figure Degree of difficulty of winters, see next page.

The temperature function is indirectly influenced by the heat stored in the sea In some respect it can be compared with a sum of cold. However, it has a greater lag and a higher compensating effect at short spells of extreme air temperatures.

Wind has only an indirect influence on the temperature function, because the daily mean temperature is used as input dat for the function. The method gives a very good corelation with total ice extension, and also provides a measure of ice thickness. Due to the fact that wind is not directly represented, however, it does not provide a measure of the degree of difficulty of ice-conditions, nor a measure of ice navigability.

Columns close to the axis represent normal winter ice-conditions, longer columns rising above the axis easy or very easy ice-conditions, and columns extending below the axis severe or very severe wintr ice-conditions.

Red columns represent mild winters, unfilled columns are normal, and blue columns severe winters. As can be seen from the figure, all of the temperaute finction values given for the Bay of Bothnia are below zero, which means that the Bay of Bothnia was ice-covered every year, even during mild winters. For both the southern part of the Baltic and the West Coast, however, the normal value lies round about zero and even slightly above, in other words ice-free waters are more normal here than ice-covered.

Vintrarnas svårighetsgrad 1920/21 - 1992/93 som en funktion av lufttemperaturen.
Degree of difficulty for the winters 1920/21 - 1992/93 as a function of the air temperature